

PDF hosted at the Radboud Repository of the Radboud University Nijmegen

The following full text is a publisher's version.

For additional information about this publication click this link.

<http://hdl.handle.net/2066/145807>

Please be advised that this information was generated on 2017-12-05 and may be subject to change.

4037

The Control of Redundancy in Joints and Muscles in the Human Arm



M.M.H.J. Theeuwen

The Control of Redundancy in Joints and Muscles in the Human Arm

een wetenschappelijke proeve op het gebied van
de Natuurwetenschappen

Proefschrift

ter verkrijging van de graad van doctor
aan de Katholieke Universiteit Nijmegen,
volgens besluit van het College van Decanen
in het openbaar te verdedigen
op donderdag 30 juni 1994
des namiddags te 1.30 uur precies

door

Marc Mary Hildo John Theeuwen

geboren op 22 juli 1967 te Weert

Promotor Prof Dr C C A M Gielen

This work was supported by the Dutch Foundation for Biophysics (NWO) and by ESPRIT Basic Research Actions 3149 and 6615

CIP-GEGEVENS KONINKLIJKE BIBLIOTHEEK, DEN HAAG

Theeuwen, M M H J

The control of redundancy in joints and muscles in the human arm /

M M H J Theeuwen - [S I s n] III

Proefschrift Nijmegen - Met lit opg ISBN 90-9007100-8

Trefw gewrichten / spieren / bewegingscoördinatie

Contents

1	Introduction and summary	1
1.1	General introduction	1
1.1.1	Redundancy on joint level	2
1.1.2	Redundancy on muscle level	4
1.2	Outline and summary	6
1.2.1	Chapters 2 and 3	6
1.2.2	Chapter 4	7
1.2.3	Chapters 5 and 6	8
1.2.4	Chapter 7	9
2	The control of arm pointing movements in three dimensions	11
2.1	Abstract	11
2.2	Introduction	12
2.3	Methods	13
2.3.1	Experimental set-up	13
2.3.2	Task	14
2.3.3	Data analysis	16
2.4	Results	17
2.4.1	Determination of mean pointing and primary directions	17
2.4.2	Dependence of primary direction on mean pointing direction	20
2.4.3	Variation of primary direction during movement	21
2.4.4	Comparison of forearm and upper arm orientation	25
2.5	Discussion	27
2.5.1	Nature of the 2-dimensional rotation surface	28
2.5.2	Relation Between Upper Arm and Forearm	30
2.5.3	Departures From the 2-Dimensional Surface	30
2.5.4	Implications for neural control	31
2.6	Acknowledgements	33

3	Are the orientations of head and arm related during pointing movements ?	35
3.1	Abstract	35
3.2	Introduction	36
3.3	Methods	37
3.3.1	Task	37
3.3.2	Experimental set-up	38
3.3.3	Data analysis	38
3.4	Results	39
3.5	Discussion	45
3.5.1	Functional implications.	46
3.6	Appendix	48
4	The Activation of Mono- and Bi-articular Muscles in Multijoint Movements	53
4.1	Introduction	53
4.2	Methods	55
4.2.1	Subjects	55
4.2.2	Task	55
4.2.3	Data Collection	56
4.2.4	Data Analysis	57
4.3	Results	58
4.3.1	Isometric Contractions	58
4.3.2	Comparison of Isometric and Isotonic Activation Direction	61
4.3.3	Comparison of Isometric and Isotonic Activation Magnitude	62
4.4	Discussion	63
5	The relation between the direction dependence of EMG amplitude and motor-unit recruitment thresholds during isometric contractions.	67
5.1	Abstract	67
5.2	Introduction	68
5.3	Methods	69
5.3.1	Set up	70
5.3.2	Experimental paradigm	71
5.3.3	Surface EMG	72
5.3.4	Intramuscular EMG	72
5.4	Theory	73
5.5	Results	75

5.5.1	Quantitative comparison between motor-unit data and EMG data.	76
5.6	Discussion	87
5.6.1	Interpretation of results.	88
5.6.2	Deviations from the circle and line fit for EMG and motor-unit behavior.	88
5.6.3	Biomechanical function	90
5.6.4	Isotonic dependence	90
6	The relative activation of muscles during isometric contractions and low-velocity movements against a load.	95
6.1	Abstract	95
6.2	Introduction	96
6.3	Methods	98
6.3.1	Experimental paradigm	98
6.3.2	Surface EMG	99
6.3.3	Intramuscular EMG	99
6.4	Results	100
6.4.1	Direction selectivity of muscle activation	102
6.4.2	Amount of muscle activation	105
6.4.3	Firing rate at recruitment	108
6.5	Discussion	110
6.5.1	Direction dependent activation of muscles.	110
6.5.2	Task dependent changes in the amount of EMG activity.	112
7	Estimating the contribution of muscles to joint torque from EMG activity.	115
7.1	Abstract	115
7.2	Introduction	116
7.3	Theory	118
7.3.1	Motor-unit recruitment data	121
7.4	Methods	122
7.4.1	Experimental paradigm	122
7.4.2	Surface EMG	123
7.4.3	Motor-unit data	123
7.5	Results	124
7.5.1	Analysis of EMG data	124
7.5.2	Estimation of contributions to joint torque based on motor-unit recruitment data.	130

7.6	Discussion	135
8	Inleiding en samenvatting	139
8.1	Algemene inleiding	139
8.1.1	Redundantie op gewrichtsniveau	140
8.1.2	Redundantie op spierniveau	142
8.2	Overzicht en samenvatting	145
8.2.1	Hoofdstukken 2 en 3	145
8.2.2	Hoofdstuk 4	146
8.2.3	Hoofdstukken 5 en 6	147
8.2.4	Hoofdstuk 7	147
	Bibliography	149
	Publications	159
	Nawoord	161
	Curriculum Vitae	163

About the cover:

The photograph on the cover is taken from a bronze statue of the Hinduistic deity Shiva, Lord of the dance (India, Chola Dynasty, 12th century AD).

Surrounded by a flaming halo, the god Shiva stands here in a completely controlled dance pose, which shows him to be the lord and master of the creation, maintenance in being and destruction of the universe. With the drum in hourglass form in his upper right hand he beats the rythm: the beginning of creation. The flame in his upper left hand makes an end to the universe. His two lower hands symbolize his protection of the world: the right gives reassurance to the faithful: the left points to his raised foot which affords a refuge for seekers. With his right leg he stands on a monstrous dwarf, who represents human ignorance and is playfully crushed by the god.

Chapter 1

Introduction and summary

1.1 General introduction

Coordination of the joints and muscles of your arm in order to perform certain tasks appears to be simple for normal humans. The reason, however, for the apparent ease with which this coordination is established, is that these tasks have been executed numerous times and that we have learned them. Most of these tasks can now be executed automatically and almost subconsciously. Questions like which muscles must be used and how strong they should contract or what angles the joints should have, are not raised explicitly. Humans have developed control strategies for muscles and joints of which they are not actively aware. Suppose, for example, that suddenly a human being would be equipped with four arms, like the Hinduistic deity Shiva on the front cover. To control these additional two arms, he could not rely on the basic skills he has acquired for use of his original two arms to be helpful for usage of the additional arms without a lot of conscious concentration. The role of these new arms will probably be limited to simple static tasks like holding objects which can then be manipulated by the original arms. Although such a human being is expected to have a larger flexibility, i.e. more degrees of freedom, he will not need it to its fullest extent for ordinary tasks because his original two arms will be sufficient. His motor system is thus redundant for these tasks.

From the very beginning it should be clear that the human motor system is not really redundant. Any damage to the effector system will become evident in a loss of performance somehow. However, for some simple tasks, the number of degrees of freedom of the human motor system exceeds the number required for the task. For example, several combinations of joint angles in wrist, elbow and shoulder correspond to the same position of the tip of the index finger in 3-D space. In such a case the

problem arises that multiple solutions are available to reach your goal and one of them has to be chosen. Which solution is the best will be determined by additional constraints. This can be compared to a journey from city A to city B. There are several alternative roads which can be taken. If time is an important constraint, you will probably take the highway. On the other hand you could also prefer a more scenic road which may lead to an other choice of roads. Depending on the constraints a different solution for the redundancy problem will be chosen. Similar redundancy problems exist for the human arm at the joint level and at the muscle level. Several hypotheses have been proposed for constraints and strategies to solve these redundancies at the joint level [90, 22, 11] and at the muscle level [18, 103, 52]. Although several hypotheses are available on how the human motor system could deal with "apparent" redundancy, not enough experimental data are available to distinguish between these hypotheses and to decide whether any hypothesis gives satisfactory explanations and predictions. A major purpose of this thesis is to provide more experimental observations and to confront these data with predictions of various hypotheses.

1.1.1 Redundancy on joint level

At the joint level, each of our arms has many degrees of freedom. For some tasks all these degrees of freedom are necessary, for example when obstacles have to be avoided or when serving coffee in a very full cup. Most tasks, however, do not require the use of all degrees of freedom. This problem arises also in robotics for multi-joint robot arms. The position of the hand in three dimensions can be obtained by many combinations of joint angles. If the control strategy for moving the hand along a path is to minimize the changes in joint angle, then it can be shown that there is hysteresis depending on the trajectory, the arm will have a different set of joint angles every time when the hand reaches the starting position. The actual orientation of an arm controlled in such a way depends on its history [60]. Traversing a trajectory several times may yield then an arm with joint angles close to, or beyond the physiological limits, which is quite unsatisfactory. Also the actual movement of the hand from one position to another will be made in a different way, depending on the actual orientation of the arm and on previous motor acts, which makes planning rather difficult.

The problem of redundancy for the human arm can be studied for a large variety of tasks. Starting with a very simple task, like pointing movements with an extended arm, seems a natural choice. For pointing with an extended arm only two of the three degrees of freedom in the shoulder are determined by the pointing direction: the elevation (up/down) and azimuth (left/right). Pointing with an extended arm does not

specify the amount of endo-/exorotation of the upper arm and pronation/supination of the forearm, which are rotations of these limbs along their long axis. When human subjects are asked to perform these tasks several times, they always use the same solution (neglecting small deviations of about 1 deg). Apparently they use a constant strategy for this problem. More surprising even, is the finding that all subjects use a very similar strategy which suggests that there must be a general constraint for this type of strategy (see chapters 2 and 3). If for this task it is fully understood how the redundancy is controlled, more complex tasks can be studied.

Pointing with an extended arm to a (moving) target was also selected as a task in our experiments because of a strong analogy with looking to a (moving) target which has been studied extensively for a long time. Both for the eye and the arm only two degrees of freedom are specified by the direction. The amount of endo-/exorotation and supination/pronation for the arm and the amount of torsion of the eye is undetermined by this specific task. For the eye, however, it is known since the observations of Donders in 1848 [16] that the torsion for a given gaze direction during fixation depends uniquely on the gaze direction. Given the orientation of the eye for one gaze direction as a reference, the orientation of the eye for all other gaze directions can be found by fixed axis rotations from that reference position, the axes of which lie in one single flat plane called Listing's plane [36]. The rotations can be represented by 3-D rotation vectors, which are parallel to the axis of rotation and have a magnitude that corresponds to the angle of rotation. For a special reference position, the so called primary position, the Listing Plane containing all rotation vectors, describing the rotation from the reference position to the actual eye position, is orthogonal to the gaze direction for that special reference position. These findings were extended for movements of the eye as well [100].

Similar results were found for the arm and head by Hepp et al. [41]. They found that the orientations of the arm could also be described by rotation vectors which were lying in a flat plane, which was considerably thicker than the plane for eye movements (standard deviations in the order of 6 degrees versus 1 degree for eye movements). They ascribed the larger thickness to the larger range of endo-/exorotation of the upper arm and supination/pronation of the forearm compared to the torsional range for the eye. Another possible explanation for the difference in standard deviation for eye and arm movements was that subjects can voluntarily change the amount of endo-/exorotation and supination/pronation in contrast to the torsional component of the eye orientation, which is not under voluntary control.

A greater flexibility and versatility of the arm was used by Hepp et al. [41] to explain the finding that the orientation of the planes of rotation vectors was dependent on the part of workspace in which the arm movements were made (roughly orthogonal to the mean pointing direction of the arm), while it is fixed for eye movements relative

to the head. The planes containing the rotation vectors of arm, hand and head were nearly parallel. A possible explanation might be that this reflected a strategy for the coordination of eye/hand movements. For a given workspace, the eye, head and hand could share a common 2-dimensional frame of reference and thus would map the 9-dimensional space of all possible orientations of eye, head and arm to a single 2-dimensional space. Computation and coordination of their interaction could thus be organized efficiently. The study of this organisation was the motivation for the research described in chapters 2 and 3.

1.1.2 Redundancy on muscle level

Not only the number of joints is redundant for some simple tasks, but also the number of muscles crossing a joint. The elbow joint, for example, is crossed by several muscles. This number exceeds the number of degrees of freedom of that joint. The elbow joint has two degrees of freedom: flexion/extension and pronation/supination (rotating the hand inward/outward). Because muscles can only pull and not push, four muscles would be enough for these two degrees of freedom. However, there are more than 7 muscles contributing to flexion/extension and supination/pronation. This means that the same torque can be generated by an infinite number of combinations of muscle activation patterns.

For flexion torques, the most important muscles are *m brachioradialis*, *m brachialis* and *m biceps*. These three muscles can provide the desired flexion torque in the elbow independently or in combination. Only the sum of their contributions is specified by the required flexion torque. Co-contraction of antagonists, *m triceps* for example, makes the situation even more complex.

The number of muscles is already redundant for flexion/extension and supination/pronation. The fact that the muscles themselves can not be considered as single coherent structures increases this redundancy. This is partly because of pure anatomical reasons, but also partly because of a very distinct control of several subpopulations of motor-units in each muscle. *M biceps*, for example, has one tendon attached to the forearm, but two tendons attached to the shoulder at different places with different mechanical leverarms. These two parts, the long and the short head, have a different activation as well. For the long head of this muscle, it has been shown that there are three subpopulations of muscle fibers each with a different activation pattern [33, 106]. *M biceps* contributes both to flexion and to supination in the elbow joint simultaneously. The activation of the subpopulations was found to depend on some specific combinations of supination and flexion torque, despite the fact that the mechanical advantage of all motor-unit subpopulations was the same [33].

The number of muscles and subpopulations of motor-units within a muscle, which acts across the elbow joint, is large and thus an infinite number of combinations of muscle patterns can contribute to the same torque in a joint. Despite this redundancy, a similar muscle activation pattern is found for all human subjects for a specific motor task [3, 21]. This suggests that some general constraint or strategy of coordination is used.

To investigate this constraint or strategy, gaining knowledge of how the muscle activity is coordinated during isometric contractions and movements in several directions, should be the first step. The torque which each single muscle generates separately can not be measured directly. However, we can measure a variety of variables which give indirect evidence for the muscle coordination. If these variables are measured during several motor tasks for the subject, the relative differences in the muscle coordination can be studied. External variables like force at the wrist, both in magnitude and direction, and position and its time derivative velocity, can be measured directly by means of strain gauges and goniometers. From these variables the total joint torques and joint angles can be calculated with inverse dynamics. With some anatomical knowledge these data can also provide insight in the muscle length and the changes in muscle length. These quantities affect the maximal force a muscle can generate due to the force-length and force-velocity relationships [69]. The internal variables, like the contributions of individual muscles to the total torque in a joint, can not be measured directly. For these measurements it would be necessary to implant force transducers in the tendons of all muscles.

An approach which is more friendly to the subject, but less direct, is the measurement of the electrical activity of muscle fibers which is called Electro Myo Gram (EMG). By means of surface electrodes placed on the skin, the electrical activity of many contributing muscle fibers together can be measured. The electrical contributions from all muscles add to one signal with different weights depending on several volume conductor properties. A variable which is often used to quantify surface EMG, is the mean rectified signal over some length of time [65]. The signals from muscle fibers close to the surface electrodes give a larger contribution than those from muscle fibers far away, due to spatial filtering which also affects the shape of the action potentials. This implies that the amplitude of the EMG signal depends on the exact location of the surface electrodes relative to the active muscle fibers. The amplitude is also affected by the thickness of the subcutaneous fat layer and the presence of blood vessels. For these reasons the absolute value of the measured surface EMG is not a useful parameter. One can only compare two EMG values with each other and make statements about the relative activity of the muscles at the times at which the surface EMG signals were recorded.

More detailed information about single muscle fibers can be obtained from the

signals measured by intramuscular electrodes. Because several individual muscle fibers are innervated by one motoneuron, together called a motor-unit, all muscle fibers activated by this motoneuron generate their action potentials simultaneously. The combined action potentials of all muscle fibers belonging to one motor-unit result into characteristic signals due to their relative geometrical position to the electrode and volume conductor properties [96]. These signals can be discriminated from the total activity measured by the intramuscular electrodes because of their characteristic waveshapes.

Force production by a muscle is achieved in a very orderly manner. The motor-units are recruited in a fixed order according to the size principle formulated by Henneman [39]. When the input to the motor-unit reaches a specific value, that motor-unit is recruited and starts to produce force. The force, at which a motor-unit is recruited, is called the recruitment threshold. During each twitch contraction of the motor-unit, force increases, reaches a maximum and then decays. After some refractory period, the motor-unit can again be activated. The frequency with which that happens is called the firing rate of the motor-unit. For a larger input signal to the motoneurons, the firing rate of all recruited motor-units increases and more motor-units become recruited. By means of intramuscular recordings the activation of individual motor-units, possibly belonging to different subpopulations, can be studied, both with respect to their recruitment threshold and with respect to their firing rate.

Because intramuscular recordings are so specific, they can reveal information on the activation of individual motor-units, which is impossible with surface EMG recordings. On the other hand these recordings give only information about very discrete parts of the muscle. Surface EMG and intramuscular recordings together can thus give insight in the activation pattern of muscles from a different perspective and can give valuable additional information. This is demonstrated in chapters 4 till 7.

1.2 Outline and summary

1.2.1 Chapters 2 and 3

To study how the redundancy in the human arm at the joint level is controlled, we studied pointing movements with an extended arm. These movements have strong analogies with the well-studied eye movements. Hepp et al. [41] made a hypothesis for a common 2-dimensional frame of reference for eye, head and hand movements. Computations and coordinations of their interaction could thus be organized efficiently. The experiments described in chapters 2 and 3 confirmed the findings by Hepp et al. [41] that the orientations of the arm, hand and head during pointing

movements could be described by rotations with axes that lie in a 2-dimensional plane. We found that the orientation of this plane was roughly orthogonal to the mean pointing direction in workspace.

This seemed to confirm the hypothesis about a common 2-dimensional frame of reference for eye, head and hand movements. The orientation of this plane would then be adjusted to the workspace of pointing directions. Analysis, however, of pointing movements within a small workspace, taken from a set of pointing movements within a much larger workspace, showed that the plane in which the rotation vectors were lying was roughly orthogonal to the mean pointing direction for that smaller workspace and not to the mean pointing direction of the larger workspace. The inevitable conclusion was that the plane of rotation vectors itself was not flat, but rather a curved surface. The fitted flat planes found for the small workspaces were just local linear approximations of the curved surface. The redundancy for arm orientations during pointing movements is removed by the restriction that the rotation vectors should be in this curved surface.

Similar results have been found, not only for the hand, but also for the upper arm and the head. They all showed rotation vectors in a curved surface, which was similarly curved, in contrast to the flat Listing's Plane for eye movements. At first glance there could still be a common frame of reference for orientations of head, upper arm and forearm. Comparison of the rotation surfaces, however, indicated that this is probably not the case because the rotation surfaces revealed significant differences despite their global familiar appearances.

1.2.2 Chapter 4

To study the control of redundancy at a muscle level, the activation of muscles has been examined first. This examination starts with the help of surface EMG first (chapter 4). Then more detailed information is obtained from combined intramuscular and surface EMG recordings (chapters 5 and 6). In the last chapter, the insights thus obtained, are used to estimate quantitatively the contribution of the muscles. How the control of redundancy at the muscle level is achieved can be determined with these tools. Hopefully, further research will be done on models to find the constraints which lead to the actual solution the motor system has chosen to solve the redundancy at a muscle level.

In chapter 4 the relative activation of several elbow and shoulder muscles is investigated for isometric contractions and for movements. EMG activity was measured for forces and movements in various directions in a horizontal plane. During isometric (static) contractions, each muscle demonstrated a specific activation pattern. For each muscle there was one direction, the preferred direction, in which that muscle

showed its largest EMG. That means that that muscle gave its largest contribution to the total required external force for that direction. For other directions, the activity, and thus the relative contribution to the externally required force, gradually decreases with the cosine of the angle between the preferred direction and the direction of the externally exerted force. Plotted in a polar plot, these cosine dependencies yield circles through the origin in the direction of the preferred direction.

For movements against an external force, the direction dependent modulation of activity could also be described by a cosine relating the angle between a preferred direction and the direction of the movement. The preferred direction of the muscles for movements appeared to be different from that found for isometric contractions, even though the measured forces at the wrist and the directions in which they were exerted were the same. That the muscles showed their largest EMG activity and hence their largest force contribution in different directions, while the total external forces at the hand was the same, means that the muscles gave different relative contributions to the external forces in these two experimental conditions. Not only the preferred direction of the muscles was different for isometric and movements. Also the measured EMG amplitude was different. For movements we found that the EMG amplitude increased relative to that for isometric contractions. Quite remarkably, an increase of EMG activity was found for all muscles. This must imply that there are different EMG-force relationships for the muscles under these conditions.

1.2.3 Chapters 5 and 6

To explain these findings, we measured EMG activity simultaneously with surface and intramuscular electrodes. The cosine dependencies we found, describing the surface EMG activity for a constant force in several directions, could be explained with the recruitment behavior of motor-units. The recruitment threshold appeared to depend only on the component of the external force in some specific, i.e. the "preferred", direction. In a polar plot the recruitment thresholds of motor-units appeared to fall on a straight line. Based on the size principle and on the finding that recruitment thresholds, of motor-units with different recruitment thresholds, were lying on parallel lines, we assume that the activity of the muscle and hence its EMG is always the same at recruitment of one specific motor-unit. Therefore, the EMG activity must depend also on the component of the external force in that specific direction, which must then be the same as the preferred direction found for surface EMG. For a constant external force this component varies with the cosine of the angle between the external force and the preferred direction. The changes in direction which were found in the surface EMG data for isometric contractions and movements could now be explained by corresponding changes in the orientation of the line fitted through the recruitment

thresholds

The changes in amplitude of the surface EMG data could also be explained quantitatively by the recruitment behavior of motor-units. If the recruitment threshold decreases, the amplitude of the surface EMG increases. A decreased recruitment threshold implies that for the same force more motor-units will be recruited and hence that the surface EMG activity will increase. The total changes in amplitude of surface EMG could be ascribed completely to changes in recruitment threshold as no changes were observed in firing rate of motor-units.

1.2.4 Chapter 7

The explanation of the increased surface EMG in terms of decreased recruitment thresholds, left the question unanswered why a larger number of motor-units was active in all muscles during movements than during isometric contractions against the same load. The force-velocity relationship could not be the only cause for the changes because then the opposite results would have to be found when subjects exerted forces in the same direction while moving in the opposite direction, which was not the case. A second finding, described in chapters 4 and 6, was that the preferred directions were different for movements and isometric contractions. Since the total exerted torque was the same, it must be concluded that the relative contribution to the torque in the joints from the individual muscles is different. Cocontraction by antagonistic muscles could be ruled out as an explanation for both findings because the EMG activity in antagonistic muscles was practically absent.

Quantification of the contribution of individual muscles to the total joint torque, instead of only vague qualitative descriptions, was necessary to understand these findings. Therefore, we constructed a method to derive the torque contributed by individual muscles from their EMG. The basic assumption is that the EMG-force relationship for several directions is a scaled version of the actual relationship between EMG activity and force produced by each muscle itself. Only the scaling constant has to be determined in order to estimate the relative contribution of a muscle to joint torque. Because one can calculate the total torque in a joint by inverse kinematics from force at the end effector, one obtains a relationship between the scaling constants and the total torque. If one does this for several directions and if the relative activation of the active muscles is different for forces in different directions, one can construct a set of linearly independent relations, from which these scaling constants can be determined.

This method works, but it is very sensitive to noise, so that it remains unclear whether it will be of any practical use. More robust is probably the similar method based on intramuscular recruitment data. This last method offers the opportunity

to measure the activation and hence the torque contribution from individual sub-populations of motor-units separately. This gives far more detailed insight into the coordination of muscles than possible by means of only surface EMG.

Chapter 2

The control of arm pointing movements in three dimensions

Adapted from: Miller LE, Theeuwen M, Gielen CCAM (1992) The control of arm pointing movements in three dimensions, *Experimental Brain Research* **90**, pp 415-426.

2.1 Abstract

In this study we have investigated pointing movements made with an extended arm. Despite the large number of mechanical degrees of freedom, limb orientation adopted during pointing could be described by rotation axes contained on a 2-dimensional curved surface. As a result of the curvature, the orientation of a linear plane approximating a small region of the curved surface is dependent on the location of the movements within the full workspace. These results account for earlier suggestions that limb orientation could be described by co-planar rotation vectors, and that the orientation of the plane moved with the workspace. Despite the additional complexity, our results indicate that the number of degrees of freedom used to position the forearm is reduced from 5 to 2 for normal pointing movements. Contributions to orientation of the wrist and hand by supination/pronation of the forearm were minor for changes in shoulder yaw angle. However, supination/pronation added significantly to orientation of the hand for changes in shoulder pitch angle.

2.2 Introduction

Pointing accurately to a distant, visual target is a task all of us have learned to do since childhood. It requires essentially no conscious thought, and is accomplished nearly as automatically as directing gaze at the same target. There are, in fact, several useful analogies which can be made between the control of gaze direction and pointing direction.

With the shoulder held in a fixed position, there are 5 degrees of freedom available to the upper arm and forearm. In our experiments, subjects were instructed to keep the elbow "comfortably extended", leaving 4 degrees of freedom. Pointing direction, however, is fully determined by only 2 dimensions, often expressed in terms of yaw and pitch angles. The amount of endo / exo-rotation of the shoulder, and supination / pronation of the forearm remains unspecified.

Likewise, a particular gaze direction may be achieved by an infinite number of combinations of eye and head positions. Having specified the direction of gaze, the orientation of the eye may still be controlled by cyclotorsion of the globe, or independent head movements. It has long been recognized that in the absence of head movements, when looking at targets at a fixed distance the orientation of the globe during fixation is entirely determined by the position of the eyes within the orbit [16]. That is to say, during normal eye movements, only 2 of the available 3 degrees of freedom are independently controlled. Listing's law states further, that a single reference orientation ("primary position") exists, such that all orientations of the eye during fixation may be reached from the primary position by a single rotation, the axis of which is perpendicular the original gaze direction, and the final gaze direction [36]. The observation of eye movements in violation of Listing's law during vestibular stimulation [64, 10] or during sleep [72] indicates that this law has a neural, rather than a mechanical basis.

The orientation of 3 dimensional rotational systems may be expressed in terms of the sequence of 3 rotations about arbitrary axes which are necessary to move from a reference orientation to a particular orientation. This system is often adopted for objects like the eye or arm, which have a well defined "direction". Two rotations (e.g. pitch and yaw) will specify the direction, followed by a rotation (torsion) around the axis in this direction. However, the final orientation is dependent on the sequence in which these rotations are applied.

This limitation is avoided if orientation is instead expressed by the axis and angle necessary to move from the reference orientation to the particular orientation by a single rotation. Use of a 3 dimensional rotation vector to specify the necessary rotation allows a convenient statement of Listing's law: All allowable orientations may be reached by a rotation from primary position with a axis of rotation lying in a

plane perpendicular to the line of sight in primary position. Adopting primary position as the reference orientation provides a system in which normal eye movements are accomplished with no torsion. Rotation vectors falling outside of this plane would correspond to orientations having non-zero torsion.

Experiments have recently been undertaken to examine the orientation of the upper limb during pointing and grasping tasks. In these experiments, the rotation vectors necessary to bring the arm from primary position to the pointing direction were calculated. Despite the large range of movement available by endo / exo-rotation of the shoulder, the rotation vectors describing upper arm orientation were reasonably well restricted to a plane [41, 91, 92]. Similar results were reported of the forearm [49]. However, a significant difference between these results and those of the eye movement system was the fact that for the arm or forearm, the orientation of this "rotation plane" and its primary direction depended on the location of the workspace with respect to the body. The dependence was such that when the center of the workspace was moved within the horizontal plane, primary direction moved in the same direction, but through a slightly smaller angle. One could assume that a single, continuous sequence of movements includes only orientations described by co-planar rotation vectors. For workspaces in varied locations, the orientation of this plane would be adjusted accordingly.

We have considered an alternative explanation for these results. Namely that the rotation planes calculated for any given restricted region of the physiological range represent only local, linear approximations of a larger, curved rotation surface. The extent and nature of the curvature might be such that it would not be obvious from the relatively small workspaces considered previously. Such a system would still have the effect of reducing the number of independent degrees of freedom of the system from 4 to 2. It is of interest to know how the brain specifies this torsional component of the movement. If regular rules can be recognized, they may be expected to lend valuable insight into the organization of the movement control systems. To the extent that there exist differences between the rotations surfaces for eye and arm, models of these interacting control systems may be significantly affected.

2.3 Methods

2.3.1 Experimental set-up

During these experiments, the orientation of the right forearm and upper arm was measured during natural pointing movements with the extended arm. Data were collected from 7 volunteers, 5 male and 2 female, ranging in age from 22 to 38 years. None had any known history of neurological or musculoskeletal disorders. All subjects

were seated in a high backed chair. Two straps were attached to the chair at shoulder height, which crossed the subject's body to fixation points on the opposite sides of the chair at hip height. We took care of allowing free rotation of the shoulder joint in all directions, while minimizing movements of both the trunk and shoulder girdle.

The positions and orientations of the upper arm and forearm were measured with a 2 camera opto-electronic system (WatSmart, manufactured by Northern Digital Inc.) capable of tracking the position in 3 dimensions of infra-red emitting diodes (IRED's). In order to increase the angle of radiation, we used clusters of 3 diodes, each oriented in mutually orthogonal directions. A cluster was attached to each of the 4 tips of a lightweight cross which was fastened to the upper arm just proximal to the elbow using a thin metal band and elastic straps. A similar cross was attached to the forearm using a bracelet placed just proximal to the wrist. The bracelet was made to fit tightly but comfortably by forming a mold of elastic dental compound between the bracelet and wrist of each subject. The vector from the proximal to the distal cluster of diodes on each cross was aligned with the corresponding limb segment and determined the "pointing direction" of the segment. Any set of 3 clusters was sufficient to determine the position and orientation of the joint. The fourth redundant cluster improved the estimates, and allowed the calculations to be made even if any single cluster was not visible to both cameras. The position of each cluster was sampled at a frequency of 100 Hz. Special care was taken of minimizing reflections. Infrared absorbing curtains were hung around the entire workspace, and other surfaces were painted with infra-red absorbing paint wherever possible.

This system allowed us to record relatively unrestricted movements within most of the natural physiological range. In the vertical (pitch) direction, the workspace ranged from approximately 45 degrees below to 45 degrees above the horizontal plane at shoulder height. In the horizontal (yaw) direction, the full workspace ranged from -90 degrees (toward the right) to +15 degrees, where 0 degrees pointed forward. This full workspace was divided into 9 small workspaces, each 30 by 35 degrees. We referred to these individual small workspaces by the numbers indicated in figure 2.1. Sixteen light emitting diodes on vertical stands indicated the corners of these workspaces. Any particular workspace could be indicated by lighting the appropriate diodes at its corners and edges.

2.3.2 Task

In these experiments, subjects made natural self-paced pointing movements between imagined targets while the arm was held comfortably extended. A single trial consisted of a continuous series of movements within a specified workspace. Subjects were simply instructed to make pointing movements which were distributed approximately

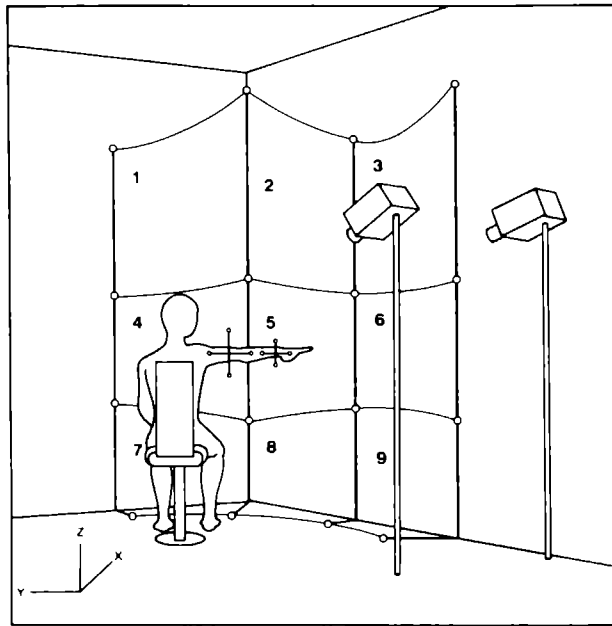


Figure 2.1: The orientation of upper arm and forearm of the subject were recorded by triangulating the positions of infrared emitting diodes on crosses attached near the elbow and wrist. The subject was instructed to point within various workspaces. These workspaces were either a single small 30×35 degree workspace (#1 - #9), a strip of 3 adjacent small workspaces, or the entire workspace. The entire workspace ranged between pitch angles of -45 to 45 degrees, and yaw angles of -90 (to the right of the subject) to $+15$ degrees.

homogeneously throughout the workspace. There were no restrictions placed on endo / exo-rotation of the shoulder or on supination / pronation of the forearm. Movements during a single trial were made within one "small" workspace, within a row or column of 3 adjacent horizontal or vertical workspaces ("strip"), or within the "full" workspace. We named the strip workspaces according to the numbers of the small workspaces of which they were composed. Shortly before each trial, the subject was informed of the location of the upcoming workspace. Several seconds later, the LEDs indicating this workspace were lit. For small and strip workspaces, subjects made pointing movements for a duration of 15 or 45 seconds, respectively. Data collection began as the subject began making movements, and continued throughout the trial. There was a pause of several seconds in-between trials and at any point the subject complained of fatigue. The particular workspace chosen for each trial

was unpredictable by the subject. During a single experiment, 35 different trials were collected, including 24 small workspaces, 10 strips, and 1 full workspace. Workspaces along the middle horizontal and vertical strips were tested most frequently.

2.3.3 Data analysis

The following data analysis was performed on each of the crosses independently. When presenting the results, we will refer to the "arm" and "forearm", which indicate the cross from which the data were collected. In this section, when referring to the general techniques, we will refer simply to the "arm", which should be understood to mean either upper arm or forearm.

At the beginning of each experiment, a standard reference orientation was determined for each cross by having the subject point to the center of the middle workspace. The orientation was expressed in Cartesian coordinates by the 3×3 matrix \mathcal{R} . The orientation of each cross was also determined throughout the movement and expressed as a second matrix, $\mathcal{A}(t)$. One can define a rotation matrix $M(t)$, by $\mathcal{A}(t) = M(t)\mathcal{R}$, such that $M(t)$, represents the orientation of the arm during movement with respect to the reference orientation, \mathcal{R} . These rotation matrices were expressed as 3-dimensional Lagally rotation vectors [35]. These vectors have a direction parallel to the axis of rotation from the reference orientation to the moving orientation. The magnitude of the vector is equal to the tangent of half the rotation angle. For small rotations, the magnitude is approximately equal to the angle in degrees divided by 100.

A consequence of Listing's law for eye movements is that these 3-dimensional rotation vectors fall on a 2-dimensional plane. A similar hypothesis has been proposed for head and arm movements within a restricted workspace [41]. Accordingly, we fitted a plane ("rotation plane") through the cloud of vectors generated by the arm movements. As a measure of the thickness of the plane and quality of fit, we calculated the root mean squared distance of the cloud of vectors from the fitted plane in a direction perpendicular to the plane.

For any arbitrary reference orientation, the orientation of the rotation plane can be defined by the vector normal to its surface. However, the direction of the rotation vectors, and therefore the orientation of the rotation plane, are dependent on this arbitrarily chosen reference. The primary position defined by Listing's law is the unique reference orientation which yields a rotation plane orthogonal to the pointing direction when the arm is in the primary position. This unique pointing direction we will refer to as "primary direction". It can be expressed either as a vector in Cartesian space, or in terms of pitch and yaw angles. Primary position and direction can be calculated from the original set of rotation vectors.

We have also devised a method for expressing the location within the full workspace of the movements for any given trial. During movements, the pointing direction vectors generate part of a spherical surface in Cartesian space which is centered on the shoulder. For movements made in different parts of the full workspace, this patch moves to different regions of the spherical surface. We refer to the normal to the plane fitted through these direction vectors as the "mean pointing direction".

The primary and mean pointing directions were calculated for the full series of movements during each trial, but also for selected portions of the data from individual trials. These portions were in fact "slices" containing only those data points having a pointing direction within specified boundaries. The slices were approximately the same size as the small workspaces. Each strip trial was divided into a number of slices by shifting a grid from left to right for horizontal strips or from top to bottom for a vertical strips. The 30 degree wide grid was shifted in overlapping 10 degree steps until the entire strip was covered.

All of the data had to meet two requirements in order to assure that the orientation of the fitted planes could be determined reliably. Cases which failed to meet either of the following criteria were rejected. In addition to calculating the thickness orthogonal to each plane, we calculated analogous measures within the plane, corresponding to "width" or "height". We required that the smallest dimension within the plane be at least 50% bigger than the thickness of the plane.

We also required that the movements be approximately homogeneously distributed throughout the workspace. As a measure of homogeneity, we divided the full workspace into a grid of 5×5 degree bins, and counted the number of pointing direction vectors which fell within each bin. We calculated the mean and standard deviation of these counts across all bins. Data were only considered for those cases in which the standard deviation of these counts was smaller than the mean.

We used several tests to determine whether tendencies were statistically significant. When comparing differences across all subjects we used Wilcoxon's Rank Sum Test. To determine whether a single estimated slope differed significantly from 0, we used a χ^2 -test. To compare whether 2 slopes differed significantly from each other we used a modified t-test. We considered differences to be significant when the test-value exceeded a confidence level of 5%.

2.4 Results

2.4.1 Determination of mean pointing and primary directions

In these experiments, subjects made self-paced movements as though pointing to various distant targets. We collected data related to the position and orientation

of the upper arm and forearm throughout these movements. Figure 2.2 contains representative data obtained during a single trial for movements within the middle horizontal #456 strip (subject SG).

The top 3 panels (A, B and C) represent the Cartesian positions of the center of the cross which was attached on the upper arm near the elbow. The 3 panels represent views from behind the subject (yielding a "front" view of the data), from the left side, and from above the subject. The axes were chosen such that the z -axis is pointing upward, the x -axis forward, and the y -axis to the left relative to the subject (see figure 2.1). In order to obtain these perspectives, some of the axes have been reversed in this and following figures. Panels A and B indicate that, as expected,

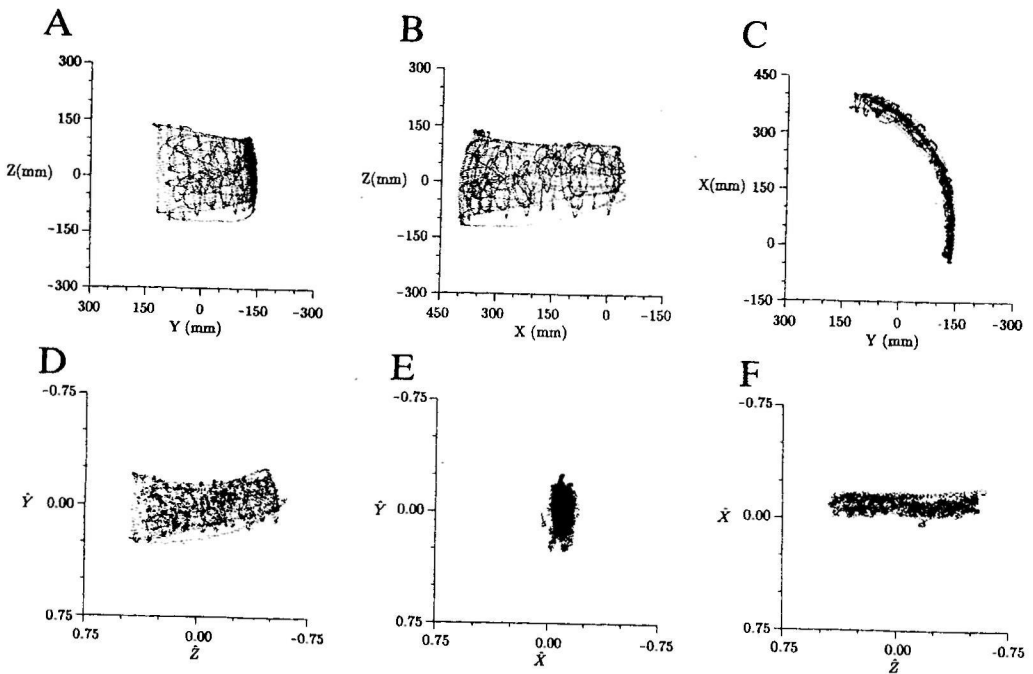


Figure 2.2: Upper arm position and orientation during a single trial. (A-C) Position of the center of the elbow cross during pointing movements within the horizontal #456 strip. Views from behind (A), from the left side (B) and from above (C) the subject. (D-F) Rotation vectors describing the orientation of the upper arm during the same trial. The vectors, shown in a front view (D), a side view (E) and a top view (F) were reasonably well approximated by a plane. The components of the vectors indicate left/right (\hat{Z}), up/down (\hat{Y}), and torsional (\hat{X}) rotations.

the movements filled the middle horizontal strip of small workspaces. Because of the relatively restricted range of the movements in the vertical direction, the view from above (panel C) clearly shows an arc projected from the spherical surface on which the cross moved. Similar data (discussed later) were collected from the forearm cross during the same movements.

The 3 panels at the bottom (D, E and F) contain rotation vectors expressing the orientation of the arm throughout the trial relative to the primary position. The \hat{z} component of these vectors represents the magnitude of the rotation of the pointing direction around the \hat{z} -axis. Rotations around this axis move the pointing direction primarily left and right. Therefore, this axis was chosen as the horizontal axis in panels D and F. Similarly, rotations around the \hat{y} -axis represent up and down movements, and it was therefore chosen as the vertical axis in panels D and E. The \hat{x} component finally, represents the amount of torsion.

The range of the \hat{z} component for the trial shown in figure 2.2 was approximately 110 degrees, equal to the full width of the horizontal workspace. The range of the \hat{x} (torsional) component on the other hand, was only about 15 degrees, and the thickness of the plane was 4.3 degrees. Considering the rotation axes to lie in a plane seems a reasonable first order approximation, given the significantly larger range of the \hat{y} and \hat{z} components.

		Upper Arm						
	Subject	CD	SG	GH	BM	LM	SM	SS
Prim. Dir WS #5	Pitch	39 1°	28 0°	5 2°	20 5°	24 2°	5 2°	23 0°
	Yaw	-38 2°	-50 5°	-57 0°	-63 4°	-41 9°	-54 9°	-74 9°
	Accuracy	4 7°	4 9°	1 9°	6 3°	6 9°	3 6°	8 4°
Thickness	Small WS	3 8° (1 2)	3 9° (0 8)	3 3° (0 8)	3 1° (0 6)	3 0° (0 5)	5 4° (1 5)	2 9° (0 6)
	Slices	4 1° (0 9)	4 4° (0 7)	4 0° (0 7)	3 8° (0 5)	3 9° (0 7)	4 6° (0 9)	3 6° (0 9)
	Strips	4 7° (0 8)	5 3° (0 8)	4 5° (0 9)	4 2° (0 6)	4 3° (0 7)	6 9° (1 2)	4 2° (0 8)
Yaw Slopes	Small WS	0 79 (0 20)	0 54 (0 08)	0 81 (0 16)	0 76 (0 17)	0 53 (0 05)	3 79 (1 79)	0 15 (0 19)
	Slices	0 91 (0 39)	0 47 (0 09)	0 63 (0 24)	0 62 (0 11)	0 45 (0 12)	=	-0 08 (0 12)
	Pitch Slopes	0 53 (0 14)	-0 25 (0 20)	-0 23 (0 15)	0 03 (0 16)	0 23 (0 16)	-0 02 (0 18)	0 15 (0 14)
Pitch Slopes	Small WS	-0 40 (0 08)	0 12 (0 08)	0 19 (0 07)	0 12 (0 11)	-0 08 (0 10)	=	0 14 (0 14)
	Slices							
	Strips							
		Forearm						
Prim. Dir WS #5	Pitch	22 3°	16 3°	6 9°	12 7°	12 7°	14 3°	-46 1°
	Yaw	-15 7°	-40 0°	-40 1°	51 2°	-35 8°	-42 9°	55 6°
	Accuracy	9 4°	5 3°	4 7°	1 7°	5 2°	3 0°	10 7°
Thickness	Small WS	6 0° (2 0)	4 6° (0 8)	4 2° (1 1)	5 0° (0 8)	4 4° (0 8)	7 0° (0 7)	4 0° (0 8)
	Slices	5 2° (0 7)	5 4° (0 6)	4 5° (0 8)	4 9° (0 8)	5 0° (0 7)	6 0° (0 0)	4 2° (0 8)
	Strips	6 8° (1 3)	6 9° (1 0)	5 7° (1 2)	6 8° (1 0)	6 1° (0 7)	2 6° (1 0)	5 8° (1 2)
Yaw Slopes	Small WS	0 52 (0 34)	0 55 (0 10)	0 78 (0 12)	0 73 (0 12)	0 30 (0 13)	=	0 12 (0 14)
	Slices	=	0 75 (0 20)	0 68 (0 36)	0 96 (0 07)	0 02 (0 06)	=	0 28 (0 14)
	Pitch Slopes	0 58 (0 30)	-0 14 (0 15)	-0 33 (0 18)	0 44 (0 07)	0 00 (0 14)	=	0 26 (0 27)
Pitch Slopes	Small WS	-1 09 (0 33)	-0 41 (0 05)	0 58 (0 24)	=	-0 30 (0 12)	=	-0 23 (0 15)
	Slices							
	Strips							

Table 2.1: Upper arm and forearm data for all seven subjects. "Prim. Dir WS #5": Mean primary direction of workspace #5. "Accuracy": Standard deviation of the angles between estimates of primary direction for several trials. "Thickness": RMS distance of vectors from fitted rotation plane. "Yaw Slopes": Slope and standard deviation of the relationship between primary and mean pointing direction yaw. "Pitch Slopes": Equivalent pitch angle measures. An * indicates there was insufficient data meeting all criteria (methods).

The orientation of the rotation plane, in figure 2 2, expressed by the primary direction vector was $(0.66, -0.68, 0.31)$. This corresponds to a pitch of 18 degrees and a yaw of -46 degrees. For each subject, primary direction was calculated for 4 separate trials which had movements restricted to the central workspace #5. From these 4 estimates, we calculated a mean vector and the angles between this mean and each of the 4 estimates. The standard deviation of these 4 angles gave a measure of the variability of primary direction for different trials. For the subject shown in figure 2 2, this variability was 4.9 degrees. These numbers are summarized for all subjects in table 2 1.

The location of the movements during a single trial was expressed by the mean pointing direction. For the trial shown in figure 2 2, the mean pointing direction was given by a pitch of 6 degrees and a yaw of -48 degrees. The variability of the mean pointing direction for repeated trials was typically less than that of the primary direction. For this subject, for the 4 trials with workspace #5, it was equal to 0.5 degrees.

2.4.2 Dependence of primary direction on mean pointing direction

Throughout a single experiment, subjects made movements within a variety of restricted regions of the full workspace.

Figure 2 3 consists of the rotation vectors belonging to 2 different trials. The movements during the 2 trials were within separate regions of the horizontal #456 strip shown in figure 2 2, and were actually collected during the same experiment.

Panels A - C show rotation vectors representing movements made within the small central workspace #5, while panels D - F represent movements made in the right adjacent workspace #6. The range of the vertical and torsional components of the movements in workspace #5 was comparable to that of workspace #6 (panels B and E respectively). However, the horizontal components of the latter movements were shifted towards the right in the $-\hat{z}$ direction (panels C and F). The mean pointing directions had yaws of -44 and -77 degrees respectively, a shift of 33 degrees. This agreed closely with the 35 degree angle between workspaces in the experimental set-up.

The primary directions for these trials had yaws of -46 and -57 degrees for workspace #5 and #6 respectively, a shift of 11 degrees towards the right. The data thus suggested a dependence of primary direction on the location of the workspace. This observation was consistent with other trials in workspaces #4, #5 and #6 for the same subject, which had primary directions that shifted progressively to the right. This finding was a general phenomenon among all subjects. The dependence

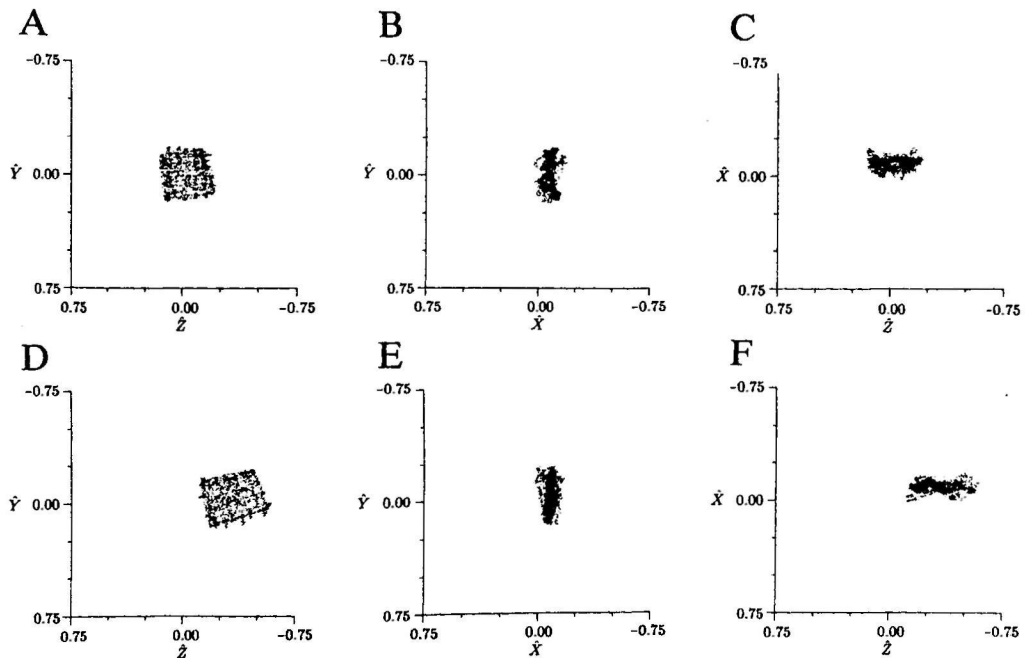


Figure 2.3: Rotation vectors for trials within the small workspaces #5 (A-C) and #6 (D-F). The rightward shift of rotation vectors from workspace #5 to #6 reflected a similar shift of primary direction. The mean pointing direction shifted 33 degrees, which corresponds to the 35 degree angle between the workspaces. The planes for each of these trials were significantly thinner than the plane for the #456 strip (fig 2.2E, 2.2F).

of primary direction on mean pointing direction could be described in a first order approximation by a line. The slopes of these lines together with their standard deviations are listed for all subjects in table 2.1.

The plane fitted to the strip workspace was thicker than that of either small workspace (4.3 versus 3.7 and 3.5 degrees for workspaces #5 and #6, respectively). The average thicknesses of all small and strip workspaces for this subject were 3.4 ± 0.8 degrees and 4.6 ± 0.7 degrees. The greater thickness of strips compared to small workspace trials was a consistent finding for all subjects.

2.4.3 Variation of primary direction during movement

The data presented so far suggest that the primary direction is dependent on the location of the workspace for different trials. These results are consistent with earlier

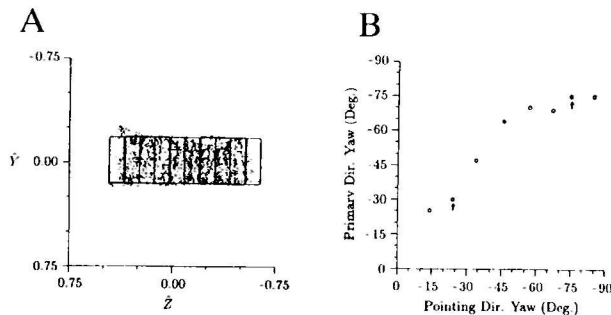


Figure 2.4: (A) Front view of the plane of rotation vectors within the #456 strip which has been divided into overlapping "slices". We calculated primary direction and mean pointing direction for the rotation vectors within each slice. (B) Primary direction yaw as a function of mean pointing direction yaw for each slice. Data points belonging to the two slices indicated by heavy boxes in (A) are marked by arrows. Primary direction yaw clearly depends on pointing direction yaw, even for slices taken from a single continuous movement.

reports [41, 91, 92, 49], which described a rotation plane, the orientation of which was adjusted for movements within different workspaces. Alternatively, the rotation plane might actually be curved. Any local estimate of primary direction would be dependent on the shape of the rotation surface in the region in which the estimate was made. This model would also account for the larger thickness measured for the strip workspaces relative to the small workspaces.

To discriminate between these hypotheses, we divided data from strip workspaces into slices with approximately the same size as a small workspace. We used overlapping slices with centers 10 degrees apart along the length of a strip. Examples of slices from the horizontal #456 strip are given in figure 2.4A. Primary direction and mean pointing direction were calculated for the data points within each slice.

Figure 2.4B shows the yaw of the primary direction of these slices as a function of the yaw of the mean pointing direction. The two symbols indicated by arrows in panel B correspond to the two slices highlighted in panel A. Figure 2.4B indicates that there was a clear relationship between mean pointing direction and primary direction among all the slices from this trial. This means that in the horizontal plane at shoulder height, primary direction of the slices changed with shoulder joint angle. The fact that the primary direction differed for different regions of the workspace during the continuous movements of a single trial means that the rotation vectors for this trial can not be adequately described by a plane. If the rotation vectors actually fell on a plane as stipulated by Listing's law, the primary direction would have been

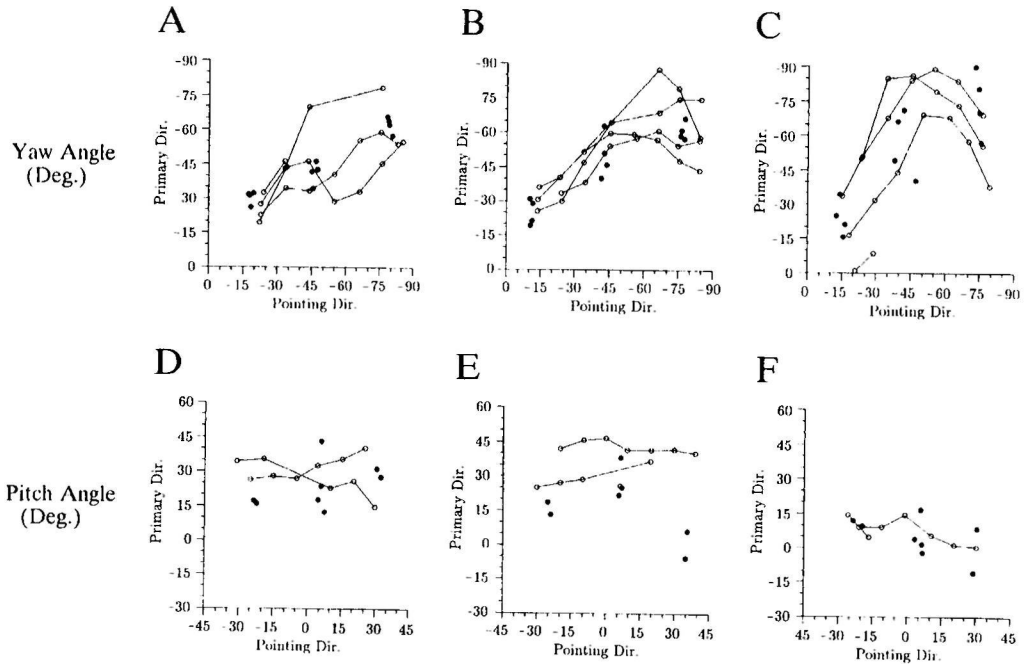


Figure 2.5: Relationship between primary direction and mean pointing direction for three subjects for small workspace trials (filled circles) and slices (open circles). Points belonging to slices from a single trial are connected. (A-C) Yaw angle relationship, (D-F) pitch angle. The small workspace trials generally fell in the same range as did the slices. In all cases, primary direction yaw increased with increased pointing direction yaw. The pitch angle relations had either zero or slightly negative slope. This indicates the rotation surface must be curved.

independent of the region of the workspace.

Figure 2.5 shows examples of the dependence of primary direction on mean pointing direction for 3 subjects (from left to right: LM, SG, GH). In panels A-C the yaw component of the primary direction is plotted as a function of the yaw component of the mean pointing direction for slices (open circles) and small workspace trials (filled circles). Points belonging to slices from a single trial are connected by lines. In panels D-F, the corresponding pitch angle relationships for the vertical #258 strips are plotted for the same subjects. In some cases there are different numbers of data points plotted for the slices from different corresponding trials (e.g. panels E and F). This occurred when data from some slices were rejected when the fitted plane failed to meet the criteria described in the methods.

In the yaw direction, there was a positive relation between primary direction and mean pointing direction for all subjects. However, in the pitch direction, most slopes did not appear to differ significantly from 0. In most cases, for both pitch and yaw, the relation between primary direction and mean pointing direction for the small workspace trials appeared to be the same as that for the slices. One exception, however, is apparent in panel E.

To evaluate these comparisons quantitatively, we fitted lines through the data points for both trials and slices and calculated slopes and standard deviations. We used a χ^2 -test to determine whether the slope of a line differed significantly from 0, and a modified t-test to determine whether the slopes of two lines differed significantly. Most subjects had a significant dependence of primary direction yaw on mean pointing direction yaw. For the data from small workspace trials, 6 of 7 subjects had slopes significantly different from (greater than) 0. For slices, 5 of 6 subjects had slopes significantly different from (greater than) 0. One subject had insufficient slices which met the criteria to calculate meaningful slopes. In no individual case, nor across the population was there a significant difference between the data from slices and from small workspace trials with respect to the 5% significance level. This indicates that the movement of primary direction for different workspaces reflects the non-linear curvature of a 2-dimensional rotation surface rather than a flat plane. Therefore the application of Listing's law to movements of the upper arm is not appropriate.

Unlike the significant positive correlation between the yaw component of primary direction and mean pointing direction, the corresponding pitch relations were less consistent. For most subjects the slopes were generally close to zero. One of 7 subjects had a significant non-zero (positive) slope for the small workspace trials. Two of 6 subjects had significant non-zero (negative) slopes for slices. For 1 subject the relations for slice data had slopes which were significantly more negative than those from small workspace trials. This difference was not significant across the whole set of subjects. Table 2.1 contains the slope and standard deviation data for all subjects.

Several of the relations in figure 2.5 appear to be non-linear. The amount of this curvature differed for different subjects, progressively increasing for the subjects represented in panels A through C. This figure also contains several examples in which the relation between primary direction and mean pointing direction differed for different trials. In some cases, the curves for different trials were parallel, perhaps as the result of offsets in initial torsion (panel C). However, in other cases, the lines connecting slices of different trials crossed each other (panel D).

We have described above that the rotation surfaces for strips were generally thicker than those of small workspaces. We also found that the thickness of the slices

typically fell between that of the small and strip workspaces. We applied statistical tests between each of these groups, and found the differences to be significant across all subjects. There was somewhat less difference between slices and small workspaces than there was between slices and strips.

2.4.4 Comparison of forearm and upper arm orientation

The data presented so far concerned the orientation of the upper arm. We also recorded data representing forearm orientation during these movements. The same kinds of analyses described above have been applied to these data. In most respects, the data from the forearm qualitatively resembled those of the upper arm. Table 2.1 lists the mean primary direction, and plane thickness for forearm and arm, for each subject.

For forearm data in the yaw direction, 4 of 6 subjects had a significant positive relation between primary direction and mean pointing direction for data from the small workspace trials. Significant positive relations occurred for 3 of 5 subjects for data from slices. Tests of the similarity between small workspace and slice data yielded no differences for individual subjects, nor across all subjects. In the pitch direction, 1 of 6 subjects had a significant positive slope for data from the small workspace trials. There were 2 of 5 cases with non-zero (both negative) slopes for data from slices. There was a significant difference between slices and trials for only 1 subject. Because of similar trends among the other subjects, the difference between trials and slices was significant across the population. Therefore for the forearm as well as the upper arm, the rotation vectors describing orientation with respect to primary direction are not confined to a flat plane. For the forearm, there is some evidence that the curvature of the rotation surface is somewhat greater for long, vertically oriented workspaces than it is for a series of small workspaces covering the same range.

We also applied statistical tests to compare the curvature of the arm and forearm rotation surfaces directly. There was no difference between arm and forearm in the relation between primary direction and mean pointing direction and forearm for the data from small workspaces. There were significant differences within the slice data, however. In the yaw direction, 4 of 5 subjects had a larger slope for forearm than for arm, but only 1 case was statistically significant. Across all subjects, this trend was not significant. In the direction plane, the forearm slopes of all subjects were more negative than the upper arm, 1 of which was significant. Across all subjects, this trend was significant. The slightly greater forearm slope for the vertical strips indicates that the rotation surface, at least for this particular workspace, was more greatly curved for the forearm than for the arm.

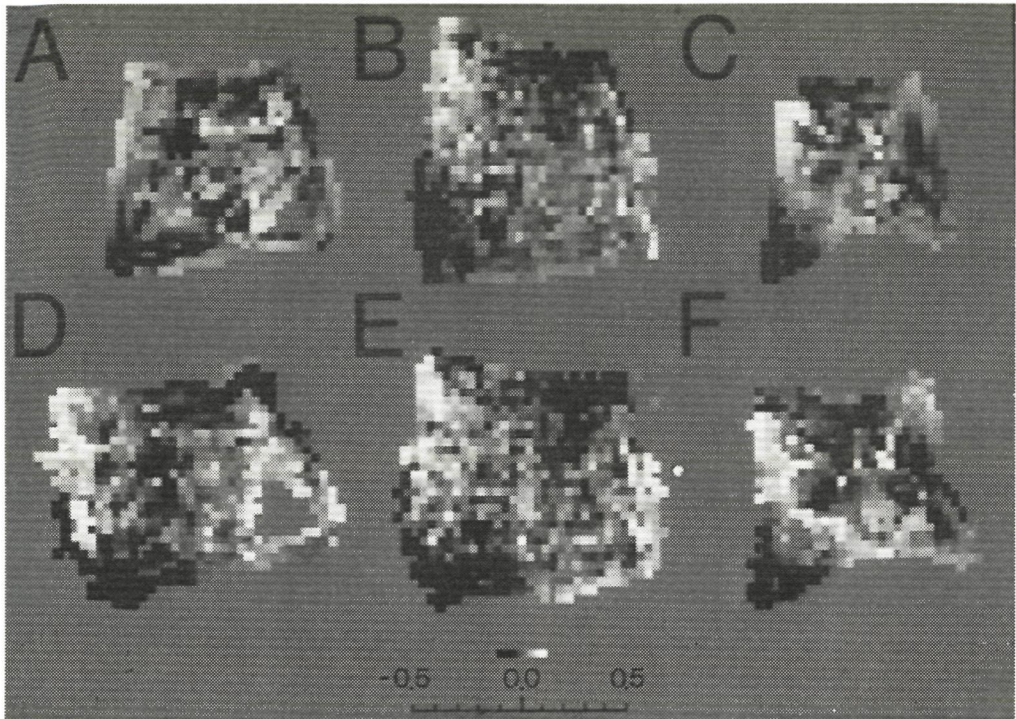


Figure 2.6: Shape of the "rotation surfaces" for upper arm and forearm. Rotation vector components on the horizontal and vertical axes represent left/right and up/down movements respectively as in figures 2.3A and 2.3D. The torsional components are indicated by the grey level. (A-C) Upper arm rotation surfaces for 3 subjects for movements of a single trial throughout the entire workspace. (D-F) Forearm plots for same trials. The light colored upper/left and lower/right corners, indicate positive torsion, remaining corners have negative torsion. Forearm had qualitatively the same shape as the upper arm, although in some cases the curvature was somewhat greater, indicating that supination / pronation added to the torsion of the upper arm.

In general, the thickness of the planes fitted to the rotation vectors for the forearm were significantly greater than those for the upper arm. As for the upper arm, the planes for trials and slices were both significantly thinner than were those of strips. However, there was no difference between trials and slices. For the forearm, the global averages for all subjects were 5.0 ± 1.1 degrees, 5.0 ± 0.6 degrees and 6.8 ± 1.3 degrees for small workspace trials, slices and strips, respectively.

We have demonstrated that a single rotation plane with a global primary direc-

tion does not adequately describe either arm or forearm orientation during pointing movements. Therefore we have adopted an alternative means by which to display the rotation vectors describing the orientation of the upper arm and forearm.

Figure 2.6 shows several examples of these plots. In each panel, the \hat{z} and \hat{y} components are displayed in the same coordinate system and with the same conventions used earlier for figures 2.2D, 2.3A, and 2.3D. In addition, we have used a grey-scale to express the \hat{x} , or torsional component of the rotation vectors. Rather than plot each rotation vector, the average torsion has been calculated for all the points within 5 degree wide bins, and this average value has been plotted. The scale at the bottom of the figure indicates the size of the individual components of the rotation vectors. This scale ranges from -0.5 to 0.5, approximately 100 degrees. The grey-scale bar above it is plotted on the same scale in order to quantify the torsional component. Pure white and black pixels represent \hat{x} components of approximately +0.12 and -0.12 respectively.

The top 3 panels in figure 2.6 represent the rotation surfaces of the upper arm for the 3 subjects displayed in figure 2.5. Panels D-F display the corresponding forearm rotation surfaces. In this format it is easy to see the relation between the arm and forearm rotation surfaces. For each subject, the shape of the upper arm rotation surface was quite similar to that of the forearm. In addition, for the middle and right columns of panels, the magnitude of curvature for the forearm was nearly identical to that of the arm. The similar amount of curvature for forearm and upper arm indicates that relatively little supination / pronation was used by these 2 subjects. On the other hand, the forearm rotation surface in panel D appears to have greater curvature than its upper arm counterpart does in panel A. For this subject, supination / pronation added to the upper arm torsion, but did not qualitatively alter the shape of the rotation surface.

2.5 Discussion

We have presented results demonstrating that "Listing's law type models" of arm pointing movements are at best, a rough approximation of the orientation of forearm and upper arm. The fixed-axis coordinate system based on a primary direction is useful to express limb torsion, but the resulting rotation vectors are not confined to a flat plane. The rotation vectors corresponding to certain regions of the workspace deviated systematically from a plane, such that a curved, 2 dimensional surface is required to describe all the orientations adequately. Although differing from Listing's law for the eye, these results indicate that a significant constraint does exist on the orientation of the limb which is adopted during pointing. However, there were also

apparently random variations in limb torsion. These consisted of orientations which did not fall along the curved surface, and corresponded to violations of Donders' law for eye movements. These two types of deviations from the linear model will be discussed below.

2.5.1 Nature of the 2-dimensional rotation surface

Despite the higher order complexities, it is possible to make useful comparisons with the linear approximations reported by several other authors. We find our results to be largely in agreement with these earlier reports. In experiments using magnetic search coils to measure arm pointing movements, the primary direction for small workspaces centered approximately in the middle of the physiological range was slightly above and to the right of the center of the workspace. When the workspace was moved from left to right with respect to the body, primary direction tended to remain workspace centered. [49, 91, 92].

However, we did not find such a large or reliable dependence of primary direction on workspace in the vertical direction. Most slopes were slightly negative or not different from zero. We also found the thickness of the planes generated during movements along a strip of 3 adjacent workspaces to be significantly greater than that of the small workspaces. We found that local estimates of primary direction for small regions of the workspace varied during a single trial in approximately the same manner as during separate trials. This could only happen if the rotation vectors for the large workspaces did not lie in a flat plane, but instead were curved in the fashion predicted by the movement of the primary direction of the small workspaces. This model also predicts the greater thickness of the strip workspaces, which would result as the deviations from the linear plane increase in magnitude with increasingly large workspaces.

The primary direction determined by a local, linear approximation of the actual rotation surface moved with the mean pointing direction in some regions of the workspace. Elsewhere it moved opposite to the mean pointing direction, and in other regions, there appeared to be no relation between the two. Furthermore, in many cases, the relation was clearly non-linear, often sigmoidal, and occasionally not monotonic. As a result, it is not possible to make a simple prediction of the relation between primary direction and mean pointing direction.

In fact, the relationships between primary direction and mean pointing direction shown in figure 2.5 can be derived from plots like figure 2.6. From figure 2.6, estimates can be made of the normal to the rotation surface at any point. The normal approximately bisects the angle between primary direction and the fixed reference pointing direction [35]. As a result, the primary direction behaves qualitatively as

does the normal. The yaw component of the primary direction depends on the \hat{x} and the \hat{y} components of the rotation vectors. At any point on the rotation surface, the yaw of the primary direction is determined by the magnitude of the torsional gradient in the vertical direction. If the torsional gradient is zero then points immediately above and below one another will have the same grey-values, and the normal will point in the direction of the \hat{x} -axis. Increased brightness gradient along the vertical axis indicates an increased $-\hat{y}$ component in the normal. This is equivalent to the increasingly negative yaw of the primary direction. Similar arguments can be made for the pitch component of primary direction, and the horizontal torsional gradient.

Given these results, we would argue that the concept of a primary direction which depends on the mean pointing direction is not a useful one. A map of spatially averaged torsion throughout the entire workspace is a much simpler means of summarizing the equivalent information. For most subjects, the rotation surface had qualitatively the shape which would result from twisting a plane along its vertical axis. With this shape, a relatively large twist can be completely obscured by noise when the surface is viewed "edge-on" as in figures 2.2 and 2.3. This is particularly true for movements within a restricted portion of the workspace. As this kind of plot has also been used for studying eye movements [99, 100], a careful investigation of those data might well be warranted.

One familiar system which generates a similar curved surface is the Fick gimbal. A telescope mount is a particular example, in which rotations occur around an earth-fixed vertical axis and a horizontal axis which depends on the amount of rotation around the vertical axis. The image of a horizontal line (e.g. the horizon) will always have the same orientation within the telescope. If arm movements would occur in an analogous fashion, a horizontal line through the hand would remain horizontal for all pointing directions. The rotation surface of a Fick gimbal has zero torsion along the horizontal and vertical meridians. The upper left and lower right corners have positive torsion, while the lower left and upper right have negative torsion. As a result, the yaw component of primary direction for small workspaces along the horizontal meridian moves with the mean pointing direction with a slope of 1.0, while the pitch component moves with a slope of -1.0 along the vertical meridian.

Quantitatively, the arm actually had a rotation surface with curvature between that of a Fick gimbal and a Listing plane. Throughout the mid-range of yaw movements for most subjects, the Fick model was a reasonable approximation of upper arm and forearm orientation. There were, however, frequent departures from a smoothly curved surface. Deviations from this model were most pronounced near the physiological limits of movement in the yaw direction, and for most pitch direction movements, especially for the upper arm. Differences between yaw and pitch may be due to the relatively complicated mechanics for vertical arm movements resulting from the nec-

essary coupling between the humerus and scapula. Likewise, the non-linear effects near the yaw limits may result from bio-mechanical constraints.

2.5.2 Relation Between Upper Arm and Forearm

Unlike earlier studies, we have measured both upper arm and forearm orientation simultaneously. This has allowed us to make a direct comparison of the movements of the two limb segments. We found the mean thickness of the rotation planes for the upper arm within the small workspaces to be 3.6 degrees. This was somewhat greater than that reported by Straumann and colleagues [91, 92], who considered only workspaces located at shoulder height. Forearm planes were somewhat thicker than those of the upper arm, with an average value of approximately 5.0 degrees, slightly less than that measured by Hore et al. [49].

In general, the shape of the forearm rotation surface was qualitatively the same as that of the upper arm. To some extent, these changes in torsion, which were measured at the wrist, were distributed across both forearm and upper arm. However, the contribution of supination / pronation to forearm torsion was generally smaller than that of endo / exo-rotation. Across all subjects, the functional dependence of forearm torsion on mean pointing direction differed statistically from that of upper arm torsion only for slices from the vertical strips. Hence in general, only for the large, vertical movements did supination / pronation add significantly to the torsion produced by endo / exo-rotation of the upper arm.

2.5.3 Departures From the 2-Dimensional Surface

While the general shape of the rotation surface appeared to be well conserved even between different subjects, there was evidence that the details of the shape varied under a variety of conditions. Figure 2.5 contains examples in which the slices taken from repeated trials formed crossing curves, or parallel curves separated by an offset. Panel E shows an example in the pitch direction in which the slices appear to differ systematically from the trials. There may also be such a tendency in the data shown in panel C as well. The differences between the shape of the large workspace (which was analysed with the slices) and the individual small workspaces reached significance only for the forearm during vertical movements. However, these statistics were calculated using a linear model. Many of these relations appeared to be significantly non-linear. It is possible that non-linear models applied to the two populations would reduce the standard deviation of each fitted curve to the extent that more of the differences between curves would become significant.

To the extent that these examples represent varied torsion for a given mean

pointing direction, they correspond to violations of a law analogous to Donders' law. Each of these graphs, however, show the relation between primary direction and mean pointing direction along a single axis. It is apparent from figure 2.6 that there is a complex dependence of these relations in the yaw direction with the mean pitch values and vice versa. Significant variation between trials in the unplotted value might account for some of the variation in slopes.

Another source of variation may have been changes in experimental conditions of which we were unaware. For example, we made no attempt to constrain the initial orientation of the hand prior to the trial. Hepp et al. [41] reported significant variation in arm torsion following a pointing movement to a fixed target when the movement was begun from varied extreme initial positions. An initial extreme torsion might be expected to add an offset throughout the trial, or an initial offset which was progressively compensated throughout the trial. More careful control of these variables might reduce the amount of these apparently random variations.

While the relation between primary direction and mean pointing direction determined from slices was generally not different from that of small workspace trials, the thickness of these planes did vary systematically. The slices were typically thicker despite the fact that they were taken from a slightly smaller region of the workspace than the typical small workspace trial. This difference might reflect hysteresis which was significant during movements throughout the large workspace, but had little effect within the small workspaces. Alternatively, it could be the result of the higher average speed of the movements throughout the long strips rather than the size per se. In addition, most of the slices from a given strip did not have edge effects related to reversal of direction at the borders of the small workspaces.

2.5.4 Implications for neural control

There are two common teleological explanations for the origin of Listing's law for the eye. One is sensory in nature, having to do with achieving orientations of the eye which minimize changes in orientation of objects on the retina for all possible eye positions. [36] The other is motor in nature, and suggests that the restriction of eye movements to two degrees of freedom is advantageous in that it simplifies the necessary control system. Recently it has been suggested that during pointing to a visual target, gaze, head and arm all move within parallel, 2-dimensional rotation spaces, and that the primary direction for each of these systems moves in the yaw direction approximately with the center of the workspace [41, 92]. This would effectively reduce the 9 degree of freedom system to the 2 dimensions necessary to specify the direction to the visual target. Our results for the arm movement system are consistent with these earlier results, but demonstrate additional complexities in

the system as well

We have shown that the rotation space for the arm is not actually linear, but rather a curved surface in 2 dimensions. Our preliminary studies on 3 subjects indicate that the rotation surface for the head is qualitatively similar to that of the arm. It is likely that these 3 systems, gaze, head, and arm, all move on similarly curved rotation surfaces. If this is true, then the planar surface generally reported for the rotation vectors of the eye in head is unlikely to have a sensory basis. Generally humans make large gaze shifts with a combination of eye and head movements. Any visual advantages conferred by a flat rotation surface would be lost for gaze movements requiring head movements along a curved surface. Instead the restricted geometry of eye movements is more likely the result of simplified motor control strategies. Similar advantages probably explain why arm orientation during pointing is also approximately constrained to a (curved) 2 dimensional surface.

The relation between movement direction and neuronal activity has been the topic of considerable study both during horizontal planar movements [23, 58] and movements in 3 dimensions [25]. Many neurons in the proximal arm region of motor cortex have direction- dependent activity during the interval prior to and during arm extension. The preferred direction of individual neurons was also found to depend on the location of the workspace. When examined at the population level, preferred directions tended to move with the center of the workspace albeit with a slope somewhat less than 1.0 [5]. However, for particular neurons, there was considerable variation in the slope of this relation. Occasionally the movement of primary direction was opposite that of the workspace location. There is a striking similarity between this description of the dependence of preferred direction on workspace location, and our description of the dependence of torsion on mean pointing direction. However, neither that study or any other has considered possible torsional components related to cell firing rate. It would be worth examining whether a significant amount of the unaccounted variability in firing rate might be related to torsional movements of the monkey's limb.

Our results have demonstrated that even during a simple pointing task, the control of arm orientation is significantly more complicated than the simple model of Listing's law applied to eye movements. Even a description of a primary direction which moves with the workspace is not adequate. Rather, we must consider a curved 2-dimensional rotation surface to describe the limb orientation during movement. The shape of the surface suggests there is some tendency among all subjects to keep the hand level, although not to the extent of a Fick gimbal system. In general, the required torsion occurred primarily as a result of endo / exo-rotation of the shoulder. However, for long, vertical workspaces, shoulder rotation was relatively restricted, and most subjects made additional supination / pronation movements.

2.6 Acknowledgements

We are grateful for many interesting and stimulating discussions with Klaus Hepp, Dominik Straumann and Jan van Gisbergen.

Chapter 3

Are the orientations of head and arm related during pointing movements ?

Adapted from: Theeuwes M, Miller LE, Gielen CCAM (1993) Are the orientations of head and arm related during pointing movements ?, *J Motor Behaviour* 90, pp 242-250

3.1 Abstract

The head, eye and shoulder are each free to rotate around three mutually orthogonal axes. These three degrees of freedom allow a given gaze or pointing direction of the eye, head or arm to be obtained in many different possible orientations. Unlike translations in 3 dimensions, 3 dimensional rotations are non-commutative. Therefore, the orientation of a rigid body following sequential rotations about 2 different axes depends on the order of the rotations.

In this paper we demonstrate that only 2 degrees of freedom are used during orienting movements of the head and pointing movements of the arm. This provides a unique orientation of head and arm for each gaze or pointing direction despite the non-commutativity of 3 dimensional rotations. This observation is in itself not new. However, we found that 1: the 2-dimensional "rotation surface", which describes the orientation of the head for all gaze directions, is curved, unlike the analogous flat plane for the eye. 2: The rotation surface for the head is curved differently from that for the arm. This result argues against the hypothesis that the orientations of head and arm are directly coupled during pointing. It also implies that the orientation of

the eye in space during gaze shifts of the eye and head is not uniquely determined for a given direction of gaze. This finding argues against a perceptual basis for the reduction of rotational degrees of freedom.

3.2 Introduction

Most biological limbs have numerous degrees of freedom available for controlling movement. This flexibility originates from multiple joints, each often having multiple rotational degrees of freedom, and from the number of muscles crossing each joint. Some parts of the body (such as the upper arm, head, and eye) can rotate about three mutually orthogonal axes. As a consequence, the pointing direction of the arm or gaze direction of the eye and head does not fully specify the orientation of the respective part of the body. The situation is complicated by the fact that rotations in 3 dimensions are not commutative (see Appendix). Therefore the orientation of an object following sequential rotations along different rotation axes depends on the order of the rotations. Beyond complicating the control system, one can easily devise circumstances in which the eye, head or arm would end up in unphysiological orientations. Perhaps to avoid these complications, the eyes, head and hand are constrained to orientations which are determined during pointing movements by the two dimensions of the gaze or pointing direction.

For the oculomotor system this problem has been recognized long ago. It was Donders [17] who noticed that the orientation of the eye did not depend on the trajectory that brought the eye into a particular position. The quantitative relation between eye orientation and gaze direction during fixation [36] and saccadic eye movements, [99, 100] has been expressed as Listing's law. It states that all orientations of the eye may be reached with an axis of rotation lying in a plane perpendicular to the gaze direction when the eye is in "primary position". It is possible to calculate the primary position from measurements of the orientation of the eye during a sequence of eye movements. The effect is to reduce the number of degrees of freedom from 3 to 2 such that the orientation of the eye depends only on fixation direction.

Recently, this problem has also been investigated for the arm and head. In these studies a plane was fitted to the rotation vectors (see Appendix) describing the arm and head orientations during pointing movements. However, for data from the upper arm [41, 40], forearm [50], and head [10, 92], the orientation of the fitted plane changed with its location in the workspace. Primary direction calculated from the planes for gaze, arm, and forearm moved in the horizontal direction approximately with the center of the workspace. This was interpreted as evidence that rotations about these three different body parts may be coupled during visually guided move-

ments [92]. A similar orientation of eye, head and hand might be advantageous in visuo-motor tasks [41]. Alternatively, the similar rotation surfaces might simply result from a common solution to the non-commutivity problem adopted by the central nervous system for all 3 systems.

Subsequently, however, Miller et al. [71] showed that, unlike the flat planes described by Listing's Law for the eye, the rotation axes for the arm do not fall along a flat plane, but rather along a 2 dimensional curved surface. The contrast between the curved surface describing arm orientations, and the flat eye planes casts some doubts on the suggestion that the orientations of arm and eye are actually coupled. It also raises the question whether the orientations of eye and head are coupled, since the rotation vectors for the head fall in a curved plane, and whether the curvature of the surface with rotation vectors is the same for the arm, hand and head. The aim of this study is to investigate these issues by measuring head, upper arm and hand orientations simultaneously during visually guided pointing movements, and to investigate whether the resulting rotation surfaces indicate that these motor systems may be actually coupled.

3.3 Methods

The orientations of the head and the right upper arm and hand were measured during pointing movements. Data were collected from six male subjects, two of whom were left handed, and ranged in age from 23 to 38 years. None had any known history of neurological or musculoskeletal disorder.

3.3.1 Task

The subjects were instructed to make natural self-paced pointing movements with the arm comfortably extended. Subjects were further instructed to attempt to fill the workspace homogeneously with both head and arm movements. There were no other explicit restrictions on orientations of the arm or head. We tested two different conditions in each experiment. In one condition, subjects were asked to make "natural arm and gaze movements" as though looking and pointing to a moving, imagined target. In the other condition, subjects made "pointing movements with the nose", simultaneously with the arm in order to increase the range of the head movements. A single trial consisted of a continuous series of movements lasting 60 seconds. The two conditions were tested alternately, each a total of 6 times in the course of a single experiment. Data collection for each trial started as the subject began movements, and continued during the remainder of the trial. A brief rest period was typically

provided between trials and for a longer time whenever the subject complained of fatigue

3.3.2 Experimental set-up

The orientations of the head, upper arm and hand were measured with two cameras of a WatSmart system capable of tracking the position in three dimensions of infrared light emitting diodes (IRED's). Crosses with IRED's on each of the four tips were attached on a helmet to measure head orientation. A second cross was fastened to the upper arm just proximal to the elbow, and a third cross was attached to the hand. The position of each of the 12 IREDs was sampled at a frequency of 100 Hz. These positions were used to determine the position and orientation of the cross and thereby the orientation of the head or limb segment. This set-up allowed relatively unrestricted movements to be made within most of the natural range. In the vertical direction, the workspace ranged from +45 degrees (above shoulder height) to -45 degrees (below the shoulder). In horizontal direction, the workspace ranged from +15 degrees (to the subject's left) to -90 degrees (to the subject's right), where 0 degrees pointed straight forward. See Miller et al. [71] for further technical details.

3.3.3 Data analysis

During movement, the orientation of each cross with respect to a fixed reference orientation was expressed as a "rotation vector" (see [35, 71] and Appendix). The direction of a rotation vector is parallel to the axis of rotation from the reference to the moving orientation. Its magnitude is equal to the tangent of half the angle of this rotation. A consequence of Listing's Law for the eye is that these rotation vectors all lie in a flat plane [35, 99]. There have been several recent suggestions that similar laws may exist for the head and arm [10, 41, 50, 91, 92]. Although it has been shown [71] that the surfaces spanned by the rotation vectors describing arm and forearm orientations are actually curved, the fixed axis coordinate system based on the orientation of the limb in primary position remains a useful means for expressing limb torsion. This produces the system with minimum global limb torsion. Consequently, we have fit the data for head and arm orientations to linear planes and calculated the resulting primary directions. Rotations about the \hat{z} axis correspond to limb movements to the left and right, while \hat{y} -axis rotations move the limb up and down. The torsional component is expressed by rotations around the \hat{i} axis.

Listing's Law constrains the rotation vectors expressed in this system to a flat plane. Two other common rotational systems may be constructed by nested gimbals (See Appendix, figure 3.5). The Fick system results if rotation around the vertical axis

is applied after rotation around a horizontal axis. Reversal of this sequence produces the Helmholtz system [7]. The rotation surfaces resulting from any of these systems may be modeled by the following equation: $\hat{x}_i = f * (\hat{y}_i - \hat{y}_0) * (\hat{z}_i - \hat{z}_0)$, where \hat{x}_i , \hat{y}_i and \hat{z}_i represent the amount of rotation along the \hat{x} , \hat{y} , and \hat{z} axes, respectively. If the limb movement systems strictly obeyed Listing's Law, f would be equal to 0 since there would be no torsion along the \hat{x} -axis. On the other hand, f would equal 1 for a Helmholtz system or -1 for a Fick system. f may actually take on any positive or negative value, depending on the sign and magnitude of the curvature of the rotation surface. Of course these surfaces represent only a subset of the infinite number of 2 dimensional rotation surfaces which might hypothetically describe limb orientations. Therefore, we calculated the correlation coefficient between the fitted rotation surface and measured rotation vectors as a measure of the quality of the model.

In order to compare two rotation surfaces, we calculated the average torsion in 5 degree wide bins throughout the workspace. Qualitative comparisons were easily made by plotting this average torsion as a function of pointing direction. The \hat{z} and \hat{y} rotation vector components determined the horizontal and vertical axes respectively, while the \hat{x} or torsional component was indicated by a gray value.

Spatially averaged torsion was also used for quantitative comparisons. The torsion can be expressed as a square matrix $X(i, j)$, expressing the torsion of the bin in row i , column j . We determined the similarity between two surfaces X and Y by calculating the correlation coefficient between pairs of points $(X(i, j), Y(i, j))$. A large correlation indicated that the two surfaces had the same type of curvature. However, a correlation coefficient provides only a measure of similarity but does not give an indication of the relative magnitude of curvature. Therefore, we also calculated the slope of the relation between points $(X(i, j), Y(i, j))$. A correlation of 1 and a slope of 1 indicate that the surfaces are the same.

3.4 Results

The orientations of the upper arm, hand and head were measured in a task in which subjects were instructed to look at and to point to targets simultaneously. The rotation vectors expressing the orientations of arm, hand and head during these movements are shown in figure 3.1. The upper three panels show the rotation vectors for the arm. The data points projected onto the $\hat{Y} - \hat{Z}$ plane present a front view of the plane that was fitted to the rotation axes. The $\hat{Y} - \hat{X}$ and $\hat{X} - \hat{Z}$ projections present side and top views. The data indicate that the rotation vectors do tend to scatter within a plane. However, in accordance with the results shown by Miller et al.

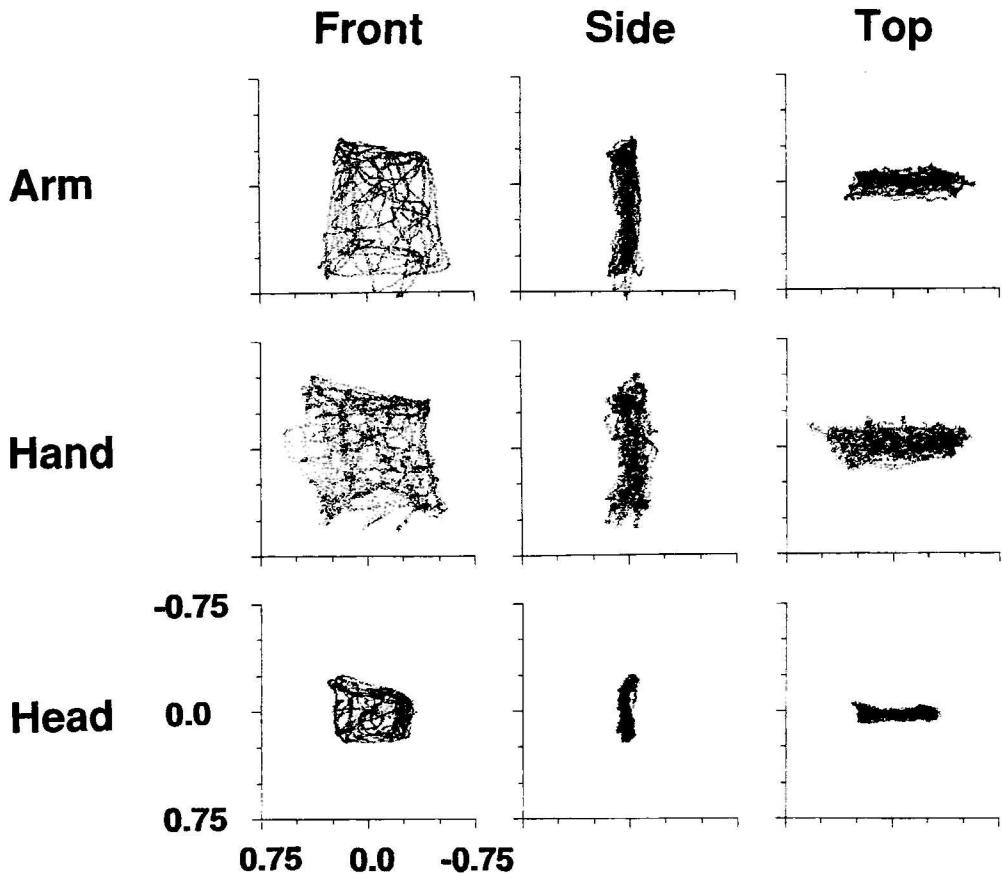


Figure 3.1: Orientations of the arm (upper three panels), hand (middle three panels) and head (lower three panels) relative to fixed reference orientations for a task in which subjects were instructed to point to and fixate imagined targets located throughout workspace. Data in the left column show front views of the planes which were fitted to the rotation vectors. The \hat{z} -component of the rotation axis is shown along the horizontal axis since it produces horizontal movements (rotations) of the arm, hand and head. The \hat{y} -component of the rotation axis is shown along the vertical axis since it produces vertical movements (rotations) of the arm, hand and head. The middle and left columns present top and side views. These views include the torsional (\hat{x} -) component of the rotation axis. In the side view and top view, this component is plotted along the horizontal axis and vertical axis respectively. The units along the horizontal and vertical axes are those of rotation vectors, where -0.75 and 0.75 correspond to approximately -75 and +75 degrees (see Appendix).

[71], closer inspection reveals that a significantly better fit to the data is provided by a curved surface. This is illustrated in figure 3.2. The panels in figure 3.2 illustrate the same data as those shown in figure 3.1, although they are shown in a different format. In figure 3.2 the torsional components \hat{x} of arm, hand and head orientations are represented on a grey-scale as a function of the \hat{y} - and \hat{z} - components of the rotation vectors. In each panel the horizontal and vertical axes represent rotations about the $-\hat{z}$ and $-\hat{y}$ axes respectively, corresponding to left/right and up/down movements. Note that the signs of both axes have been reversed in these plots in order to make them correspond more closely to the resultant movement. There is positive torsion for directions in the upper-left and lower-right part of work space. Torsion in the upper-right and lower-left has opposite signs. This representation shows quite clearly that the rotation axes do not fall on a flat plane, but rather along a curved surface.

The middle row of panels in figure 3.1 shows the data for the hand. These data look very much like the data for the arm except for the fact that the side and top views show that the fitted plane is thicker for the hand than for the upper arm. The middle panel in figure 3.2 shows that the thickness results from the greater curvature of the hand rotation surface. This reflects the contribution of supination and pronation of the forearm, which affects the torsion measured at the hand. This observation corresponds to the results of Miller et al. [71] who found that supination/pronation contributes significantly to the orientation of the hand, especially for workspaces having a large vertical range. Despite the greater curvature, the general shape of the hand rotation surface was very similar to that of the arm.

In figure 3.1 the lower panels show the data obtained for the head. The lower/left panel shows that the work space for rotations by the head is much smaller than that for the arm and hand. Generally rotations along a vertical axis (left/right movements) occurred over a larger range than rotations along a horizontal axis (up/down). The same conclusions are evident from the lower panel in figure 3.2. The thickness of the fitted plane was also much less than that for the upper arm and hand. This was a consistent finding for all subjects. The mean thickness of the planes for all subjects was 4.7 deg for the upper arm, 6.6 deg for the hand and 2.7 deg for the head. An Analysis of Variance ($F(2,10) = 106.9$, $p < 0.005$) indicated that these differences were significant. The rotation surfaces depicted in the three panels in figure 3.2 are clearly all curved, and share some features. However, they differ at least in the magnitude of the curvature, as well as in the range of the workspace which they include.

In order to study head movements over a larger range, we instructed subjects to "point" with the nose, thereby minimizing the eye movements typically made when looking to an eccentric target. The results for the normal and "nose pointing"

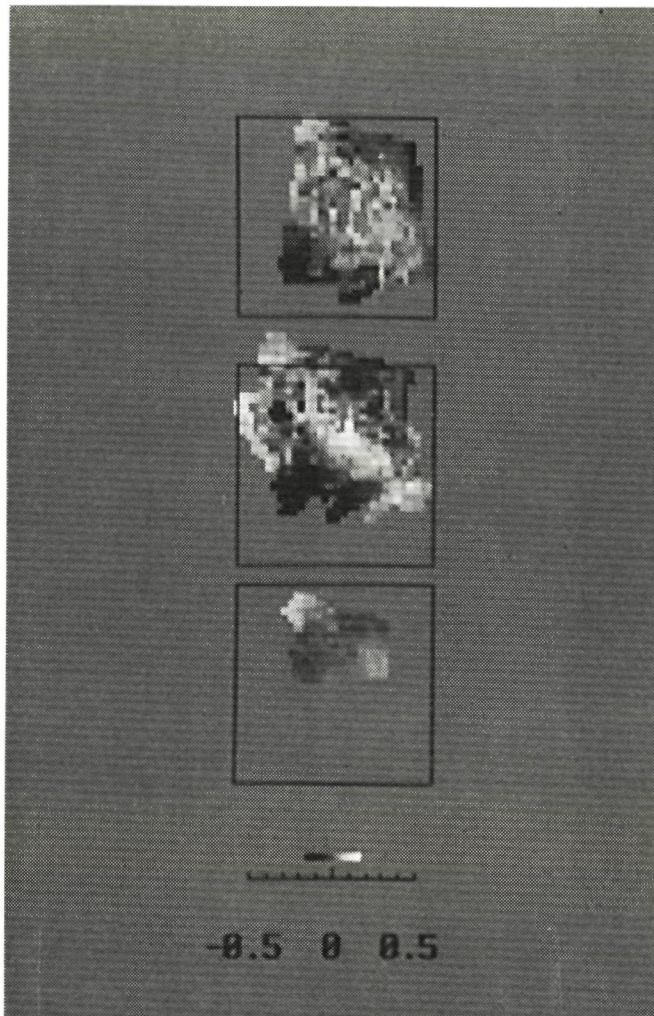


Figure 3.2: This figure shows the same data from figure 3.1, plotted in a format which reveals the curvature of the rotation surface. From top to bottom the panels show the rotation surfaces for the arm, hand, and head respectively. The \hat{z} - and \hat{y} - components of the rotation vectors are plotted with the same conventions used in the first column of figure 3.1, while a grey scale was used to indicate the average torsion in 5 degree wide square bins. Solid black corresponds to about -18 degrees and white to +18 degrees. The large square is 120 degrees on a side and is shown to indicate the \hat{y} - and \hat{z} - components of the rotation vectors in each panel relative to the others.

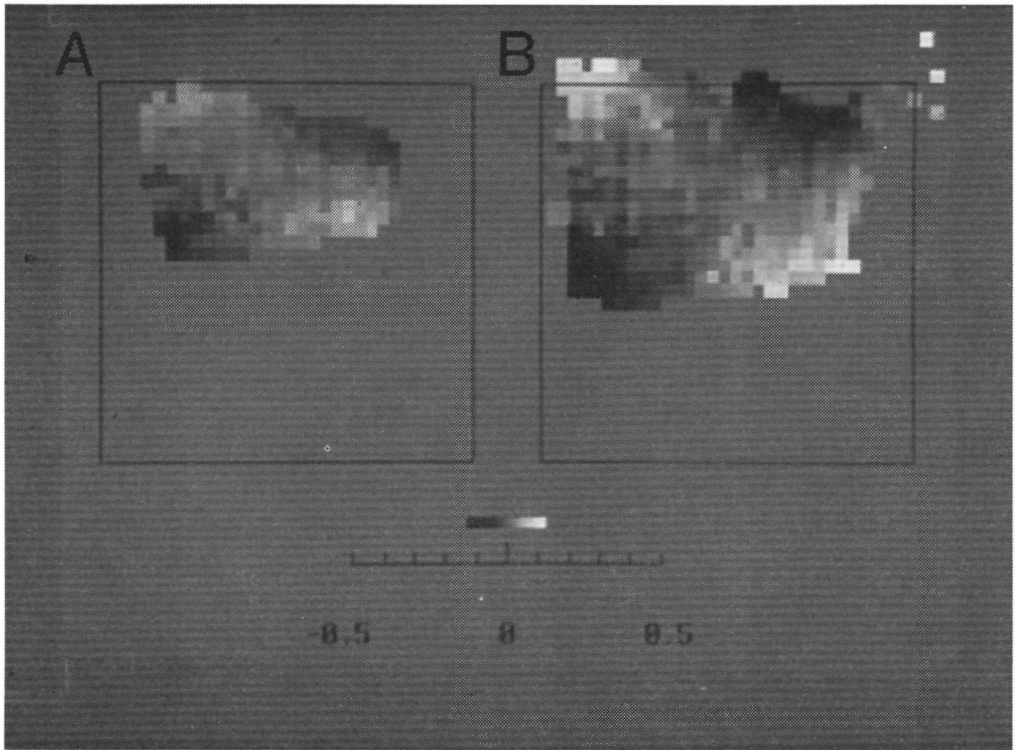


Figure 3.3: Torsion components for the head in a natural condition (A) in which the subject fixated imagined targets throughout the workspace, and (B) in a condition in which the subject was specifically instructed to "point with his nose" throughout the same workspace. All other details as in figure 3.2.

movements of the head are shown in the panels A and B of figure 3.3, respectively. The range of head movements is considerably larger in the latter condition, and the workspace is more nearly square. For the range of head positions common to the two conditions, the correlation coefficient between the rotation surfaces in this figure was 0.69, and the slope was 0.95. This indicates that the two surfaces had very similar curvature, of nearly identical magnitude. A significant difference was found for only 1 of the 6 subjects (ANOVA: $F(1,49) = 5.82$; $p < 0.05$).

A similar analysis was done to investigate whether the instruction to "point with the nose" had any effect on the orientations of the hand and upper arm. There was a difference found for 1 subject for the head / arm comparison, and a single (different) subject for the head / hand comparison. Apparently, the instruction had at most a small effect on the shape of the rotation surfaces.

subject	MF	GH	SG	MT	EA	LM
arm	0.45 (0.04)	0.63 (0.04)	0.38 (0.01)	0.44 (0.02)	0.46 (0.03)	0.27 (0.02)
hand	0.47 (0.04)	-0.34 (0.04)	0.47 (0.03)	0.69 (0.02)	0.61 (0.03)	-0.39 (0.02)
head	0.43 (0.04)	-0.77 (0.04)	0.64 (0.02)	0.74 (0.10)	0.76 (0.06)	-0.72 (0.04)

Table 3.1 The mean Fick index of the fitted rotation surface for the arm, hand and head for all six subjects. Standard deviation is given in brackets. A value of 1 (+1) would correspond to the Fick (Helmholtz) gimbal system. A flat plane (Listing) would correspond to a value of zero.

The data in figure 3.2 and 3.3 clearly show differences in the amount of torsion for arm, hand and head for movements in the same workspace. The range of the grey levels (torsional components) is smallest for the head and largest for the hand. Also the shape of the surfaces differ. For example, panel 2B (the hand) has a diagonal light grey band running from upper left to lower right, while panel 3B (head "nose pointing") has a center which shows grey levels indicating near zero torsion. If the hypothesis that arm, hand and head movements are coupled, were true, the curvature of the rotation surfaces should be the same for arm, hand and head. We used two different tests to compare these surfaces. First, a curved surface was fitted to the data as explained in the methods. This fitting procedure yielded a "Fick"-index f and a correlation coefficient indicating the quality of the fit (see Appendix). The results are shown in table 3.1 and indicate that the Fick index consistently fell between -1 and 0 for all subjects for the arm, hand and head, indicating that the shape of the fitted rotation surface was between that of a Fick-gimbal system and a flat plane. In general, both the Fick-index, and the correlation coefficient between the data points and the fitted surface, were higher for the head than for either the hand or the arm.

Since the Fick-index was significantly smaller than zero for all conditions for all subjects, the orientations of arm, hand and head cannot be described by a flat plane, as is suitable for the eye. Nor can they be described as a Fick-gimbal system either, since the Fick-index was significantly different from -1 for virtually all cases (with the exception of head orientations for one subject).

As a second approach, we calculated the slope and correlation coefficient between pairs of measured rotation surfaces. The mean correlation for repeated measures of the same part of the body was 0.6, indicating a considerable variability between trials. The correlation between head/hand, head/arm and arm/hand pairs for single trials was generally lower than the correlation for the same part of the body on repeated trials. In an Analysis of Variance, the correlations for head/hand, head/arm and arm/hand combinations appeared to be significantly different at a 5% significance level for all subjects. This result indicates that the curved surfaces that describe the

orientations of hand, arm and head during a single trial are different

Since the correlation coefficient for data from different limbs is just a measure of the similarity of shape of the rotation surfaces, but not a measure for the curvature of the rotation surface, we plotted the amount of torsion for corresponding \hat{y} - and \hat{z} - components of the rotation vectors for different limbs (see Methods). The slope of the linear regression line is a measure for the relative curvature of the relative curvature of the rotation surfaces. The results indicated that the mean curvature for all subjects is a factor of 2.24 higher for the hand than for the arm, and a factor of 4.97 higher than for the head. Summarizing, the curvature is highest for the hand, followed by that for the arm and head (in that order).

3.5 Discussion

The experimental data in this study support earlier observations [40, 41, 71, 29] that the orientations of the upper arm, hand and head are each uniquely defined for any given pointing or gaze direction. This observation corresponds to an application of Donders' Law to these movements. However, unlike the eye, the rotation vectors describing arm, hand, and head orientations are better described by a curved surface, than a flat plane. Hence each of these systems failed to meet the constraints imposed by the analogy of Listing's Law.

As mentioned in the Results section, the Fick-index was most negative for the head, followed by that for the hand and arm. It may therefore seem contradictory that the curvature of the rotation surfaces was highest for the hand, followed by that for the arm and head. The explanation is that neither the hand nor the arm rotation surfaces were as well modeled by a surface which was on the continuum between Fick and Helmholtz, as was the head. Hence, although they were more greatly curved, both the correlation with the fitted surface, and the Fick-index, were closer to 0 for arm and hand. This qualitative difference in orientations for head and arm is evident in figure 3.2. Panels A and B (for arm and hand) suggest a "ridge", with lighter bins from the upper left to the lower right. In contrast, the lower panel (head) suggests a diagonally oriented "saddle", with darker bins in the lower left and upper right corners and lighter bins in the other corners. This "saddle" is more nearly like a Fick-surface than is the "ridge" for arm and hand. This qualitative difference was found for all subjects, corroborating the conclusion that the orientations of hand and arm are different from that of the head.

There were small instruction related differences in the rotation surface of the head resulting from attempts to make relatively large head movements, which would correspond to violations of Donders' Law. However, the differences were small, and

insignificant for most subjects. Although both head and eye movements (relative to the head) obey Donders' Law, our results suggest that for eye movements in space (i.e. for combined eye and head movements) Donders' Law is violated. This can be understood if one realises that all rotation vectors of the eye relative to the head fall in a flat plane while rotation vectors for the head in space fall on a curved surface. This implies that for gaze movements in oblique directions the torsional component of gaze depends on whether a change in gaze direction is caused by an eye or head movement. These violations would be evident only for oblique gaze directions since the torsion is zero along pure horizontal and pure vertical movements, for both the eye and the hand.

3.5.1 Functional implications.

Whether the rotation surfaces we have described are related to the different musculoskeletal anatomy of the three systems, or to a neurological origin cannot be answered directly by our present data. However, it seems unlikely that such qualitatively similar curvature would result biomechanically given the large anatomical differences between the three systems.

Several functional schemes have been proposed to explain the reduction of degrees of freedom for eye and limb movements. For the eyes, Helmholtz (1866) proposed a role for perception. He pointed out that Listing's Law minimizes the changes in orientation of the retinal image for small movements in any arbitrary direction. If the eye or the head moves as a Fick-gimbal system, the eyes would always remain oriented along a horizontal line, which might also serve a perceptual purpose. However, this perception-based explanation seems unlikely. Large gaze shifts are usually accomplished with a combination of eye and head movements, as is clearly demonstrated by the difference in panels A and B in figure 3.3. Even if the rotation vectors for both the eye and head would fall in a (flat) plane, the torsion component of gaze would not be uniquely defined for combined eye and head movements unless the eye and head movements are in the same direction. For a curved surface of rotation vectors, as found for the head, the torsion component of gaze for a given gaze direction is different for different combinations of eye and head movements. As a consequence, Donders' law is violated for gaze and any visual advantages conferred by the flat rotation plane of the eye in head would be lost for gaze movements which require head movements having a curved rotation surface.

It has also been proposed [41] that the reduction in degrees of freedom may simplify the coordination between hand, arm and head movements during visuomotor tasks. Our results show that while the rotation surfaces for head, hand and arm share some features, the shape and magnitude of curvature for the three systems

differ significantly. One could also argue that since the center of the rotation axes is different for the head and the arm, the rotation surfaces would have to be different in order to maintain equal changes in orientation for fixating and pointing to targets that are not at infinity. The rotation surfaces would then differ by a specific direction-dependent amount of torsion. This was not observed. Therefore, it is apparently not true that the control of orientation for eye, head and arm are all reduced to the same 2-dimensional curved surface of rotation vectors. Nonetheless, a strategy which reduced the number of explicitly controlled degrees of freedom might still be advantageous if implemented in each system independently.

The fact that rotations in 3-D do not commute, has major implications for models of motor control. In the oculomotor system, it has been shown that the motor program for fast eye movements (called saccades) is driven by a signal representing motor error: the difference between the desired (target) position and the actual eye position. When a saccade is made, a large burst of activity is generated in order to bring the eye to the target position. This burst of activity continues until the difference between target position and eye position has become equal to zero. In a model proposed by Robinson [86] the difference is obtained by subtraction of the target position and the current eye-position during the saccades. However, the subtraction causes the orientation of the eye to depend on the order of previous rotations, because of the non-commutivity of 3-D rotations. This observation has necessitated a revision of Robinson's model. In the model proposed by Tweed and Vilis [99], Listing's Law is implemented by using a "product" operation of quaternions, rather than subtraction of eye rotations. This model requires quite different neuronal circuitry than the Robinson model. The generalization of these eye movement models to other rotational systems, has implications for modelling of limb movements and for comparison of differences and similarities in the control of eye and limb movements.

Initially [99] it was proposed that Listing's Law was implemented at the motor programming stage. However, later evidence [78] showed that the motor programs are made based on the difference between the desired target position and actual position of the eye and that the implementation of Listing's Law takes place at a rather peripheral level. This is compatible with the results of Caminiti et al. [5] for arm movements and Georgopoulos et al. [24] who found that motor cortical neurons code movement direction. Since quite different muscles are involved for the same movement direction at different parts of workspace, these electrophysiological results in motor cortex suggest that the fine-tuning of the motor program for the plant mechanics takes place at a level downstream of motor cortex.

3.6 Appendix

Commutativity of translations in 3 dimensions is taken for granted in everyday life. That is, if I move North 3 meters, then 3 meters to the East, and finally up 3 meters, I will arrive at the same location as if I had performed the sequence of movements in the reverse order. Three dimensional rotations, however, are not commutative. Figure 3.4 demonstrates this property for a die subjected to sequential rotations about the vertical and horizontal axes. It should be immediately apparent that the final orientation of the die is dependent on the order in which the rotations are applied.

The pointing or gaze direction in space is completely determined by two dimensions, leaving the third dimension unspecified. The consequence of non-commutativity for rotational systems, is that the orientation of the eye (or limb), for any particular looking direction, is dependent on the path which brought the eye into that position. As explained in the Introduction, however, the orientation of the eye relative to the head is uniquely determined by the direction in which the eyes are oriented in the orbit. This observation, that eye orientation is constrained to only two of the mechanically available three degrees of freedom has been called "Donders' Law".

The orientation of a rigid body can be easily expressed as a single rotation from a reference orientation. A rotation along any axis in three dimensions may be described by the direction of the rotation axis (2 parameters) and by the angle of rotation (1 parameter). Several systems for the description of rotation and orientation are in common usage. We have adopted rotation vectors (also called Lagally vectors), which are both an efficient means of expressing rotations, and are easily manipulated mathematically [35]. The rotation vector $\vec{r} = \tan \frac{\theta}{2} \vec{l}$ has a direction in space parallel to the unit axis of rotation \vec{l} , and its length (L) is equal to the tangent of half the rotation angle θ . For small values of $\frac{\theta}{2}$, expressed in radians, $\tan \frac{\theta}{2}$ can be approximated by $\frac{\theta}{2}$. Multiplication of this value by $2 \frac{180}{\pi}$ yields the angle of rotation in degrees. A useful approximation to interpret the length L of the rotation vector into the angle of rotation, having an error less than 15 % for angles of rotation up to 80 degrees, is then $\theta = 100 * L$.

Another common description for rotations uses quaternions [99]. A quaternion q has 4 parameters $q = q_0 + \vec{q}$, where $q_0 = \cos \frac{\theta}{2}$ and $\vec{q} = \sin \frac{\theta}{2} \vec{l}$ with θ the angle of rotation and \vec{l} , the 3-D unit vector in the direction of the rotation axis. Since a quaternion has 4 components, it is redundant. This is caused by the fact that a quaternion has length 1: the first component q_0 is chosen such that $q_0^2 + |\vec{q}|^2 = 1$.

A 3x3 rotation matrix, having 9 coefficients, may also be used to express a rotation, but it is obviously highly redundant. These three representations of rotations (rotation vectors, quaternions, and rotation matrices) are the most frequently used

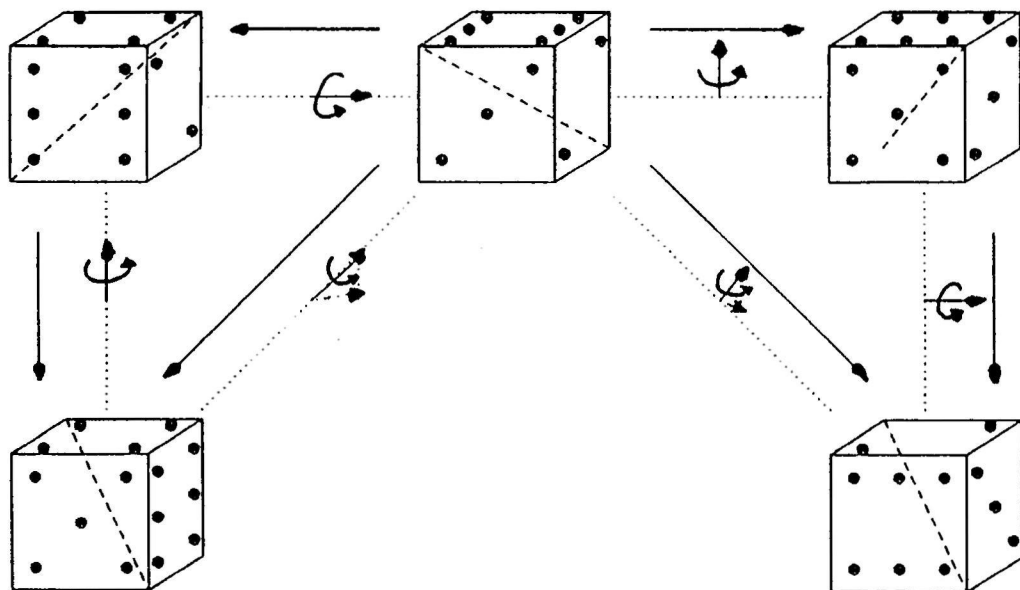


Figure 3.4: Illustration of the fact that rotations do not commute. This can be seen by looking to the changes in orientation of the center die. If we first apply a rotation of 90 degrees along a horizontal axis we obtain the die in the left upper corner. Applying then a rotation of 90 degrees along a vertical axis, gives the die in the lower left corner. However, if we reverse the order of rotations, thus first a rotation around a vertical axis (right upper die) and then a rotation along a horizontal axis, we find the die in the lower right corner. This die has clearly a different orientation (different numbers on corresponding sides). This example shows that rotations along two axes which are not parallel do not commute. Also note that the dice at the lower left and lower right can be obtained starting from the same starting position (middle die) by different rotation vectors. From these dice we can also see that one pointing direction, which is here illustrated by a dashed body diagonal through the corner of the sides with the 3, 5 and 6, does not specify the orientation of the dice. Both lower dice can be obtained by one rotation from the center dice (rotation vectors for these rotations are shown on the diagonal dotted lines). In both cases the pointing direction has the same final direction, but the final orientation is different.

representations for 3-dimensional rotations. Transformations from one representation into another are straightforward.

Rotation vectors provide a simple means of expressing Listing's law, or the func-

tional dependence of three-dimensional eye orientation on the two dimensions of the looking direction. The allowable orientations, when expressed as rotation vectors relative to "primary direction", are all confined to a plane which is perpendicular to the line of sight when the eye is in primary position. In the oculomotor literature this plane is called "Listing's plane". In order to describe rotation axes in other systems relative to Listing's plane, we define a cartesian system with the \hat{x} -axis along the line of sight in primary position. Hence for Listing's Law, which states that all rotation vectors fall in a plane orthogonal to \hat{x} , the x -component should be zero.

For the upper arm and hand, we showed that the corresponding rotation vectors lay in a 2-dimensional curved surface, rather than in a flat plane. Nonetheless, this system still represents a reduction from three degrees of freedom to two.

Another convention for expressing orientation uses a series of three rotations to define each of the three dimensions. Such a system can be modeled geometrically as a series of nested gimbals. Because of the non-commutativity of rotations, the order nesting of these gimbals is important, and different orders result in different "standard" systems. Two of these systems are shown in the top half of figure 3.5 next to a mechanical system which obeys Listing's Law. In a "Fick" system, the horizontal (\hat{y} -) rotation axis is nested within a frame containing a vertical (\hat{z} -) rotation axis. This is equivalent to the convention that the rotation component along the y -axis is made first, followed by the rotation component along the \hat{z} -axis. For this system the \hat{x} -component of the rotation vector is equal to minus the product of the y - and \hat{z} -components of the rotation vector: $x = -y \cdot z$. This system keeps the retinal vertical in line with the environmental one [73]. For a "Helmholtz" system, the order of nesting of the y - and z -axes is reversed. The \hat{x} -component of the rotation vector in a Helmholtz system has the opposite sign from that of the Fick system: $x = +y \cdot z$. Using the same notation, a "Listing" type system would have $f = 0$. Therefore, the three discrete cases can be described by the general equation $x = f \cdot y \cdot z$, with $f = -1$ for a Fick system, $f = 0$ for a Listing system, and $f = 1$ for a Helmholtz system. We have called this parameter f the "Fick-index".

The bottom half of figure 3.5 shows the rotation surfaces which would result from each of the gimbal systems. The solid lines mark the rotation surface as it curves systematically away from the flat "Listing" plane, shown by dotted lines. The curvature of the Fick system is qualitatively much like that of the head, although it differs in magnitude.

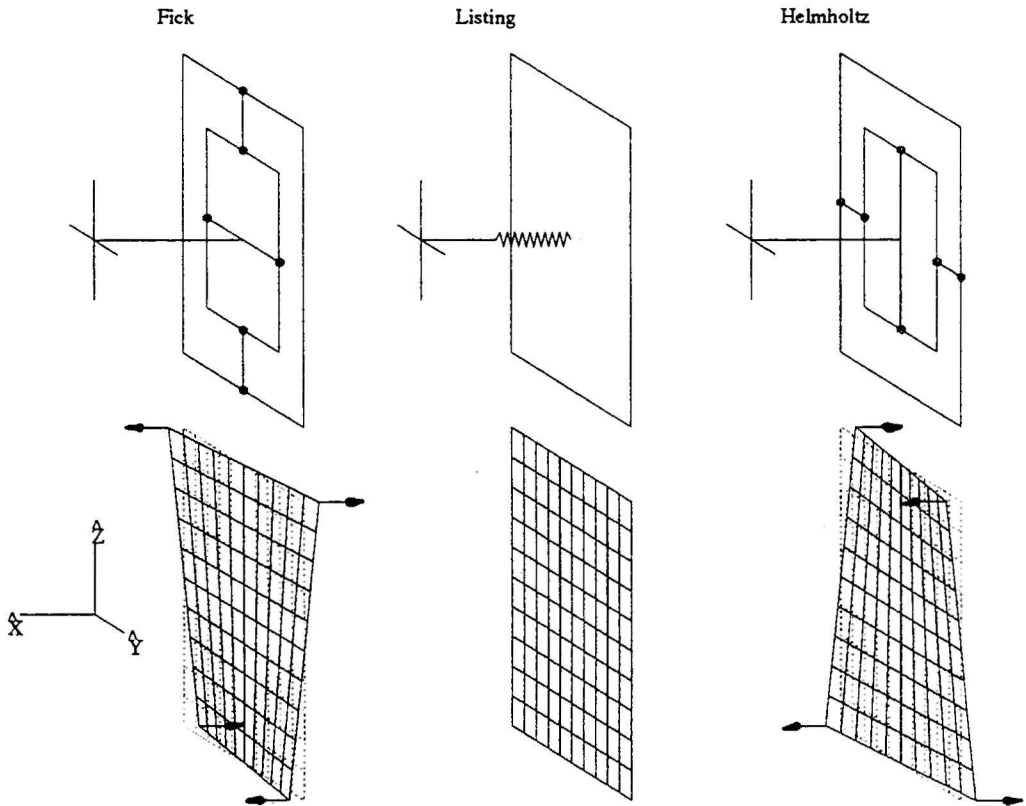


Figure 3.5: The top row shows from left to right a Fick-gimbal system, a system which meets with Listing's Law and a Helmholtz-gimbal system. All these systems impose a specific orientation for the cross mounted on a stick for each pointing direction of the stick. All sticks and crosses are shown in the same primary position. For the middle system, the stick is attached to a plane by a spring which determines the orientations of the cross for all pointing directions of the stick. The rotation vectors corresponding to all orientations obtained during pointing directions lie in a flat plane (Listing plane) as shown below this system. For the Fick-gimbal system the horizontal rotation axis lies inside a frame which rotates around a vertical axis. Only for purely horizontal and vertical rotations will the Fick-gimbal and the Listing system give the same rotation vectors. For oblique movements of the pointing direction of the stick, the rotation vectors will not lie in a flat plane but on a curved surface. This curved surface is shown at the lower left corner. The dotted flat plane (Listing plane) is shown for reference. For the Helmholtz-gimbal system, shown in the upper right corner, the horizontal and vertical rotation axes are nested in reversed order with respect to the Fick-gimbal system. Consequently the sign of the torsion changes.

Chapter 4

The Activation of Mono- and Bi-articular Muscles in Multijoint Movements

Adapted from: Miller LE, Gielen CCAM, Theeuwes M, Doorenbosch C (1992) The Activation of Mono- and Bi-articular Muscles in Multijoint Movements. In: Caminiti R, Johnson PB, Burnod Y (eds) *Control of Arm Movement in Space. Neurophysiological and Computational Approaches*. Springer, Heidelberg, pp 1-15.

4.1 Introduction

For several reasons the coordination of muscle activation patterns in various movement tasks is still poorly understood. One of the problems in understanding the relative activation of muscles is that biological limbs are supplied with multiple joints which provide great flexibility for producing various movements. Furthermore, each joint is crossed by a number of mono- and biarticular muscles. Despite this large number of degrees of freedom, the activation pattern for movements is rather stereotyped for a given subject [32, 33, 106] and frequently shows very little variability between subjects [33, 106]. Apparently, some constraints (presumably with biomechanical, neural, or anatomical origins) are present which impose restrictions on the set of possible muscle activation patterns.

In a previous study [106] it was shown that the activation of a muscle could not be understood simply from the mechanical advantage of that single muscle. Rather, the effect of all other muscles acting across the same joint had to be taken into

account. For example, *m. triceps*, the activation of which contributes to torque in the extension direction only, is also activated for torques in supination direction. This can be understood by considering the activation of *m. biceps* for torques in supination direction. Since the insertion of the biceps at the radius is such that it causes both supination and flexion torques, an extensor muscle has to be activated to compensate for the torque component in the flexion direction in order to obtain a net torque in the supination direction alone. This relationship between the relative activation and the mechanical advantage is complex enough for muscles acting across a single joint, but becomes even more complex for biarticular muscles.

Recently, Tax et al. [93, 94] have shown that the activation of *m. biceps* (a biarticular muscle) and *m. brachialis* (a monoarticular elbow flexor) in isotonic contractions differs in two important respects from that which occurs during isometric contractions. First, the recruitment threshold of motor-units in *m. biceps* was lower for isotonic shortening than for isometric contractions. Second, the firing rate of motor-units in *m. biceps* at recruitment was higher during isotonic shortening than during isometric contractions. Both effects are consistent with *m. biceps* making a larger contribution to elbow torque. An effect opposite to that in *m. biceps* was found for *m. brachialis* and *m. brachioradialis*. For these muscles, the recruitment threshold was higher, and the firing rate at recruitment lower, during isotonic shortening contractions than during isometric contractions. These results led Tax et al. [95] to conclude that motor-units were operating in two different modes in isometric and isotonic contractions. However, since they studied one dimensional movements about a single joint (flexion/extension in the elbow) it is quite possible that the different motor-unit behavior in these muscles depends not only on the nature of the movement task (isometric versus isotonic contraction) but also on the direction of the movement and of the force exerted by the hand.

Van Ingen Schenau [52] has presented theoretical concepts which predict different roles for mono- and biarticular muscles. He suggests that some movements against an external force can be made much more efficiently when biarticular muscles are used in place of their mono-articular agonists. According to van Ingen Schenau et al. [51], the role of biarticular muscles is especially important for some movement directions where the torque and displacement in a particular joint have the opposite sign. In these circumstances, the lengthening muscle would produce negative work or, in other words, would dissipate energy rather than contribute work. Under these conditions, biarticular muscles can improve efficiency by reducing this energy dissipation. Some theoretical results and quantitative predictions on the relative activation of mono- and biarticular muscles have been presented by Gielen and Ingen Schenau [28]. These were corroborated by later results presented by Gielen et al. [27] indicating that the relative activation of *m. biceps longum* and *m. brachioradialis* differed in isometric and

isotonic contractions. In this chapter we study the relative activation of other mono- and biarticular muscles in the human arm in order to investigate the correspondence with the theoretical predictions.

In summary, this study aims to investigate the different roles of mono- and biarticular muscles in the human arm by studying the relative activation of these muscles in isometric and isotonic contractions against an external load acting from different directions at the wrist.

4.2 Methods

During these experiments, the electromyographic (EMG) activity of the muscles brachioradialis, biceps caput longum, triceps caput longum, and triceps caput laterale was measured while subjects produced forces in various directions about the wrist within the horizontal plane. Muscle activation was compared during isometric and isotonic force production. Further details are given below.

4.2.1 Subjects

Data were collected from six volunteer subjects, four male and two female, ranging in age from 23 to 52 years. None had any known history of neurological or musculoskeletal disorders. Each subject was seated in a chair with the right forearm supported at approximately shoulder height in a cloth sling. The sling was suspended from the ceiling such that the relaxed arm was maintained in a horizontal position and very little force was required to displace the relaxed arm in the horizontal plane. In the standard test position, the upper arm was held with 0° ante flexion, the elbow was 90° flexed, and the forearm was in the midprone position.

4.2.2 Task

Forces were applied to the subject's arm via a lightweight aluminum bracelet fixed around the wrist. The bracelet was made to fit tightly but comfortably by forming a mold of elastic dental compound between the bracelet and the subject's wrist. A yoke was attached via steel cables to the top and bottom of the bracelet, so that the assembly was free to rotate around the hand in the horizontal plane. The yoke was attached to a single cable leading to a torque motor used to deliver isotonic loads. During the movements, the motor produced a constant tension in the cable and the subject was instructed to move the hand slowly in the direction opposite to the applied force. The velocity of the hand varied somewhat for different subjects,

and to some extent in the different directions, and typically ranged between 8 and 13 cm/s. This corresponds to joint angular velocities of 10 - 20 °/s.

During the initial five experiments it was not possible to measure force during the movements. Instead, the isotonic force was calibrated prior to each experiment by using the motor to pull on the load cell used for the isometric measurements. During the last three experiments (subjects CD2, MT2, and LM) we were able to measure both isometric and isotonic forces directly and the force exerted at the hand was the same to within 0.2 N in both conditions. The initial limb position was arranged such that the wrist passed through the test position during data collection. In order to deliver forces in different directions, the motor was moved to different positions about the subject. Figure 4.1 contains a schematic drawing of the subject's posture and displays the convention we have adopted for naming the directions of movement.

In the isometric condition, the length of the cable was fixed such that the subject's arm was placed in the test position. A meter placed in front of the subject indicated the amount of tension in the cable. Data collection began when the force exerted by the subject was equal to that in the isotonic condition. For each subject, ten trials were collected in each direction, five isometric and five isotonic. The sequence of force directions was chosen randomly, but the ten trials in each direction were always collected as a block. For the five initial subjects, EMG activity was measured in 12 directions which spanned 360° at 30° intervals. Similar measurements were repeated for a greater number of directions for two of the original subjects and one additional subject. In these last three experiments, data were collected at 15° intervals throughout two 120° arcs centered on the maximum activation direction for biceps and triceps. For most subjects, it was impossible to collect data in directions near 135° because of geometrical constraints introduced by the force delivery method.

4.2.3 Data Collection

EMG data were collected using Ag/AgCl surface electrodes. The signals were differentially amplified and filtered with a 50 Hz notch filter and a fourth order Bessel filter with a passband of 10-150 Hz. The signals were sampled with a 12 bit A/D converter at 400 Hz. Tension in the cable was measured with a load cell constructed from four semiconductor strain gauges wired in a Wheatstone bridge configuration. The force signal was also sampled at 400 Hz.

Infrared light emitting diodes were attached to the wrist, elbow, shoulder, and neck, and their positions were calculated with a Watsmart opto-electronic system at 100 Hz. In addition to absolute position in three dimensions, all relevant joint angles could be calculated. The collection of position, force and EMG data was synchronized by the Watsmart system. Data were collected for 5 s in experiments with the first

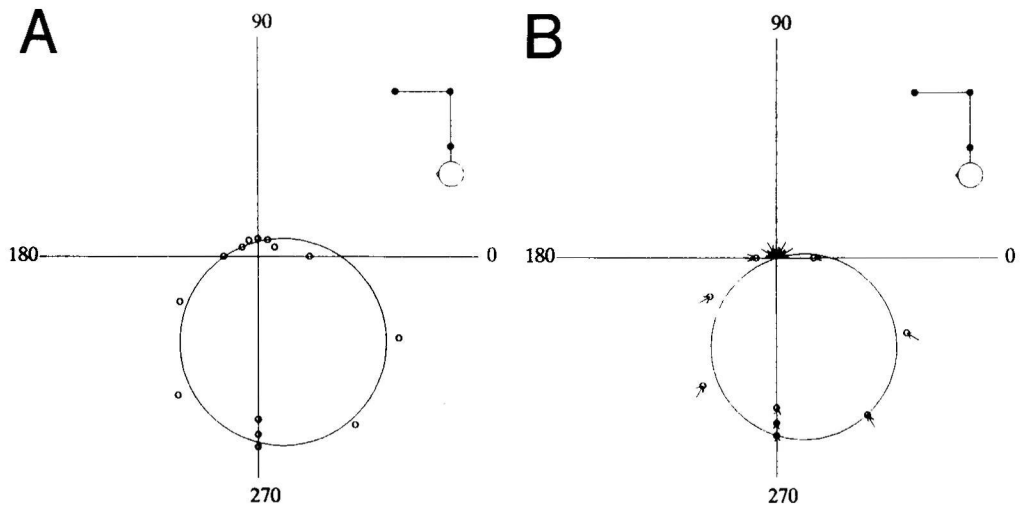


Figure 4.1: Procedure for analyzing EMG data. A: The averaged EMG activity of *m. brachioradialis* obtained for isometric contractions in various directions at a constant force. The distance of each point from the origin indicates the amount of EMG activity in a particular force direction. The orientation of each point indicates the direction of force exerted by the subject. B: The same data after subtraction of the small amount of direction independent background EMG activity. The fitted curves are least RMS error circles through the data points. Inset shows schematically the position of the subject

three subjects, and for 3 s for the last three.

4.2.4 Data Analysis

All EMG signals were digitally rectified prior to their analysis. The isometric data were analyzed first by finding the segment of data within each trial having a stable force of the intended amplitude. Average position and EMG amplitude were subsequently calculated across that time segment, which typically varied in duration between 1.0 and 2.5 s. Next, the average wrist position during these measurements was determined for each block with five isometric trials. Analogous EMG averages were obtained during the isotonic contractions by averaging the data obtained when the wrist was within 6 cm of this average isometric position. Finally, the mean EMG level measured with the relaxed arm in the measurement position was subtracted from each average. By these procedures, a single, average EMG was calculated for each muscle for the isometric and isotonic forces in each direction.

In order to compare our data with earlier predictions based on single motor-unit recordings, it was necessary to transform the "critical firing level" (CFL) curves in joint torque space [55] to constant force EMG amplitude curves in cartesian space. These theoretical considerations have been discussed before [27], and it is sufficient here to note that the linear CFL typical for m. biceps and m. brachioradialis motor-units [106, 55] maps to a circle which passes through the origin. Changes in slope of the CFL are equivalent to changes in orientation of the circle.

We used a two step procedure to fit circles to the average EMG data, as shown in figure 4.1. Figure 4.1A shows a polar plot of the average EMG amplitude for m. brachioradialis during isometric contractions. The force direction is that exerted by the subject. A circle has been fitted to these points, that does not pass through the origin because of the presence of a small amount of background activation in the muscle in the off direction. Rather than force the circle through the theoretically expected point, we assumed that this background activation was present for all directions, and reduced the amplitude of the EMG in each direction by the minimum distance from the circle to the origin. Figure 4.1B shows the shift and the new position of each point and the final fit, which passes through the origin. In most cases, this correction was quite small, usually less than 10% of the maximal activity.

4.3 Results

Earlier single motor-unit recordings have suggested a different role for m. biceps and m. brachioradialis during isometric and isotonic contractions [93, 94, 95]. However, these earliest experiments tested activation in only one direction, and hence could not address the possible direction dependence of the effect. Our own experiments have been designed to investigate this effect and further to elucidate the source of the apparent differences.

4.3.1 Isometric Contractions

Figure 4.2 is a polar plot of averaged EMG activity during isometric contractions as a function of the direction of applied force. The direction corresponds to the direction of the force vector exerted by the subject. The open symbols indicate m. biceps activity and the filled symbols indicate that of m. brachioradialis. A circle has been fitted to each set of data points using the technique described earlier. Two parameters may be obtained from the best fit circle, namely the radius and the location of the center. The latter parameter defines the orientation of the circle, and hence the direction of maximal activation of the muscle, while the radius is a measure of the magnitude of the activity.

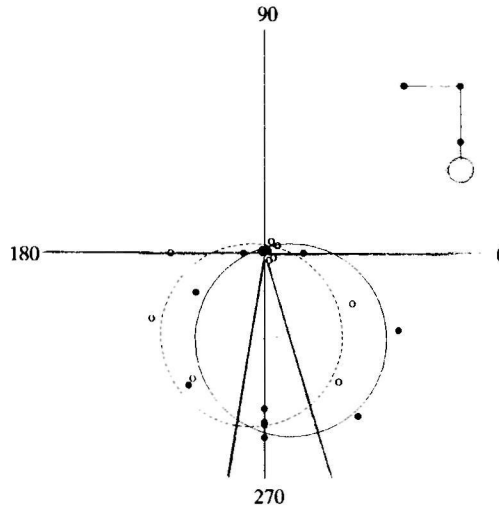


Figure 4.2: Polar plot of averaged EMG activity in m. biceps caput longum (open symbols) and m. brachioradialis (filled symbols) for isometric contractions after correction for background EMG activity. The circles (broken and solid lines) are the best fit circles for m. biceps and m. brachioradialis, respectively. The different orientations reflect the different mechanical roles of mono- and biarticular muscles. Note that the activation in direction 270° was typically measured several times as a control

In this example, the activity of both muscles is well described by the circles, which have clearly different orientations, consistent with the different mechanical actions of the two muscles. M. brachioradialis crosses only the elbow joint and has no direct role in producing torques at the shoulder. M. biceps, however, is a biarticular muscle, contraction of which causes flexion torque at the elbow and anteflexion torque at the shoulder. The orientation of m. biceps activation is shifted with respect to that of m. brachioradialis by -26° , such that it has greater activity in the directions which require shoulder anteflexion torque.

Table 4.1 lists the orientations of these muscles for all subjects tested and indicates that, with two exceptions, the relative orientation of the data for these muscles was similar to that shown in figure 4.2. Subject CD was tested twice, and each time had large biceps activity in nearly all directions, making the orientation of the best fit circle essentially meaningless. The activity in extension directions may have been the result of co-contraction intended to stiffen the limb. There was, however, no corresponding m. triceps activity in the flexion directions. The m. brachioradialis data from subject TT were fitted only very poorly by the circle, with the result that

EMG	Subject	Direction(°)		Shift(°)	Ratios		Force (N)	
		IM	IT		Ratio	270°	IM	IT
M biceps	CD1	*	*	*	*	1.9	27.7 ± 0.3	-
	CD2	*	287	*	*	1.8	16.6 ± 1.0	16.6 ± 0.6
	EO	261	259	-2	1.7	1.7	24.2 ± 0.9	-
	LM	215	246	31	1.3	2.6	15.5 ± 0.2	15.3 ± 0.4
	MT1	232	238	6	1.6	1.5	24.2 ± 0.8	-
	MT2	220	259	39	2.3	2.6	31.1 ± 0.8	30.5 ± 0.6
	PS	243	*	*	*		23.8 ± 1.1	-
	TT	250	257	7	1.9	2.3	26.9 ± 0.1	-
M Bra-Rad	CD1	293	293	0	1.3	1.7		
	CD2	281	283	2	1.1	1.5		
	EO	287	276	-11	1.2	1.2		
	LM	265	259	-6	1.5	1.7		
	MT1	290	277	-13	1.2	1.3		
	MT2	301	291	-10	1.7	2.4		
	PS	241	237	-4	1.3			
	TT	*	285	*	*	2.7		
M triceps longum	CD1	62	74	12	1.7			
	CD2	90	93	3	1.6			
	EO	82	96	14	1.0			
	LM	65	72	7	1.1			
	MT1	73	88	15	1.1			
	MT2	72	82	10	1.3			
	PS	68	*	*	*			
	TT	85	76	-9	1.5			
M triceps lateralis	CD1	-	-	-	-			
	CD2	107	108	1	1.4			
	EO	54	83	29	1.1			
	LM	81	99	17	2.4			
	MT1	68	81	13	1.1			
	MT2	65	83	18	1.2			
	PS	64	*	*	*			
	TT	101	111	10	2.3			

Table 4.1: EMG and force data during isometric (IM) and isotonic (IT) conditions. Columns 3 and 4 list the orientation of the best fit circle. Column 5 indicates the difference between the two conditions. No entry is made for those cases in which either condition was not adequately fit by the circle. Columns 6 and 7 give the ratio of the radii of the best fit circles in the IT and IM conditions and the mean activations in direction 270°, respectively. The mean and standard deviation of the forces are indicated in the last two columns. The symbols - and * stand for not measured and unacceptable fit, respectively.

its orientation was inappropriately skewed in the negative direction from the cluster of points having greatest EMG amplitude. In the remaining cases the orientation of the circle was a reasonable estimate of the direction of maximal muscle activation. The different orientation of data for m.biceps and m. brachioradialis for these five cases appeared to be statistically significant in an analysis of variance ($F(1,4) = 9.00$; $p < 0.05$).

Both heads of m. triceps were oriented approximately opposite the two elbow flexors. Across all subjects, there was no consistent difference between the orientation of caput longum and laterale of m. triceps during isometric activation.

4.3.2 Comparison of Isometric and Isotonic Activation Direction

Figure 4.3 contains two plots similar to those of figure 4.2. The filled symbols in figure 4.3A indicate the activity of m. biceps during isometric force production while the open symbols are those of the isotonic condition. Data were collected for this subject at 15 intervals, centered approximately on the maximal activation directions of the elbow flexors and extensors. As a result, a portion of the active region of m. biceps was not measured. Nonetheless, the circles fit the existing points quite well, and reveal a distinct shift of the isotonic activation toward the positive direction.

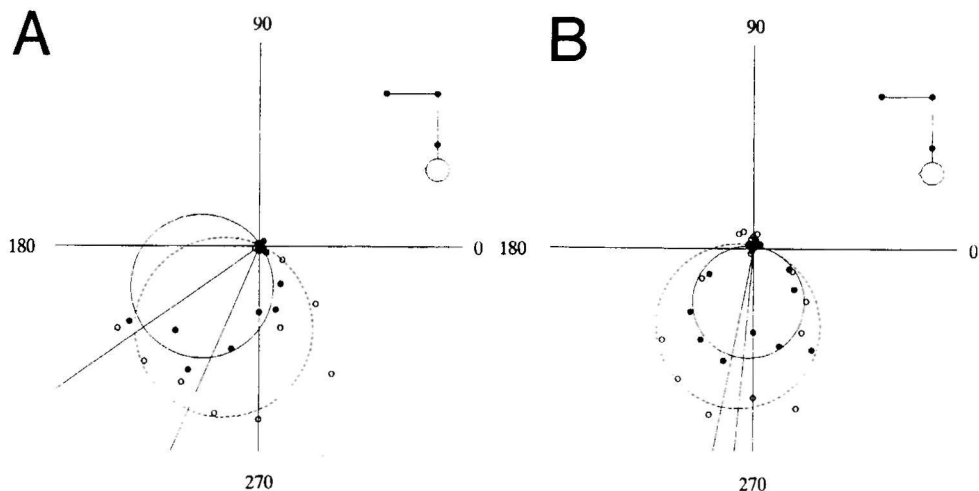


Figure 4.3: Polar plots of averaged EMG activity in m.biceps caput longum (A) and m.brachioradialis (B). Filled and open symbols refer to EMG activity in isometric and isotonic conditions, respectively. The different orientations of the fitted circles reflect the different roles of these muscles during isometric and isotonic contraction

Figure 4 3B shows the activity of *m* brachioradialis, obtained simultaneously with the data in figure 4 3A. It indicates a shift of considerably lower magnitude in the negative direction.

The isotonic *m* biceps and *m* brachioradialis orientation directions for all subjects are listed in table 4 1 along with the isometric orientations. With the exception of subject CD noted above, the shift in orientation of *m* biceps activity between the isometric and isotonic conditions was either positive or not significantly different from zero. A Wilcoxon rank sum (WRS [61]) test applied to the seven reliable cases indicated that the shift in orientation was significant ($p < 0.05$). For *m* brachioradialis, there was a negative or zero shift in all cases except that of subject TT, for whom, as noted above, the orientation of the circle was inappropriate. The WRS test applied to data from all subjects except TT indicated that the difference in orientation for isometric and isotonic contractions was significant ($p < 0.05$) for *m* brachioradialis. During isotonic force production, the orientation of maximal EMG activity of both heads of *m* triceps tended to shift toward more positive directions. However, only for the lateral head the shift statistically was significant (WRS test, $p < 0.05$).

4.3.3 Comparison of Isometric and Isotonic Activation Magnitude

Table 4 1 lists the force levels for each subject, expressed as the mean and standard deviation across all trials. The force variation within the measurement period of an individual trial was generally smaller than the variation across trials. Since we were unable to measure the isotonic force directly for the first five subjects, only the isometric force is listed in the table. It may be that in these cases the isotonic force was several Newtons larger than the isometric force because of the small amount of additional friction force in the motor. In the other experiments, force was the same in the isometric and isotonic condition.

Figure 4 3 shows data for isometric and isotonic contractions. In these trials, isometric and isotonic forces were closely matched for this subject. However, the isotonic activation was significantly larger than the isometric. The ratios of the radii of the fitted circles were 1.25, 1.45, 1.1 and 2.4 for *m* biceps, *m* brachioradialis, and *caput longum* and *laterale* of *m* triceps, respectively. Table 4 1 lists the corresponding radii for all other subjects. The ratio was never less than 1.0, although in a few cases it was not significantly different from 1.0.

The ratio of isotonic to isometric activation in the direction of 270° is of particular interest because it corresponds to the single direction tested in the motor-unit experiments referred to earlier [93, 94, 95]. In those experiments, *m* biceps motor-units were recruited at lower forces isotonicly and fired at a higher rate, while *m*

brachialis and m. brachioradialis motor-units were recruited only at somewhat higher forces isotonically. Therefore, we would expect to find the isotonic enhancement of m. biceps activation and EMG to be greater than that of m. brachioradialis. For the subject shown in figure 4.3, average isotonic m. biceps EMG activity was 2.6 times greater than the isometric average, while that of m. brachioradialis increased only 1.7 times. Table 4.1 lists the corresponding ratios for all subjects, and indicates a similar relation between these muscles for all but subject TT. Although the difference was not statistically significant at a 5% level, the trend is qualitatively consistent with the earlier observations of Tax and colleagues.

Figure 4.3 suggests that this effect is at least partially due to the shift in orientation of the circle that describes the muscle activation in the isometric and isotonic conditions, and is not simply the result of an intrinsic difference between isometric and isotonic activation. For example, despite the generally increased EMG activity during isotonic force production, directions between 150° and 225° have ratios of approximately 1 or less than 1. Therefore, the relative contribution of m. biceps and m. brachioradialis in isometric and isotonic conditions depends on the direction of the force or movement.

4.4 Discussion

The main result of this study is the finding that the relative activation of elbow flexors and extensors is different in isometric and isotonic contractions. The shifts in orientation of EMG activity which occurs isotonically are in opposite directions for mono- and biarticular flexor muscles in the human arm. Earlier Tax et al., [93, 94, 95] showed that the activation of m. biceps, m. brachioradialis, and m. brachialis is different for isotonic and isometric conditions. These authors found that the recruitment threshold for motor-units in m. biceps was lower for isotonic than for isometric contractions. In addition, the firing rate at recruitment was higher for isotonic flexion movements than for isometric contractions. For m. brachioradialis just the opposite effects were found, both for the recruitment threshold as well as for the firing rate at recruitment. These observations may explain why the ratio of EMG activities for isotonic and isometric contractions was higher for m. biceps than for m. brachioradialis. However, they cannot explain why the ratio exceeded 1 for m. brachioradialis. If the recruitment threshold is raised and the firing rate is decreased in isotonic contractions, one would expect to measure a lower EMG activity with surface electrodes. The low movement velocity makes the force-velocity relationship an unlikely explanation. Another possible explanation, co-contraction of antagonistic muscles, could also be ruled out since m. triceps was not active for contractions in the direction

270°. The clarification of this issue requires combined recordings of muscle activity with surface and intramuscular electrodes, which will be the object of further study.

The shift in EMG activity as a function of the direction of force can be understood from a functional point of view. For example, the monoarticular brachioradialis muscle is a pure flexor muscle for the elbow. Based on the mechanical effect of this muscle, the largest activity for isometric contractions would be expected in the flexion direction, i.e. near 270° in figures 4.2 and 4.3. For theoretical reasons, and in accordance with earlier motor-unit studies, during isometric contractions for force directions different from the maximum, we expect the data points to fall along a circle centered on the maximal direction. This agrees quite well with the experimental data (see table 4.1).

Let us now consider the role of m. brachioradialis in isotonic contractions. For contractions in a direction between 180° and 360° a flexion torque at the elbow is required. However, flexion of the elbow is required for movements in a direction between 225° and 45° and elbow extension is required for movements in other directions. This implies that if m. brachioradialis is activated for movements in the region between 180° and 225° against an external force, it must deliver negative work to the movement since it is lengthening. If m. brachioradialis is delivering negative work, other muscles must deliver an amount of work that exceeds that delivered by the hand by at least that amount of energy dissipated by m. brachioradialis. Clearly, this is a rather inefficient way of making this movement.

A means of producing force in these directions with improved efficiency is to assign a larger role to m. biceps. The change in muscle length is much smaller for m. biceps than it is for m. brachioradialis since the lengthening imposed by elbow flexion is (at least partially) counteracted by the simultaneous flexion of the shoulder. Therefore, this hypothesis predicts a shift in orientation of the circle that describes the data for isometric contractions for m. biceps and m. brachioradialis. In directions between 270° and 315° a similar conflict between shoulder torque and change in shoulder angle also predicts a larger role for m. biceps. Since m. biceps also contributes to elbow torque, it predicts a smaller activation for m. brachioradialis.

Two important conclusions follow from these considerations. First, a larger role is predicted for m. biceps in directions between 180° and 225° and between 270° and 312°. A consequence may be that a circle no longer describes the activation of m. biceps in the isotonic condition, which may explain the deviation of the data from a circle that was obtained for some subjects. Secondly, the decreased activation of m. brachioradialis for contractions in the region between 270° and 315°, which corresponds to the shift of the circle in our data to negative directions (table 4.1), can only be understood if one notices the increased activation of m. biceps in this region. This illustrates the point, made earlier by van Zuylen et al. [106], that the activation

of a muscle can only be understood if one takes into account the mechanical effect of all muscles acting across the same joint

A complete analysis of the motor-unit data presented by Tax et al [93, 94, 95] requires a quantitative comparison between motor-unit activity and EMG activity recorded with surface electrodes. For isometric contractions a quantitative comparison can be obtained when some plausible assumptions are made. The first assumption is that a motor-unit is recruited whenever a particular input threshold is exceeded [39]. This implies that all combinations of elbow and shoulder torque for which a motor-unit is recruited correspond to combinations of torque requiring a particular constant input to the motor-unit. Experimental data [55] have shown that the combinations of torques for which a motor-unit is recruited generally fall along a straight line. Since joint torque and force at the hand are related by a linear transformation [47, 27], there is a line in the horizontal force plane that gives all the forces for which the input to the motor-unit is constant.

This line corresponds to the combination of shoulder and elbow torques associated with constant input to the motor-unit during force production in different directions. Note that, under these conditions, the force at the hand is not constant. Since our experiments used constant force in various directions, it follows that the input to the motor-units was no longer constant. A simple geometrical argument shows that the straight line for constant activation transforms to a circle for constant force. Most EMG data in our study are well described by a circle. However, in some conditions, for *m. biceps* in particular, the data were clearly not well described by a circle. Notwithstanding a possible explanation provided earlier, this may also be related to the fact that a population of *m. biceps* motor-units has recruitment torques which do not fall along a straight line, but rather along a concatenation of line segments [106]. The constant-force EMG data should then fall along a concatenation of arcs, each having a different center and radius.

Preliminary data for *m. triceps* indicate that the circle describing EMG activity as a function of force direction also shifts its orientation between isometric and isotonic contractions. This suggests that, in general, the activation of muscles depends on the nature of the motor task in addition to the force being produced (see also [3]). A similar conclusion was reached earlier by Capaday and Stein [6] who found a modulation of the *m. soleus* H-reflex in human walking and standing. Moreover, our results are compatible with the different role of motor-units in the anterior sartorius muscle in the cat during active lengthening and shortening [Loeb 66]. While this confirms that the enormous complexity and flexibility of the motor system is indeed used in typical motor tasks, it also suggests that understanding the flexibility of the motor system will require study of muscle coordination in various movement tasks. The frequently studied activation in isometric contractions may at best provide a

cartoon of the motor system and may be insufficient to allow us to understand the motor system fully.

Chapter 5

The relation between the direction dependence of EMG amplitude and motor-unit recruitment thresholds during isometric contractions.

Adapted from Theeuwen M, Gielen CCAM, Miller LE, Doorenbosch C (1994) The relation between the direction dependence of EMG amplitude and motor-unit recruitment thresholds during isometric contractions. *Exp Brain Res*, in press.

5.1 Abstract

The activation of muscles can be studied by measuring the activity of a representative set of single motor-units in a muscle or by measuring the surface electromyographic (EMG) activity of a muscle that results from the contribution of a large number of motor-units. In this study we have developed a model showing how the direction dependence of the amplitude of the electromyographic activity during isometric contractions can be understood from the recruitment thresholds of single motor-units when force is applied in various directions within a plane. The model predicts that the direction with the largest EMG activity (called the "preferred direction") corresponds to the direction in which the largest number of motor-units is recruited. If

one assumes homogeneous activation of a population of motor-units, this preferred direction can be shown to be equivalent to the direction in which the recruitment threshold of the motor-units is smallest.

The experimental data show that for most muscles in the human arm, the amplitude of surface EMG for a constant, isometric force at the wrist was proportional to the cosine of the angle between the muscle's preferred direction and the direction of force. As predicted by the model, the preferred direction coincided with the direction in which the recruitment threshold of motor-units was smallest.

M. deltoid anterior had a more complicated directional sensitivity for surface EMG that could not be well fit by a single cosine function. This effect could be explained by the finding of two sub-populations of motor-units within that muscle, each with a different recruitment behavior.

5.2 Introduction

Numerous studies have investigated how mono- and bi-articular muscles in the arm contribute to forces imposed in various directions at the wrist. This is not a trivial problem since the same force at the hand can be obtained by different relative contributions of muscles in the human arm. In these studies the contribution of each muscle was estimated either by measuring its surface EMG or by measuring the recruitment behavior of single motor-units.

Buchanan and colleagues [2, 3] measured the variation in the amplitude of EMG activity in human arm muscles for constant isometric forces at the wrist in various directions. Their results demonstrated that these muscles were active over a broad range of force directions. Similar results were obtained later by Flanders and Soechting [21], who fitted cosine functions to the EMG data in order to determine the direction dependence of the activation.

Other studies [32, 106, 93, 94, 95] have recorded the activity from single motor-units. Based on the "size principle" [37, 38, 39] these studies assumed that the force at which a motor-unit is recruited corresponds to a condition of constant input to the motoneuron soma, regardless of the direction of force. Contrary to the cosine fit for the surface EMG data, the recruitment force of motor-units as a function of force direction appeared to depend linearly on joint torques and could be fitted adequately by a straight line [55, 32, 33]. The relationship between joint torques and recruitment threshold was the same for all motor-units in a given population, supporting the notion of homogeneous activation of the motor-unit pool and a fixed recruitment order.

In summary, in these latter experiments, motor-unit activity was studied at equal

levels of excitation in contractions in different directions. By contrast, in the surface EMG experiments, force amplitude was held constant while variation in EMG amplitude was measured as a function of the direction of imposed force.

The relation between surface EMG and single motor-unit activity has been of interest for some time. Summarizing the general agreement in literature, the main contribution of motor-unit activity to the amplitude of surface EMG is by recruitment, while variation in firing rate contributes to a smaller extent [14, 83, 62]. Changes in the firing rate of motor-units, together with the conduction velocity of action potentials along the muscle fibers, have greater impact on the spectrum of the surface EMG signal. Rarely have both methods been used simultaneously for a quantitative analysis in conditions of natural muscle activation, making it difficult to relate the results of both kinds of studies to one another.

In this manuscript we intend to investigate the direction-dependent relation between motor unit recruitment and surface EMG for isometric force in various directions. We have developed a model which describes the relationship between surface EMG and the recruitment behavior of single motor-units. The basic assumption is that there is a homogeneous activation of a population of motor-units and that the recruitment order is determined by the "size principle" [37, 38] which states that when two motor-units receive the same excitation, the order of recruitment is determined by the size of the motoneuron soma. These assumptions predict a similar recruitment behavior for all motor-units in a given population. With the model it becomes possible to predict how the EMG activity of a muscle changes for various directions of isometric force when the recruitment behavior of representative motor-units is known. We have collected both surface EMG and single motor-unit data simultaneously in order to test the underlying assumptions and predictions of this model.

5.3 Methods

The EMG activity of several muscles acting across the elbow (m. brachioradialis, m.biceps caput longum, m.triceps caput longum, m.triceps caput breve) and shoulder (m.biceps caput longum, m.triceps caput longum, m.deltoid anterior, m.deltoid posterior) was measured by means of both surface and intramuscular electrodes during experiments in which subjects exerted isometric forces at the wrist in various directions within a horizontal plane. Data were collected from eight volunteer subjects, six male and two female, ranging in age from 23 to 53 years. None had any known history of neurological or musculoskeletal disorder.

5.3.1 Set up

Because the set up as used for the experiments described in chapters 5, 6 and 7 is almost the same, it will be described here in detail. The explanation about the experimental set up for movements concerns the experiments in chapters 6 and 7 only.

Each subject was seated in a chair with the right arm at approximately shoulder height and supported by a cloth sling (see figure 5.1A). The sling was suspended from the ceiling such that the relaxed arm was maintained in a horizontal position and very little force was required to move the relaxed arm in the horizontal plane. In the standard test position, the upper arm was held in a position of zero degrees ante flexion, the elbow was flexed by 90 degrees, and the forearm was in the mid-prone position.

A lightweight aluminum bracelet was fixed around the wrist of the subject. The bracelet was made to fit tightly but comfortably by forming a mold of elastic dental compound between the bracelet and the subject's wrist. A cable was attached to the bracelet via a yoke, and also to a servo motor. The cable passed through several pulleys on a metal arm that could be rotated about a vertical axis passing through the wrist of the subject (see figure 5.1A). This arrangement allowed the direction of force or movement to be varied within a horizontal plane at shoulder height. This direction was indicated by the angle with respect to the forearm, such that the direction of the vector pointing from the wrist to the elbow corresponded to zero degrees (see figure 5.1B). The angle increased with rotations counterclockwise as in normal polar coordinates. Strain gauges were incorporated in the cables to the yoke and the sling in order to measure force in the horizontal and vertical directions, respectively, the latter due to exo-/endorotation and ab-/adduction torques at the shoulder. The output signals of the strain gauges were displayed on an X/Y oscilloscope in order to assist the subject in controlling the horizontal force and to maintain a constant level of vertical force.

The system could be configured to present either an isometric load or a weak elastic load to the subject. For isometric contractions, the cable was clamped to the metal frame. The total stiffness of the system, including the soft tissues of the wrist, was about $5 \cdot 10^3 \text{ N/m}$ for forces smaller than 10 N and about $4 \cdot 10^4 \text{ N/m}$ for forces exceeding 10 N. As a result, displacements at the wrist of less than 3 mm occurred for forces of 50 N. In the movement condition, the clamp was removed, and the position of the wrist was fed back to the torque motor such that torque was increased in proportion to wrist displacement in order to simulate an elastic load. Typically, force at the wrist increased by 2 N/cm, to which was added a constant force offset.

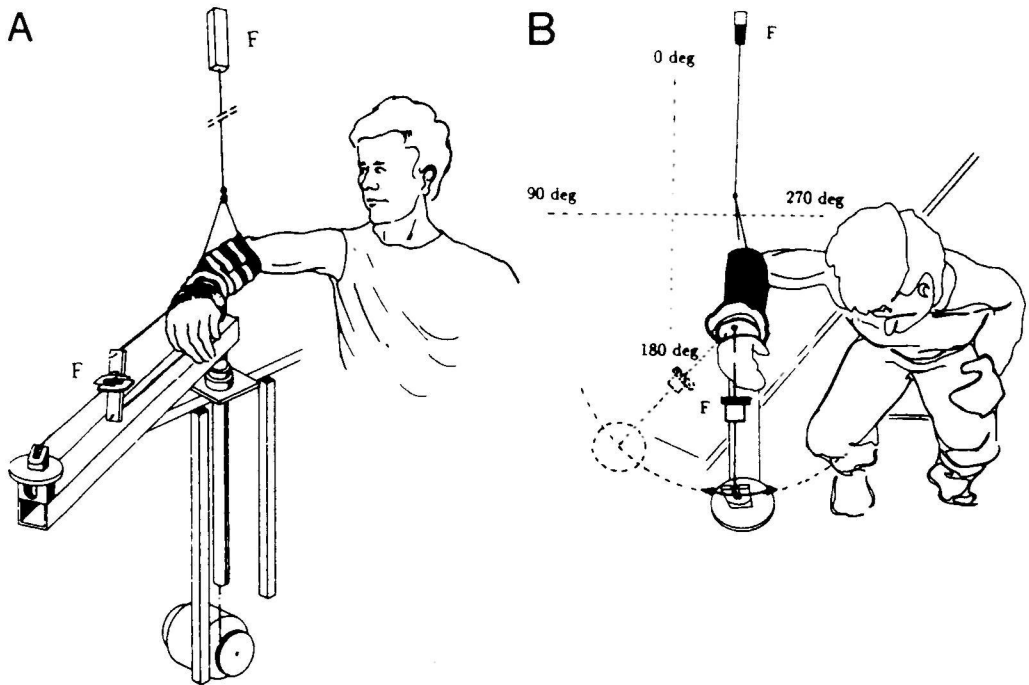


Figure 5.1: Schematic overview of the experimental set-up. Panel A shows a front view. The forearm was suspended by a cloth sling attached to the ceiling such that the relaxed arm was in a horizontal plane. A strain-gauge (indicated by symbol F) in the sling measured forces in the vertical direction. A bracelet was placed around the wrist, and connected to a cable with another force transducer. The cable ran parallel to a metal bar, which could be rotated about a vertical axis through the elbow of the subject. The cable ran across a pulley, then returned to the vertical axis within the metal bar to another pulley located on the vertical rotation axis, from which the cable ran to a torque motor. In the isometric condition, the cable was clamped to the metal frame such that no movement was possible. Panel B shows a top view, explaining the representation of the direction of force and movement.

5.3.2 Experimental paradigm

Subjects were asked to exert slowly increasing isometric forces (rate approximately 3 N/s) from a completely relaxed state to a force of approximately 50 N in various directions in the horizontal plane. Each test direction was selected from a random sequence, and tested three times in succession. Between each new direction, the EMG activity was measured with the arm in a completely relaxed condition in order

to correct the EMG signals for background activity. For a typical subject a force of 50 N in elbow flexion direction corresponds to approximately 25% of maximum voluntary contraction (MVC) in the flexion direction. However, since MVC is substantially less for different force directions, 50 N fell in the range from 25% to 50% over the whole range of directions. Therefore, we have expressed force in Newtons, rather than in terms of %MVC, which is direction dependent.

5.3.3 Surface EMG

Surface EMG data were collected using Ag/AgCl surface electrodes. The signals were differentially amplified and filtered with a 50 Hz notch filter and a fourth order Bessel filter with a passband of 10-150 Hz. The signals were sampled with a 12 bit A/D converter at 400 Hz. Force signals were simultaneously sampled at 400 Hz and could be measured with an accuracy of 0.1 N.

The surface EMG data were digitally rectified, and the mean rectified EMG activity was measured in the period when the force was within 15% of a fixed test force (typically 40 N). Next the mean EMG activity for a given direction was obtained by averaging over the three test trials. Finally, the rest EMG signal, determined when the muscle was relaxed, was subtracted from the mean EMG amplitude obtained in the isometric trials. By these procedures, a single, average EMG value was calculated for each muscle and each direction. Polar plots were constructed of the EMG amplitude as a function of the direction of the applied force, and for reasons explained in the Theory section, a circle passing through the origin was fitted to these data.

5.3.4 Intramuscular EMG

Bipolar recordings of single motor-unit activity were obtained between a pair of nylon coated, 25 μm diameter wires inserted into the muscle within a hypodermic needle. The needle was inserted into the muscle between the two surface electrodes in an effort to record signals from the same part of the muscle. Typically four of those wires were inserted in a single needle, and the best pair was selected for the recording. After insertion of the wires, the needle was removed.

The intramuscular signals were differentially amplified and filtered with a fourth order Bessel filter with a passband of 300-5000 Hz and recorded on an FM tape recorder, for later off-line processing. Single motor-units were discriminated using a window discriminator. Typically one or two motor-units could be detected in each signal. The window discriminator detected action potentials with positive (negative) peaks above (below) an adjustable threshold level, but rejected action potentials which also exceeded a second higher (lower) level. Only peaks of waveforms with

amplitudes within the window formed by these threshold levels were accepted. Occasionally a third or fourth motor-unit was present. In that case discrimination by the window discriminator was in general not possible due to overlap of peak amplitudes with the first or second motor-unit. In those cases when action potentials of multiple motor-units were present, the data-analysis was done with the commercially available BrainWave spike analyser. The discrimination process was visually controlled to ensure that all detected peaks belonged to the same motor-unit. This was done by displaying the sampled action potentials on a computer monitor to check for irregularities in motor-unit firing and to check for a constant action potential shape. Moreover, it was verified that the shape of the action potentials of the motor-units was the same for all directions of exerted force. The order in which the motor-units became active never changed, even for different directions of force.

The moment at which the motor-unit became active with a regular firing pattern was compared with the force record, and the force at recruitment was determined for each trial. Trials during which motor-units were firing irregularly were excluded from analysis. Polar plots were constructed for the recruitment force data as a function of the direction of applied force. Straight "recruitment lines" were fitted to the data points. These lines are similar to the critical firing level lines of ter Haar Romeny et al. [32] and van Zuylen et al. [106]. The recruitment lines represent lines of constant input to the motor-units, according to the size principle [37, 38].

To summarize, in these experiments we collected two types of data, each offering a different measure of muscle activation. The direction of force was varied, and data were collected during slow ramp increases of force. The amplitude of surface EMG activity was measured as the ramp passed through a fixed test level, while motor-unit recruitment was determined by measuring the force at which a given motor-unit first became active. The surface EMG reflects the activation of (or input to) the muscles, which varied as a function of direction during constant force (or output). The recruitment threshold reflects a constant level of excitation (input) to the motor-unit during varied force (output).

5.4 Theory

In this section we will show theoretically, that given a population of motor-units, one can transform the direction dependent recruitment thresholds of the motor-units into the surface EMG activity of the muscle which would result from a constant force in various directions. The transformation requires that we make four assumptions. 1) A homogeneous activation of the motoneuron pool of the population of motor-units. 2) That the response of single motor-units to activation (both in terms of recruitment

and firing rate) is constant and independent of the direction of force 3) Because motor-units are recruited according to the size principle [39], muscle activation and the amplitude of surface EMG are constant whenever a given motor-unit is recruited 4) A linear force-EMG relationship (that has been reported frequently in the literature [80, 65, 30], such that linear interpolation of EMG activity can be used to predict EMG activity at any force level

Results obtained earlier by ter Haar Romeny et al [32, 33] and by van Zuylen et al [106] for motor-units in the human arm during isometric flexion/extension and supination/pronation contractions, demonstrated that recruitment thresholds fell on straight parallel lines when displayed in a polar plot as a function of the direction of exerted force The same observation was made in this study This observation, which will be extensively documented later in this paper, will be used to derive a relation between motor unit recruitment thresholds and surface EMG

Figure 5 2A is a polar plot displaying the recruitment thresholds (as distance to the origin) for three hypothetical motor-units These recruitment thresholds correspond to points of constant activation of the muscle The concentric circles correspond to circles of constant force In figure 5 2B the recruitment thresholds of each motor-unit are connected to several parallel "recruitment lines" Recruitment lines are lines of constant activation and thus of constant surface EMG activity A given force in the direction perpendicular to these lines would activate the greatest number of motor-units, and cause the largest surface EMG activity In other directions, fewer motor-units would be activated, and there would be proportionately less surface EMG activity Only the component of the force perpendicular to the recruitment lines contributes to a higher surface EMG activity This component (and hence the surface EMG amplitude) is proportional to the cosine of the angle between the direction of exerted force and the direction of the normal to the recruitment lines

Given a linear EMG-force relationship, surface EMG activity is proportional to the component of the exerted force perpendicular to the recruitment lines The direction orthogonal to the recruitment line is indicated by ϕ_r For a force F in a particular direction ϕ , the amount of surface EMG activity EMG is then given by

$$EMG = cF \cos(\phi - \phi_r) \quad (5.1)$$

with c a proportionality constant EMG activity for various directions is given by Equation (1) If the force F remains constant for all directions, this equation describes a circle of radius $\frac{cF}{2}$ which passes through the origin, and has its center in the direction ϕ_r (see figure 5 2C) By measuring both motor-unit recruitment and surface EMG amplitude simultaneously, we have the means to test this model of the relation between the two types of signals

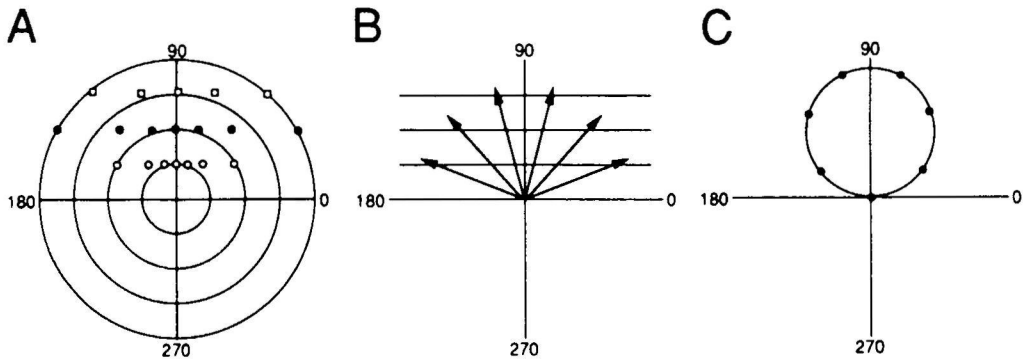


Figure 5.2: Panel A shows recruitment thresholds for three hypothetical motor-units (one symbol for each motor-unit) for various directions. The circles are circles of constant force. Connecting all recruitment thresholds of each motor-unit as done in panel B, yields parallel lines (recruitment lines). On each line the activation of the muscle and hence its surface EMG are constant. For illustrative purposes some forces are indicated by arrows. Only the component of the forces at the wrist orthogonal to these lines contributes to an increase in muscle activation and EMG. In case of a linear force-EMG relationship, EMG is proportional to the component of the force orthogonal to the recruitment lines. For a constant force EMG amplitudes fall on a circle through the origin and with a center in the direction orthogonal to the recruitment lines (panel C).

5.5 Results

In the course of these experiments, we have recorded data from a total of 50 motor-units together with surface EMG from the same muscles. A significantly larger number of motor-units were recorded without simultaneous EMG. These additional-units reinforced our observations, but were not included in the primary quantitative analysis.

One of the model assumptions was that of a linear EMG / force relationship. This relation could be verified experimentally for our experimental conditions. Figure 5.3 shows these data for *m.brachioradialis*. The various symbols refer to surface EMG activity recorded for force applied in several different directions. For all directions, there was a linear relationship, with correlation coefficients of 0.97, 0.99, 0.98, and 0.99 for directions 0 deg, 300 deg, 270 deg, and 240 deg, respectively. Similar results were obtained in all other muscles for all subjects, for force levels up to approximately 40 N, which corresponds to approximately 20% of maximal voluntary contraction in the direction 270 deg. Correlation coefficients for all directions fell in the range

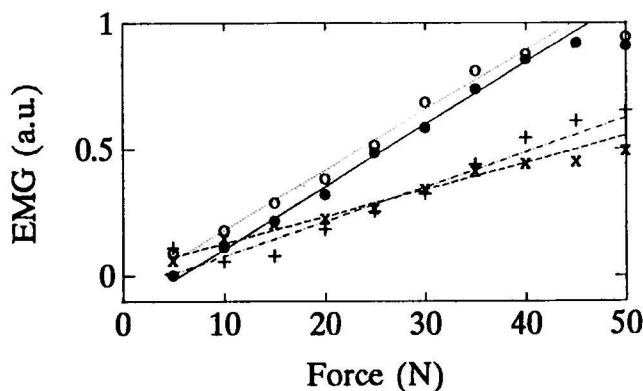


Figure 5.3: EMG-force relationship for various directions of isometric force. EMG was measured with surface electrodes from *m. brachioradialis*. The EMG at rest for each direction has been subtracted. Different symbols refer to data obtained for different directions of isometric force (+: 0 deg; x: 240 deg; o: 270 deg; •: 300 deg). Deviations from a linear relationship become apparent at forces higher than 40 N.

0.92-0.99.

5.5.1 Quantitative comparison between motor-unit data and EMG data.

Figure 5.4A shows recruitment forces of two motor-units in *m. brachioradialis* obtained during a single experiment. The recruitment forces are plotted in polar coordinates as a function of the direction of applied force. The inset figure indicates the orientation of the trunk, the upper arm, and the forearm of the subject as explained in the methods (see also figure 5.1).

Figure 5.4A shows that the force necessary to recruit a motor-unit was different for forces in different directions. This corresponds to constant muscle activation resulting from changing force at the wrist. The recruitment forces for these two motor-units in this figure were well fitted by straight lines. The orientation of these lines may be described by their normal (\vec{F}_r). The motor-unit was recruited at the lowest force level for forces in the direction of this normal. The orientations of the recruitment lines for the two motor-units shown in figure 5.4A were 300 deg (S.D. 2 deg) and 292 deg (S.D. 7 deg), which were essentially parallel, within experimental accuracy. With the exception of *m. deltoid anterior* (described below), this was generally true for all motor-units from a given muscle (see also figure 5.5 and table

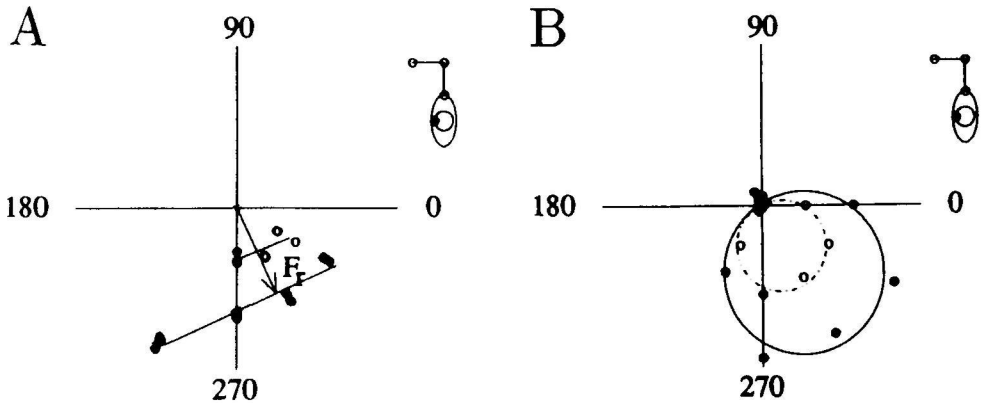


Figure 5.4: The force at recruitment of 2 motor-units for various directions of isometric force is indicated in panel A in polar coordinates (i.e. the recruitment force corresponds to the distance from the origin). Different symbols refer to recruitment thresholds of different motor-units. A straight line is fitted to the data for each motor-unit. Panel B shows the amount of EMG activity for a constant isometric force in polar coordinates. The amplitude of EMG is represented by the distance of the symbol to the origin. The different symbols refer to constant force levels of 25 N (open circles) and 40 N (filled circles). A circle is fitted to the data for each force level. Note that different-units are plotted in panels A and B. Symbols in the polar plots in A and B represent forces and EMG, respectively.

5.1). We will therefore assume that forces at recruitment for the motor-units from a single muscle lie on straight parallel lines or line segments, as already indicated by the results of ter Haar Romeny et al. [32, 33] and by van Zuylen et al. [106].

Figure 5.4B shows a polar plot of EMG data, obtained in the same experiment from the same muscle as the motor-unit data shown in figure 5.4A. Each point shows the mean, rectified surface EMG as a function of the direction of the force exerted at the wrist. For this example, the model appears to be well supported. The recruitment thresholds of the two motor-units are well described by straight, parallel lines, and the surface EMG is well fitted by a circle. Furthermore, there is close correspondence between the orientation of the two recruitment lines and that of the fitted circle. In the following section we will give a quantitative comparison of these characteristics for a larger number of cases.

Figure 5.5A shows a polar plot of the forces at recruitment for three motor-units recorded simultaneously in the m.brachioradialis for a second subject. The orientations of the recruitment lines describing the recruitment data for these motor-units

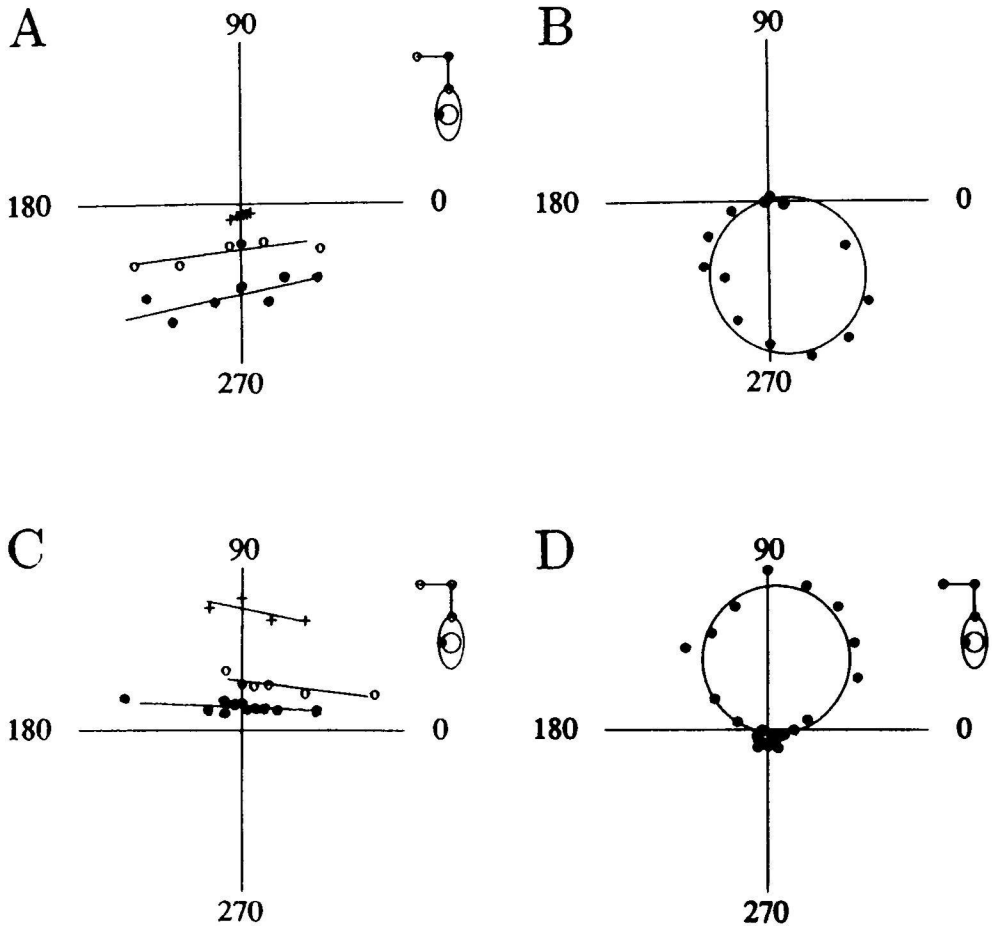


Figure 5.5: Forces at recruitment of motor-units for isometric contractions in various directions are indicated in the panels A and C. The distance of the symbols to the origin corresponds to the recruitment force. Different symbols refer to recruitment forces of different motor-units. Straight lines are fitted to the data of each motor-unit. The data in panel A was obtained from m. brachioradialis, in panel C from m. triceps caput lateralis. Panels B and D show EMG activity for a constant force in various directions obtained simultaneously by surface electrodes from the same muscles as the recruitment data shown in panels A and C, respectively. The distance from the symbols to the origin corresponds to the amplitude of the EMG-activity in that direction for a force of 40 N. Circles are fitted to the data.

are 267 deg (S.D. 2 deg), 281 deg (S.D. 4 deg) and 288 deg (S.D. 2 deg) for the motor-units with the low, middle, and the high recruitment thresholds, respectively. The corresponding correlation coefficients were 0.86, 0.86 and 0.93. The mean correlation coefficient for all motor-units recorded from m. brachioradialis from all subjects was 0.84 (S.D. 0.13). For all motor-units in m. brachioradialis the correlation coefficient was significant at a 5% level. Therefore, the hypothesis that recruitment data may be represented by straight lines appears to be valid for this muscle.

Figure 5.5B shows a polar plot of mean, rectified EMG activity for m.brachioradialis which was recorded simultaneously with the motor-unit data shown in figure 5.5A. As in figure 5.4B, this circle fits the surface EMG activity quite well, in agreement with earlier results [27]. In figure 5.5B, the circle is oriented in a direction of 285 deg (S.D. = 3 deg). This orientation agrees quite well with the mean orientation of the recruitment lines for the three simultaneously recorded motor-units shown in figure 5.5A (279 deg ; S.D. = 11 deg). The orientation is also very close to that of the recruitment lines for all recorded motor-units from m.brachioradialis (286 deg ;S.D. = 10 deg, see table 5.1). Table 5.1 summarizes the orientation of the surface EMG data and the simultaneously recorded motor-units for a variety of subjects and muscles. Any differences in orientation between intramuscular and surface electrode data were not significant for any subject. Table 5.1 includes only data for subjects from which surface EMG and intramuscular activity were recorded simultaneously.

Figure 5.5 also shows data from another mono-articular elbow muscle, the m.triceps caput laterale. Panel C shows recruitment forces for individual motor-units while panel D shows the corresponding mean surface EMG activity at a fixed force level. The recruitment data are well described by straight, parallel lines, and the surface EMG data are well described by a circle having approximately the same orientation as the recruitment lines (83 deg. for EMG versus 88, 89, and 94 deg for the three motor-units recruitment lines). For all subjects, there was also a close correspondence between the orientation of the EMG data and the orientation of the motor-unit recruitment lines (see table 5.1), as for m. brachioradialis. The orientation of the circles was slightly different for different subjects. However, this variability was not significantly different from the variability in the orientation of the motor-unit recruitment lines (SD - 17 deg. for surface EMG and 9 deg. for the motor-unit data). The variability between subjects was almost the same for the lateral head of m. triceps as for m. brachioradialis.

The data in figure 5.5 clearly suggest that a straight line provides a good description of the motor-unit recruitment thresholds for these muscles. The mean correlation coefficient between recruitment data and recruitment lines for all muscles was 0.75 (S.D. 0.17). A statistical analysis revealed that the linear correlation coefficient calculated for each set of motor-unit recruitment thresholds, was significant with respect

Subject	Surface EMG	Recruitment Line
Biceps Caput Longum		
EO	247(5)	268(6)
BC	265(6)	254(3)
LM	217(2)	273(9)
MF	269(4)	264(5)
MT	274(10)	239(6), 274(4)
CD	275(3)	272(2), 279(6)
Brachioradialis		
EO	285(2)	267(2), 281(4), 283(9), 288(2)
MT	287(6)	291(2), 283(4)
CD	301(2)	292(7), 300(2)
Triceps Caput Longum		
BC	71(4)	92(5), 94(10)
LM	100(2)	82(2)
MF	70(2)	95(7)
MT	73(3)	90(8), 80(13)
CD	88(5)	82(3)
Triceps Caput Lateralis		
LM	112(4)	102(3), 74(4)
MT	64(3)	80(6)
CD	88(5)	91(9)
SG	94(5)	74(3), 91(3)
AM	83(3)	88(1), 89(2), 94(2)
Deltoideus Anterior		
LM	199(3)	181(7), 183(4)
MF	206(3)	99(4)

Table 5.1: This table contains the mean directions and standard deviations of circle fits for surface EMG at constant forces in various directions (middle column) and for recruitment lines for single motor-units in various directions (right column). The fits are listed for the muscles m.biceps caput longum, m.brachioradialis, m.triceps caput longum, m.triceps caput lateralis and m.deltoideus anterior. For each muscle the fits are given for each subject. Each circle fit corresponds to a single experiment. The multiple data for each recruitment line in the right column corresponds to recruitment data of single motor-units obtained during the same experiment from which the surface EMG data were obtained.

to a 5% significance level for 35 out of 41 motor-units. For the other 6 motor-units, the variability in recruitment threshold was relatively large. However, there was no indication for any of the remaining 6 motor-units, that a significantly better fit could have been obtained by a smooth nonlinear function. Therefore, we conclude that the motor-unit recruitment data for these muscles lie on straight lines, in accordance with earlier reports by van Zuyl en et al. [106] and Jongen [55].

Figure 5.6 shows data for two bi-articular muscles. Recruitment thresholds for a motor-unit in *m.biceps caput longum* are shown in figure 5.6A, and the corresponding surface EMG data in figure 5.6B. For *m.triceps caput longum* the same types of data are shown in figures 5.6C and 5.6D. Since both these muscles act across both the elbow and the shoulder joints, their preferred directions differ from those of their mono-articular synergistic muscles. The preferred direction falls between the directions of maximal shoulder flexion and elbow flexion for *m.biceps caput longum* and between the directions of maximal shoulder extension and maximal elbow extension for *m.triceps caput longum*. For these bi-articular muscles, the EMG data and motor-unit data were in good agreement (see table 5.1) just as for the mono-articular muscles. The mean orientation of the motor-unit data was 265 deg (12 deg) and 83 deg (16 deg) for *m. biceps caput longum* and *m. triceps caput longum*, respectively. The corresponding preferred directions for EMG data were 255 deg (19 deg) and 72 deg (14 deg). Within experimental accuracy, the preferred directions for motor-unit activity and EMG were the same. For each of these bi-articular muscles, only a single population of motor-units was found, and all EMG data were fitted adequately by a circle. Hence, despite their more complicated mechanical actions, the bi-articular muscles behaved in a fashion similar to the mono-articular muscles with respect to their orientation selectivity.

Unlike all other muscles we tested, our data reveal a good correspondence between the surface EMG preferred directions and the recruitment lines for most, but not all motor-units in *m. deltoid anterior*. Although the number of motor-units recorded in *m. deltoid anterior* was relatively small, for three out of eight subjects we found that they tended to fall into two different groups. One group of motor-units ($N = 5$) had recruitment lines which were oriented very near to those of the surface EMG data. A second group of motor-units ($N = 4$) had recruitment lines orientated nearly 90 degrees away from those of the first group. This is illustrated in figure 5.7, which shows recruitment forces for two different motor-units that were collected in a single session, along with surface EMG. Panel A shows motor-unit data for which the correspondence between recruitment line and preferred direction (in panel C) was as good as for any of the other muscles described earlier. However, panel B shows motor-unit data, in which the orientation of the recruitment line does not correspond to the preferred direction of EMG, but differs from it by about 90 deg., despite

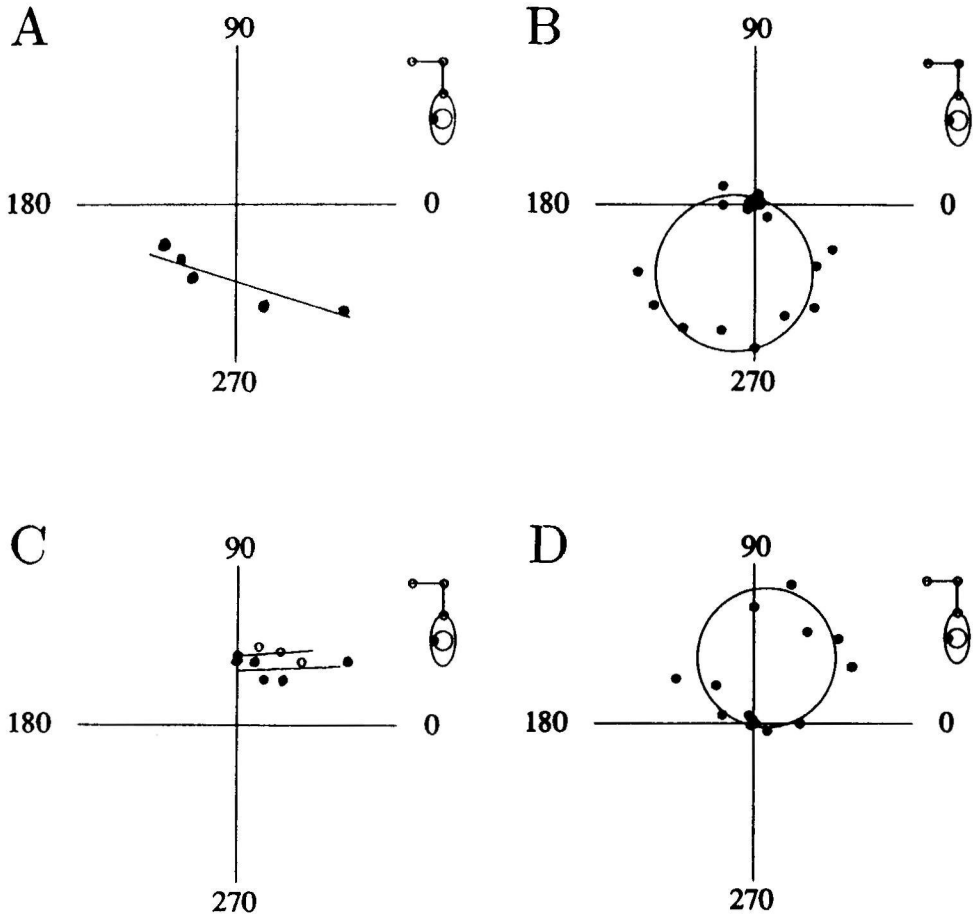


Figure 5.6: Forces at recruitment of motor-units in bi-articular muscles for isometric contractions in various directions are indicated in the panels A (m. biceps caput longum) and C (m. triceps caput longum). The distance of a symbol to the origin corresponds to the recruitment force. Different symbols refer to recruitment forces of different motor-units. Straight lines are fitted to the data of each motor-unit. Panels B and D show the EMG activity obtained by surface electrodes simultaneously with the recruitment data shown in panels A and C, respectively. The distance from the symbols to the origin corresponds to the amplitude of the EMG-activity in that direction for a force of 40 N. Circles are fitted to the data.

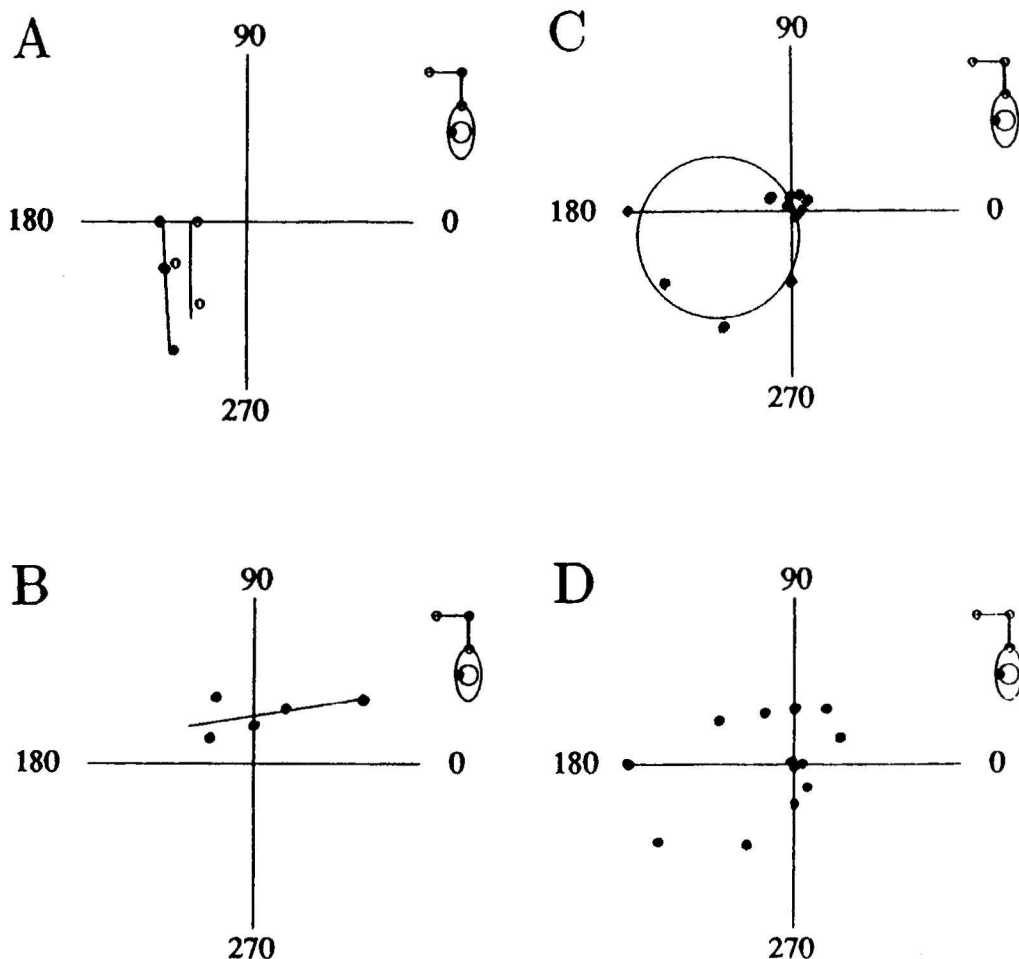


Figure 5.7: Forces at recruitment for motor-units from two subpopulations in m.deltoideus anterior for isometric contractions in various directions are indicated in panels A and B. The distance of a symbol to the origin corresponds to the recruitment force. A straight line is fitted to the data. Panels C and D show EMG activity of m.deltoideus anterior for a constant isometric force (40 N) in various directions. Data in panels A and B were obtained simultaneously with the EMG data shown in C. A circle is fitted to the data. In panel D the contribution of two subpopulations of motor-units, examples of which are shown in panels A and B, results in a surface EMG activation which no longer can be fitted by a single cosine function. Two lobes of activity are centered around the directions orthogonal to the subpopulation recruitment lines.

the fact that the intramuscular wire electrodes for both motor-unit recordings were inserted in between the two surface electrodes. For each of the individual motor-units which showed a behavior as illustrated in figure 5.7B, the correlation coefficient of the recruitment data with the straight recruitment lines was higher than 0.75, the mean correlation coefficient for all motor-units. Therefore, there was no indication that these motor-units had a recruitment behavior which did not correspond to data falling on a straight line.

The discrepancy between the orientation of surface EMG and that of the motor-unit recruitment data appeared to be very consistent in repeated experiments. For all contractions (typically at least 30 contractions for each motor-unit) we found a consistent recruitment behaviour. Since we found both types of motor-units simultaneously during one single experiment, it is unlikely that co-activation or a different activation due to a different interpretation of the motor task [94, 95] could explain the difference. The most plausible explanation seems to be that m. deltoid anterior has several sub-populations of motor-units, each activated with different directional characteristics. This is corroborated by the fact that the EMG data for m. deltoid anterior was often not well fit by a circle. This observation is described in more detail below by quantitative tests of the quality of the circle fit for various muscles.

The upper part of figure 5.8 shows data for m. brachioradialis, m. biceps brachii (long head), m. triceps (lateral head), and m. triceps (long head) replotted from previous figures. In each case, the circle appears to provide a good fit to the data for each muscle. However, we also tested this relation quantitatively, looking for systematic deviations of the data from a circle. For each muscle, we plotted the measured EMG amplitude as a function of the EMG activity predicted by the cosine function fitted to the data. In order to pool data from various subjects for recordings from a given muscle, the diameter of the circle was normalized to one. Data on the one half of the circle (usually the right or upper half) were plotted with positive sign while data on the other half were plotted with a negative sign.

For a perfect match between actual and predicted data, all data points should fall on a straight line passing through the origin with a slope of 1. The results are shown in the lower half of each panel of figure 5.8. For the four muscles shown in figure 5.8, there is a good correspondence across all subjects between actual and predicted EMG amplitude. The correlation coefficients were 0.96, 0.89, 0.96, 0.98 for the data of m. brachioradialis, m. biceps (long head), m. triceps (lateral head), and m. triceps (long head), respectively. For these four cases, the regression line passed through the origin and had a slope very close to one. Table 5.2 summarizes the results for all muscles.

Unlike the muscles pictured above, the response of m. deltoid anterior was often not adequately fit by a circle. Since two sub-populations of motor-units were found in

muscle	slope	intercept	corr. coeff.
m.brachioradialis	0.96(0.02)	0.02(0.01)	0.96
m.biceps caput longum	1.02(0.05)	0.04(0.03)	0.89
m.triceps caput longum	1.03(0.02)	-0.01(0.01)	0.98
m.triceps caput breve	1.05(0.03)	0.00(0.01)	0.96
m.deltoideus posterior	0.92(0.03)	0.01(0.01)	0.95
m.deltoideus anterior (1)	0.99(0.09)	0.00(0.05)	0.72
m.deltoideus anterior (2)	1.01(0.05)	0.00(0.03)	0.91

Table 5.2: For each muscle (first column) this table shows the slope, intercept along the vertical axis and the correlation coefficient for the best straight line that is fitted when measured EMG is plotted as a function of predicted EMG, such as in figures 5.8 and 5.9.

m.deltoideus anterior, each with a different recruitment behavior (see figures 5.7A and

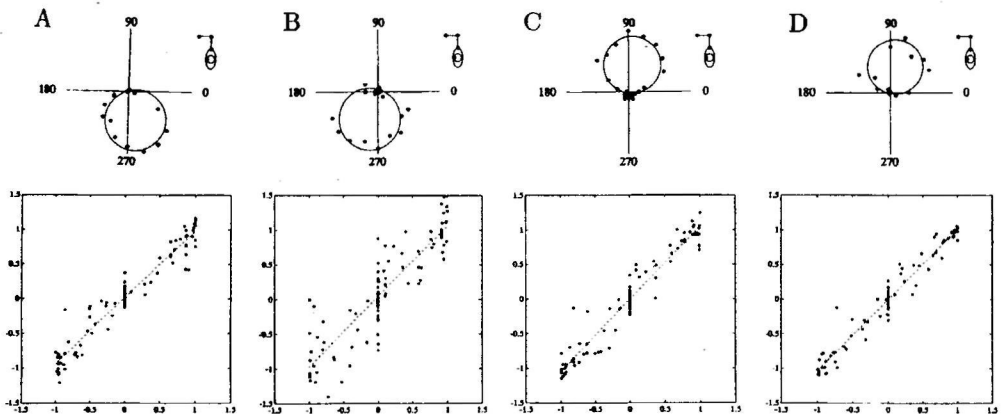


Figure 5.8: Upper part shows polar plots of surface EMG data obtained for isometric contractions for m. brachioradialis (A), m. biceps (long head) (B), m. triceps (lateral head) (C), and m. triceps (long head) (D). Lower part shows a comparison of measured EMG activity (vertical scale) and EMG activity according to circle fit (horizontal axis). All panels in lower part show data obtained in different experiments from different subjects from a single muscle pooled in the same plot. The maximal predicted activity (corresponding to twice the radius of the circle) is normalized to one for each set of data. Data at the direction clockwise or counterclockwise were plotted with positive or negative sign, respectively, in order to illustrate any asymmetries in the fit.

5.7B), our model would predict that the surface EMG data should be described by the summation of two circles having the orientations of the recruitment lines describing the two motor-unit sub-populations.

In order to test this hypothesis, we compared the quality of the fit to a single circle with that of the sum of two circles. The results are shown in figure 5.9. Panels A and B demonstrate the fit with one and two circles respectively, for a typical data set from a single subject. The EMG data reveal two lobes, which are better fitted by two

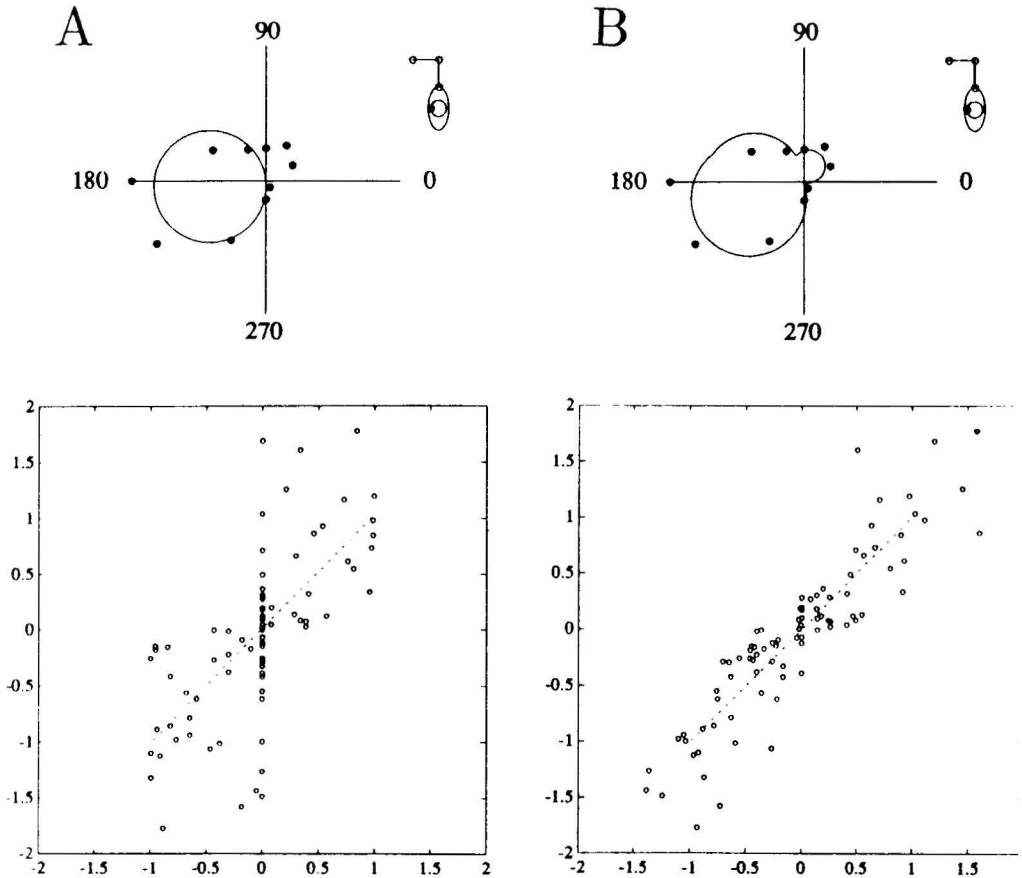


Figure 5.9: Upper part shows EMG activity measured from m. deltoid anterior fit with a single (upper left) and with two circles (upper right). The lower part gives a comparison of all the data obtained from m.deltoid anterior pooled in the same panel with regard to a fit by a single circle (lower left) or by two circles (lower right).

circles than by one (see top panels in B and A, respectively). When the deviation of the data with the circle fit are plotted in scatter plots, large deviations from a straight line become obvious (see lower panel in A). Data points in the first quadrant, for which no activity is predicted, appear along a vertical line in the middle of the panel. When scatter plots were constructed from all the data from m deltoid anterior for all subjects, the scatter along the diagonal was substantially smaller for the fit with two circles (lower panel in B) than for one (lower panel in A). This becomes evident in the correlation coefficient which increases from 0.72 to 0.91 (see table 5.2).

The preferred directions of the two circles describing the surface EMG data for m deltoid anterior are in close agreement with the orientations of the recruitment lines of the two motor-unit sub-populations. The mean orientations of the recruitment lines of the motor-unit sub-populations across all subjects were 99 and 192 deg (SD = 12 deg). The mean orientations of the two circles fitted to the surface EMG data for all subjects were 100 deg and 215 deg (SD 18 deg). The fact that the difference between motor-unit and surface EMG orientation was within the experimental error, supports the idea that the deviations of EMG activity found for m deltoid anterior can be explained by the recruitment behavior of the two motor-unit sub-populations.

5.6 Discussion

The main result of this study is that we have been able to demonstrate a quantitative way to relate the direction dependent patterns of motor-unit recruitment behavior to the pattern of muscle activation measured by the amplitude of surface EMG during isometric contractions. We found that for most of the muscles we measured, the amplitude of surface EMG for a constant force in the horizontal plane was proportional to the cosine of the angle between a muscle-specific preferred direction and the direction of force. Surface EMG can therefore be fitted by a circle which passes through the origin and which has a center in the preferred direction. Furthermore, the forces at recruitment for motor-units belonging to these muscles lay on straight lines with the normal of each line pointing in the preferred direction for the muscle. For m deltoid anterior, the EMG activity had to be described by a summation of two circles, corresponding to the recruitment behavior of two distinct sub-populations of motor-units. Within a single sub-population, the recruitment lines of all motor-units were parallel. This provides evidence for the notion that a given population of motor-units receives a homogeneous activation during isometric contractions.

5.6.1 Interpretation of results.

In agreement with previous results [32, 33, 106, 55] we found that recruitment thresholds for various directions could be described by straight lines which were parallel for different motor-units within a given muscle. The most plausible explanation for this finding is that all motor units in a given population receive a homogeneous activation and that the recruitment order is fixed according to the "size principle" [4, 85]. Although some questions have been raised with regard to the size principle [31, 105] we never saw any reversal of recruitment thresholds within a sub-population of motor-units. It has been speculated that the size principle may be valid only for the slowly contracting motor-units of a motor-unit pool in strict accordance with the motor-unit axon size and muscle-unit size. Our results do not address this possibility, since our data were collected for relatively small force levels, corresponding mainly to the activity of slowly contracting motor-units. If this were true, the results of our study could not be extrapolated to higher force levels.

5.6.2 Deviations from the circle and line fit for EMG and motor-unit behavior.

Other studies of the direction dependence of surface EMG amplitude during isometric muscle activation have been performed by Buchanan et al. [2, 3] for flexion/extension in the elbow and exo-/endorotation in the shoulder and by Flanders and Soechting [21] for forces in the vertical plane. The latter authors fitted their data with cosine functions, just as we did. For some postures, Flanders and Soechting found a significantly improved fit by the use of multiple cosine functions. Their explanation for this phenomenon was based on the complex activation of those muscles. In short, they suggested that a muscle can be activated during the production of force which is in a direction not directly related to the mechanical advantage of the muscle. Such an activation may be necessary in order to compensate for the activation of other muscles which make a contribution both in the desired force direction as well as in another unwanted direction. For example, van Zuylen et al. [106] showed that m. triceps was active for isometric contractions in the supination direction. This muscle produces only an extension torque around the elbow joint, having no mechanical effect on supination or pronation torque. Its involvement in the supination task can be understood if one realizes that it is in compensation for the flexion torque produced by the m. biceps, which produces unwanted flexion torque as well as supination torque. The argument by Flanders and Soechting implies that in complex tasks the activation of a muscle might be better fitted by multiple cosine lobes, one lobe corresponding to the direction in which that muscle alone has the largest mechanical advantage and

one or more lobes for other directions in which the muscle compensates for unwanted mechanical contributions from other muscles. Although this explanation may be valid, the complex EMG data found by Flanders and Soechting [21] might also have been due to the fact that the arm was not supported. As a result, the gravity-related torque in the elbow and shoulder would have varied with arm position, causing a variable, position dependent torque in elbow and shoulder.

Another explanation for the deviations from a circular arrangement of the EMG data found by Buchanan et al. [2, 3] and by Flanders and Soechting [21] is that the forces in their studies exceeded a level of 25% of maximal voluntary contraction. If the EMG-force curve deviates from a linear relationship, the line of reasoning in this manuscript predicts that the EMG data will fall along an ellipse, rather than on a circle. The typically observed nonlinearity in the EMG-force relation is a slope which decreases with increasing force. In that case, the short axis of the ellipse would be in the preferred direction and the long axis would be orthogonal to the preferred direction. This is qualitatively in agreement with the results of Buchanan et al. [2, 3] and by Flanders and Soechting [21].

Other studies of motor-unit recruitment have been performed by ter Haar Romeny et al. [33] and by van Zuylen et al. [106]. They studied isometric contractions of human elbow muscles during supination/pronation and flexion/extension. For almost all muscles in their study, they found several sub-populations of motor-units, each with a specific direction related activation. For *m.biceps caput longum*, which contributes to both flexion and supination of the forearm, they found three distinct sub-populations. One sub-population of motor-units became active only for supination torque and the recruitment thresholds fell on a straight line of constant supination torque. Another sub-population became active only for flexion torques. A third sub-population (the largest in number of motor-units) received input related both to supination and to flexion torque. In the latter case, the recruitment behavior of the motor-units was characterized by a concatenation of three line segments. In such a case, we would predict a similar concatenation of 3 cosine functions, each with an orientation corresponding to the orientation of one of the line segments. In our study we did not find motor-units with a recruitment behavior that could be described by a concatenation of straight line segments. Unless there are motor-units in human arm muscles involved in flexion/extension in elbow and shoulder which have a recruitment behavior different from a straight line, it is unlikely that the multiple lobes in the surface EMG data obtained in this study and by others [21, 2, 3] can be explained by the segmented recruitment behavior of motor-units.

A more likely explanation for the presence of multiple lobes of activity in surface EMG is based on the presence of a similar number of sub-populations of motor-units. If a muscle has several sub-populations of motor-units, each with a different activation

pattern, the surface EMG data would correspond to a weighted superposition of the direction sensitivities of each individual sub-population. Take, for example, the case of the two sub-populations of motor-units pictured in figure 5.7. Both sub-populations contribute to the surface EMG in proportion to the cosine of the angle between the direction in which the force is exerted and the sub-population specific preferred direction. For directions in which both sub-populations are active, the EMG would be proportional to a weighted sum of the contributions to EMG caused by each individual sub-population. This weighted sum may have a single broad lobe (when the preferred directions are close, for example within 60 deg) or two separate lobes (when the preferred directions are far apart, such as for the deltoid anterior motor-units in figure 5.7).

5.6.3 Biomechanical function

The preferred direction of mono-articular muscles does not always coincide with their mechanical working direction. For example, the direction of maximal flexion torque for the elbow is 270 degrees, since in this direction, the externally exerted force and the lever arm (i.e. the forearm) are perpendicular (see figure 5.10). However, the mono-articular elbow flexor *m. brachioradialis* does not have a preferred direction of 270 deg, perhaps because a force in this direction requires flexion torque in the shoulder as well, which can not be provided by *m. brachioradialis*. Another reasonable hypothesis would be the force direction that would result from flexion torque exerted only at the elbow. This direction is 315 degrees, where the force direction and the lever arm (i.e. line between wrist and shoulder) are parallel. In fact, the preferred direction of *m. brachioradialis* is between these two directions, with an orientation near 290 degrees.

The bi-articular *m. biceps caput longum* contributes both to flexion in the elbow and to flexion in the shoulder. Its preferred direction (near 255 deg) lies between the direction for which maximal elbow flexion torque is required (270 deg) and the direction for which maximal shoulder torque is required (225 deg). The fact that this muscle has a larger lever arm at the elbow than at the shoulder may explain the fact that the preferred direction is closer to the direction in which maximal elbow torque is required.

5.6.4 Isotonic dependence

The relationship between the direction dependence of surface EMG and intramuscular recruitment data for individual motor-units, which is described in this study, was only tested under isometric conditions. Miller et al. [70] have described differences

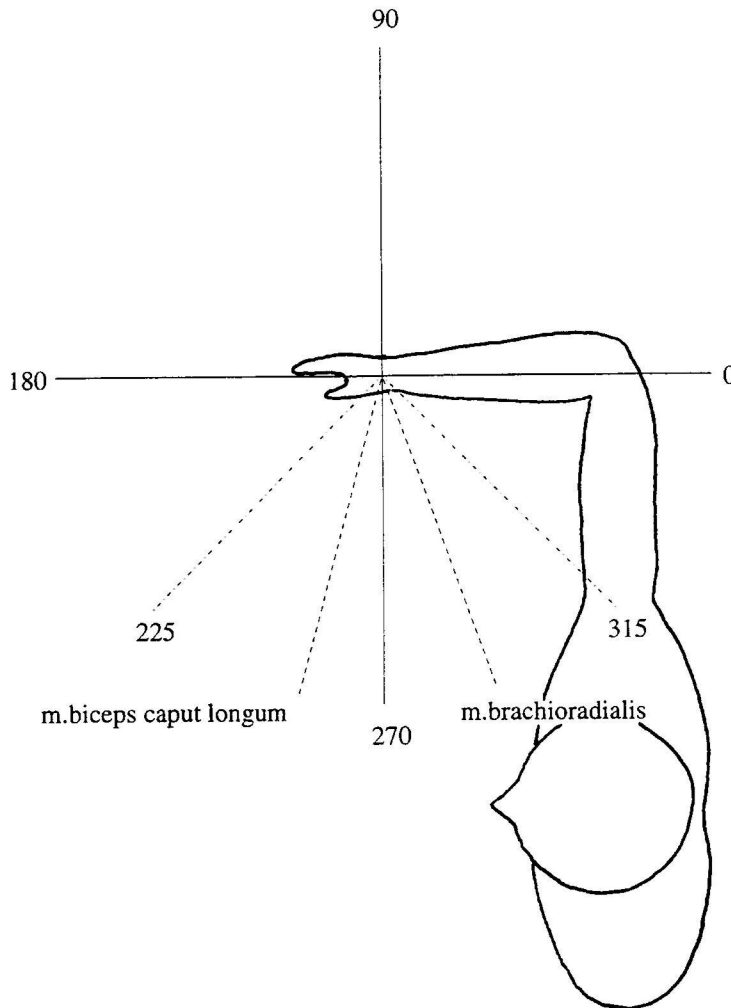


Figure 5.10: The direction of approximately 290 deg in which a maximal activity of the mono-articular elbow flexor m.brachioradialis is measured for a constant force in all directions, lies in between the direction of maximal elbow torque (270 deg) and the direction in which there is no shoulder torque (315). The biarticular m.biceps caput longum contributes both to elbow and shoulder flexion. Since the contribution to elbow flexion is larger than to shoulder flexion, due to its tendon insertions, the direction of maximal activity for m.biceps caput longum (255 deg) lies closer to the direction of maximal elbow flexion (270 deg) than to the direction of maximal shoulder flexion (225 deg).

in the preferred direction of these muscles between isometric and isotonic conditions. Moreover, the amplitude of the surface EMG was consistently higher in isotonic conditions than in isometric conditions for all muscles [27, 70]. The different preferred direction for surface EMG probably reflects a different orientation of the recruitment lines under isotonic conditions. A change in orientation of recruitment lines can explain a different preferred direction for the surface EMG, but it does not explain the general increase of EMG amplitude. Since the velocities during the experiments of Miller et al. [70] were low (about 5 deg/s), it is unlikely that the increase in EMG activity can be accounted for by the force-velocity relationship. The discrepancy between the amplitude of surface EMG recordings for isometric and isotonic conditions may be related to the observation by Tax et al. [93], that recruitment and firing rate at recruitment can be modulated independently. A given force might be produced by a greater number of motor-units (given a lower recruitment threshold) firing at a lower rate. Since motor-unit recruitment contributes more strongly to surface EMG amplitude than does rate modulation, the force contributed under these conditions would be associated with increased surface EMG amplitude. The effects on surface EMG of this trade-off between firing rate and recruitment threshold are not well understood. Further experiments including the recruitment and rate modulation of motor-units under isotonic conditions are needed to gain more quantitative insight into the relationship between surface EMG and motor-unit data.

Chapter 6

The relative activation of muscles during isometric contractions and low-velocity movements against a load.

Adapted from Thecuwen M, Gielen CCAM, Miller LE (1994) The relative activation of muscles during isometric contractions and low velocity movements against a load *Submitted to Exp Brain Res*

6.1 Abstract

Surface EMG and motor-unit activity were measured in human arm muscles during isometric contractions and during movements against an elastic load. The direction of force applied at the wrist and of movement direction were varied in a horizontal plane.

During isometric contractions the direction in which the largest EMG activity was measured corresponded to the direction in which motor-units had the smallest recruitment threshold, for each muscle. The same was found for movements against an elastic load. However, this direction was different for isometric contractions and for movements. Because the magnitude and sign of these changes varied for different muscles, this resulted in a different relative activation of muscles for the two conditions.

The amplitude of the surface EMG during contractions against an elastic load was generally significantly larger than that for isometric contractions against the

same load. For *m. brachioradialis* isometric conditions yielded occasionally increased EMG activity. The change in EMG activity could be attributed completely to changes in motor-unit recruitment thresholds leading to proportionate changes in the number of recruited motor-units. However, the initial firing rate of motor-units at recruitment was the same under both conditions and, therefore, did not contribute to changes in amplitude of surface EMG activity.

6.2 Introduction

Since the work by Bernstein [1] the problem of how to control the large number of degrees of freedom in the skeleto-motor system has received considerable attention. Most biological limbs have multiple joints and multiple muscles crossing each joint, which allows a given movement to be made in a variety of ways. Despite this large number of degrees of freedom, it has generally been believed that the muscle activation pattern to produce a particular movement or force was quite consistent for a given subject. For example, Buchanan et al. [2, 3] reported that the direction of force for which the EMG activity of a given muscle reached a maximum value, corresponded closely to the direction of greatest mechanical advantage of the muscle. However, these findings were made more complicated by the observation by van Zuylen et al. [106] that certain muscles were activated for forces in directions in which their mechanical advantage was zero. For example, *m. triceps brachii* is activated during supination of the forearm although it contributes mechanically to elbow extension only. The activation during supination compensates for the flexion torque generated by *m. biceps brachii*, which has a mechanical advantage both for supination and flexion. This illustrates that the activation of a given muscle may not always be predictable on the basis of its mechanical advantage alone, but requires that the mechanical advantage of all muscles acting across the joint be considered.

For some joints, such as the elbow [32, 33, 106], there is much experimental data on the relative contribution of the major muscles to isometric forces. However, a few years ago Tax et al. [93] found that the relative contribution of muscles to torque in a joint is not fixed but, instead, depends on the motor task. They found that the recruitment threshold of motor-units in some muscles was considerably lower during movement than during isometric contraction. For example, in *m. biceps brachii*, the recruitment threshold of motor-units decreased by about 40% during elbow flexion movements against a load compared to that for isometric elbow flexion. For other muscles (e.g. *m. brachioradialis*), the recruitment threshold was shown to be increased. Closely related experiments revealed similar differences when subjects were instructed to control either force or position [95]. This led the authors to

conclude that the differences in recruitment threshold could be ascribed to differences in central activation. Unfortunately, a more detailed explanation for the observed differences could not be given.

These results indicate that the selection of a particular muscle activation pattern by the central nervous system is dependent on the motor task. This proposition has led to a search for an understanding of the constraints which may be imposed by the nervous system in order to reduce the number of degrees of freedom [101, 50, 12]. One of the suggestions which allowed for a different activation during movements and isometric contractions came from Van Ingen Schenau [52]. He predicted a special role for bi-articular muscles during movements which would improve the limb's mechanical efficiency. For certain directions of movement, torque and changes in joint angle are oppositely directed. Under these conditions, mono-articular muscles would be actively lengthened, and thus would dissipate work, rather than contribute positive work. Because of their geometry, bi-articular muscles would dissipate less energy because their length change is moderated by the changes in angle of the other joint.

The results of Tax et al. [93, 94, 95] are impossible to apply to this hypothesis, because they studied isometric contractions and movements in one direction only. Therefore, we decided to study activation of the human elbow and shoulder muscles during movements and forces in various directions within a horizontal plane in order to investigate to what extent the relative activation of the muscles was affected by the direction of movement or isometric force.

The amplitude of both force and EMG activity depends both on the number of recruited motor-units as well as on the firing rate of those motor-units. Recording from single motor-units has the advantage that both the recruitment threshold and firing rate at recruitment can be studied independently. The latter is important since it was shown [93] that there may not be a fixed relation between force and firing rate at recruitment. Furthermore, the relative contribution of recruitment and firing rate to force and EMG is not known in detail. Therefore, we measured muscle activation both with surface EMG electrodes and with intramuscular electrodes which allowed the recording of the activity of single motor-units. With these methods, we have investigated the direction dependent activation of muscles during two motor tasks, isometric contraction and movements against an external elastic load. We have shown that the differences in EMG activity between isometric and movement conditions can largely be accounted for by accompanying changes in recruitment threshold of motor-units.

6.3 Methods

Subjects were instructed to exert isometric force at the wrist in various flexion directions within the horizontal plane, or to make movements of the hand in these directions against an external elastic load. The EMG activity of several flexor muscles acting across the elbow (m. brachioradialis, m. biceps caput longum) and shoulder (m. biceps caput longum, m. deltoideus anterior) was measured by means of both surface electrodes and intramuscular wire electrodes. In five experiments surface electrode recordings were also made from extensor muscles in order to verify that there was no co-contraction. All data were collected from seven male volunteer subjects ranging in age from 23 to 40 years. Some of these subjects were tested several times. None had any known history of neurological or musculoskeletal disorder.

6.3.1 Experimental paradigm

A detailed description of the experimental set up can be found in chapter 5. In these experiments, subjects were tested in two experimental paradigms, the isometric condition and the movement condition. Between these conditions, the EMG activity in a completely relaxed condition was measured in order to compensate for any noise or background activity. In all conditions, the subjects were instructed to maintain the vertical force at the elbow at a constant level. The two test conditions and the rest measurement were measured as a block, for a given direction. The directions were chosen in a random order.

For a typical subject, a force of 40 N in elbow flexion direction corresponded to approximately 20% of Maximum Voluntary Contraction (MVC). However, since MVC was different for different force directions, the force of 40 N fell in the range between 20% and 40% over the full range of directions. Therefore, we have expressed force in Newtons, rather than in terms of MVC.

In the isometric condition, subjects were asked to exert slowly increasing isometric forces (approximately 3 N/s) from a completely relaxed state to a force of approximately 50 N. Data were collected throughout the entire duration of the ramp. Each direction was tested three times in succession.

In the movement condition, subjects were asked to move the wrist in a direction opposite to the pulling direction of the cable beginning approximately 5 cm from the isometric test position. The subject was instructed to move the wrist slowly but at a constant velocity (about 2 cm/s) against the load provided by the torque motor. After a displacement of about 2 cm (when the arm was moving at a constant velocity) data collection began. For these low hand velocities the shortening of flexor muscles was rather small (about 2% rest length per second) such that any effects of the force-

velocity relationship were small. On subsequent trials, the preload was increased in steps of 6 N from 6 to 36 N. Across the 6 cm movement range, force increased by approximately 12N, such that the force level in subsequent trials overlapped. This allowed the recruitment threshold and initial firing rate to be determined in at least two trials. This condition is similar to the "increasing preload" condition introduced by Tax et al. [94, 95].

In order to compare the results found under the isometric condition with those found during the movement condition, data were only considered for analysis when the position of the wrist was within 3 cm of the isometric test position. The resultant maximal angular differences in elbow and shoulder joint angle were thus 6 degrees and 4 degrees, respectively.

6.3.2 Surface EMG

Surface EMG data were collected using Ag/AgCl electrodes. The signals were differentially amplified and filtered with a 50 Hz notch filter and a fourth order Bessel filter with a passband of 10-150 Hz. The signals were sampled with a 12 bit A/D converter at 400 Hz. Force signals were simultaneously sampled at 400 Hz and could be measured with an accuracy of 0.1 N.

The surface EMG data were digitally rectified. For both isometric and movement trials, the mean rectified EMG activity was calculated during the period in which force was within 15% of a fixed test force (typically 40 N). Next, the mean EMG activity for a given direction was obtained by averaging over all trials. Finally, the mean activity for each muscle in the relaxed rest condition was subtracted from this mean EMG activity. By these procedures, a single average EMG value was calculated for the two conditions for each muscle and for each direction. Polar plots were constructed for the EMG amplitude as a function of direction. For theoretical reasons explained in an earlier paper [97], we fitted a circle which passed through the origin to these data.

6.3.3 Intramuscular EMG

Bipolar recordings of single motor-unit activity were obtained using nylon coated, 25 μm diameter wires inserted into the muscle with a hypodermic needle. The needle was inserted into the muscle between each pair of surface electrodes in an effort to record signals from the same part of the muscle. Typically four of those wires were inserted by a single needle, and the best pair was selected for the recording. After insertion of the wires, the needle was removed.

The intramuscular motor-unit action potential signals were differentially amplified and filtered with a fourth order Bessel filter with a passband of 300-5000 Hz and

recorded with a BrainWave system, which stored the time and waveform of each action potential with a sampling frequency of 16 kHz.

Single motor-unit action potentials were then discriminated from the intramuscular EMG signals using any of several criteria, such as template matches and principal components. We monitored the discrimination process carefully in order to ensure that all detected peaks belonged to a given motor-unit. This was done by displaying the sampled action potentials on a computer monitor to check for irregularities in motor-unit firing and to check for a consistent action potential shape. In particular, we verified that any changes in shape of the action potentials of the motor-units (especially during movements) were gradual such that we were sure, that all recordings were obtained from the same motor-unit.

The forces at recruitment for each trial were determined using both the discriminated motor-unit data and the force data. For high force levels, we sometimes observed that a motor-unit generated one or two action potentials followed by a period of silence (typically about 0.5 to 1.5 seconds) before it started firing at a regular frequency. These cases (about 25% at the highest force levels) were excluded from further analysis. Polar plots were constructed for recruitment force as a function of the direction of applied force. Straight lines, subsequently called recruitment lines, were fitted to the data for each motor-unit, similar to the critical firing level (CFL) lines of ter Haar Romeny et al. [32], van Zuylen et al. [106] and the recruitment lines of Theeuwes et al. [97]. The recruitment lines represent lines of constant excitation to the motor-units, according to the size principle [37, 38, 39].

The number of recruitment threshold data points was sometimes limited, because of the high forces necessary to recruit the motor-units in directions far from their optimal recruitment directions. As a result, the standard deviation of the orientation of the fitted recruitment line was occasionally rather large.

6.4 Results

We recorded a complete set of data from a total of 26 motor-units. The left column of figure 6.1 shows examples of the EMG activity recorded from *m. brachioradialis* (upper left), *m. biceps brachii caput longum* (middle left), and *m. deltoid anterior* (lower left) during isometric contractions (filled circles) and during movement (open circles). In both conditions, force at the wrist was 40 N. The amount of EMG activity is plotted in a polar plot in which the distance from the origin is a measure of the EMG amplitude, and the direction relative to the origin corresponds to the direction of the force at the wrist. The EMG data were fitted by a circle (solid line for isometric contractions and broken line for movement task). It can be seen clearly that both the

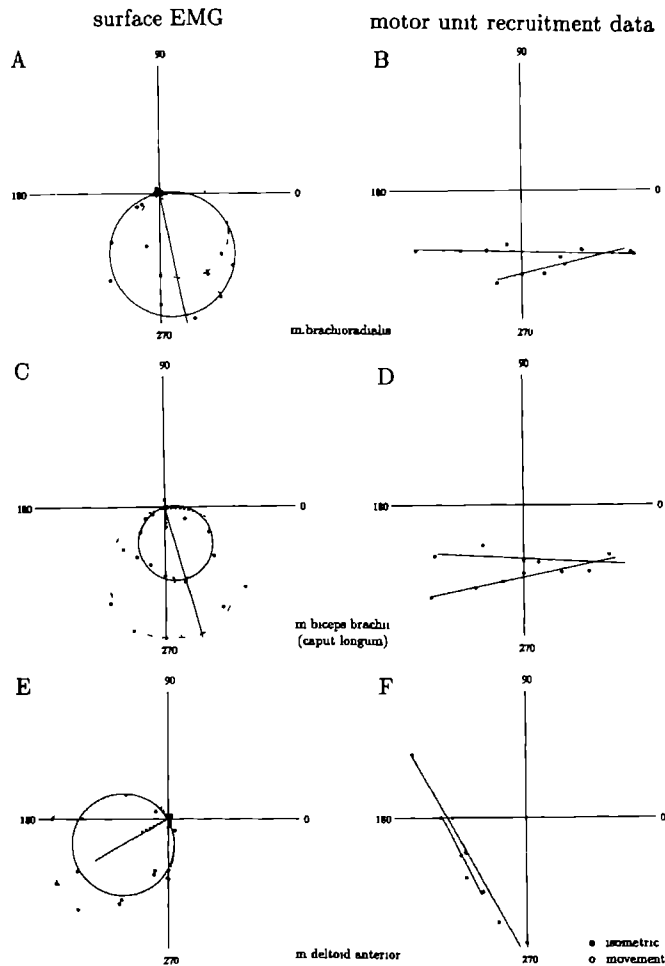


Figure 6.1: Surface EMG (left column) and motor-unit data (right column) for m. brachioradialis (top), m. biceps brachii caput longum (middle), and m. deltoid anterior (bottom). EMG data are plotted in polar plots. Each symbol represents the amount of EMG activity in polar coordinates. Filled circles (open circles) refer to data collected in the isometric (movement) condition. Fitted circles are shown by solid lines and broken lines for the isometric and movement conditions, respectively. Right column shows motor-unit recruitment thresholds in polar coordinates. Filled symbols (open symbols) refer to recruitment thresholds in isometric (movement) condition. Straight lines are least squares linear fits to the recruitment thresholds in the two conditions.

orientation and the amplitude of the EMG data differed between the two conditions

The right column in figure 6.1 shows polar plots of the recruitment thresholds of motor units for the same set of muscles shown in the left column. Both sets of data were collected simultaneously. The distance from the origin of each symbol represents the average force at which a motor-unit was recruited for forces in a given direction. In agreement with previous results [55, 32, 33, 97] the recruitment thresholds of motor-units for isometric contractions fell along a straight line. A straight line also appeared to characterize the recruitment behavior of motor-units in the movement condition (see figures 6.1 and 6.2) the mean correlation coefficient for the recruitment thresholds was 0.92 (SD = 0.09) and 0.89 (SD = 0.12) for the isometric and movement conditions, respectively. The range of correlation coefficients for individual recruitment lines fell between 0.63 and 1.00. The correlation coefficients for the recruitment lines for all but 7 motor-units in either condition were significant at a 5% level. For the remaining 7 motor-units the recruitment threshold was rather high and it could only be determined in 3 or 4 directions because of irregularities in the firing rate at recruitment in directions away from the preferred direction (see Methods section). Due to this small number of data points for these motor-units, the 5% significance level was relatively high in these cases. However, in none of these 7 cases was there any evidence for significant differences from a straight line.

Figure 6.1 also shows that the distance from the origin to the recruitment lines was different for the movement condition and for the isometric condition. This implies that a different number of motor-units were recruited during movement than during an isometric contraction at the same force. This appeared to be qualitatively in agreement with the difference in EMG activity in the movement condition.

Figure 6.1 shows that the differences in recruitment behavior during the two conditions can be characterized by a change in orientation of the recruitment line, and by a change in the distance of this line from the origin. These differences are clearly related to the analogous changes of orientation and amplitude that occurred in the EMG activity for the two conditions. These differences will be examined in more detail in the next sections.

6.4.1 Direction selectivity of muscle activation

The three arm muscles (*m. biceps brachii*, *m. brachioradialis* and *m. deltoid anterior*) each had a different direction selectivity. This was expressed by the differences in orientation of the circle which fits the EMG data (see table 6.1) for each muscle in both conditions and by the different orientation of the motor-unit recruitment thresholds. Mean values for the orientation of the circles and their standard deviation in this study were 287.0 (9.3), 265.7 (13.5) and 163.0 (61.6) deg for the isometric

Subject	$\frac{R_{mov}}{R_{met}}$	$\frac{\theta_{met}}{\theta_{mov}}$	$\frac{FR_{mov}}{FR_{met}}$	ϕ_{met}^{mu}	ϕ_{mov}^{mu}	ϕ_{met}^{cmg}	ϕ_{mov}^{cmg}
Brachioradialis							
SG	0.88	0.81	0.7	275	277	279	283
	0.78	0.76	1.1	268	283	281	300
	1.02	1.01	0.9	286	282	286	282
AM	1.56	1.25	1.0	273	285	297	275
		1.16	0.7	270	288		
		1.48	1.0	290	297		
LM	0.89	1.01	1.2	280	302	284	292
MF	1.59					294	313
PH	1.41	1.84	1.2	266	258	274	296
BM	1.39					303	308
BB	0.81	0.96	0.9	280	270	285	275
		0.78	1.0	277	263		
		0.82	0.9	272	268		
Mean	1.15	1.08	0.96	276.0	279.4	287.0	291.6
Std Dev	0.33	0.34	0.17	7.4	13.8	9.3	13.8
Biceps caput longum							
SG	1.45	1.64	1.0	277	245	279	284
		2.53	1.3	276	255		
AM	1.56	1.16	0.7	256	261	256	258
		1.23	0.9	260	264		
		1.20	1.0	259	269		
LM	1.02					246	259
MF	1.80	1.32	1.0	282	267	286	276
		0.96	0.9	283	271		
PH	1.87	1.69	1.1	268	261	260	255
BM	1.20	1.17	1.0	273	270	266	259
		1.02	1.1	268	267		
BB	1.19					267	287
Mean	1.44	1.39	1.00	270.2	263.0	265.7	268.3
Std Dev	0.32	0.46	0.16	9.6	8.0	13.5	13.6
Deltoides Anterior							
SG	1.30	1.43	1.1	205	206	208	205
		1.03	0.9	204	184		
		1.03	1.0	209	210		
		1.09	0.9	206	209		
AM	1.26					124	148
PH	1.08					207	208
BM	1.37					73	101
BB	1.01	1.42	1.2	216	176	203	173
Mean	1.20	1.20	1.02	208.0	197.0	163.0	167.0
Std Dev	0.15	0.21	0.13	4.8	15.8	61.6	44.4

Table 6.1: Surface EMG and motor-unit data for m. brachioradialis (top), m. biceps brachii caput longum (middle) and m. deltoid anterior (bottom) for all subjects. This table shows the ratio of radii of the fitted circles to surface EMG in movement (mov) condition and isometric (met) condition (column 2), the ratio of recruitment thresholds in isometric and movement condition (column 3), the ratio of initial firing rates in movement and isometric conditions (column 4). Columns 5, 6, 7, and 8 show the orientation of the motor-unit recruitment line in isometric condition and in movement conditions (ϕ_{met}^{mu} and ϕ_{mov}^{mu}) and the orientation of the circles fitted to the EMG data in isometric and isotonic conditions (ϕ_{met}^{cmg} and ϕ_{mov}^{cmg}), respectively. For each muscle, the mean values are shown at the bottom of each part.

condition and 291.6 (13.8), 268.3 (13.6) and 167.0 (44.4) deg for the movement condition for m.brachioradialis, m. biceps brachii caput longum, and m. deltoid anterior, respectively. Although the mean values for the isometric and the movement condi-

tion were relatively close for each muscle, the differences were large and significant for individual subjects in many cases (see table 6.1). The difference in orientation between the isometric and movement conditions was significant with respect to a 5% level for 6 out of 9 experiments for *m. brachioradialis*, for 4 out of 7 experiments for *m. biceps caput longum* and for 3 out of 5 experiments for *m. deltoid anterior*. The fact that the standard deviation in the mean orientation of EMG activity for *m. deltoid anterior* is rather large, is presumably due to the fact that *m. deltoid anterior* has two subpopulations of motor-units, each with a different recruitment behaviour [97]. Because of changes in the position of the recording electrodes, the EMG activity recorded with surface electrodes may be dominated by one or the other subpopulation giving rise to a different orientation of the circle fit.

Figure 6.2 shows the recruitment behavior for several motor-units in each muscle. In addition to the correlation coefficients reported in the previous section, this figure illustrates in another way that for both conditions the recruitment data could be described by straight lines. For either condition, all motor-units within a given muscle, which were recorded simultaneously, had recruitment lines having approximately the same orientation (see table 6.1). The variability in orientation of the recruitment lines within a condition was about 10 deg, indicating that the lines were approximately parallel. The parallel shift of the recruitment lines in each condition indicates that the motor-units were recruited in a fixed order for all directions of force and movement.

The orientation of the lines which describe the recruitment data was significantly different for isometric contractions and for movements for the examples shown in figures 6.1 and 6.2. The mean orientation of the recruitment lines for the two experimental conditions for all motor-units is shown in table 6.1. The difference in orientation for the isometric and movement conditions was significant with respect to a 5% level for 6 out of 11 motor-units for *m. brachioradialis*, for 5 out of 10 motor-units for *m. biceps caput longum* and for 3 out of 5 motor-units for *m. deltoid anterior*. In 48 out of 52 pairs of motor-unit and surface EMG data, including both the isometric and movement conditions, the orientation of the recruitment line was not significantly different from the orientation of the circle fitted to the corresponding EMG data with respect to a 5% significance level. This suggests that the orientation of the EMG data can be explained by the recruitment behavior of the motor-units in the muscle.

These results demonstrate that the relative activation of muscles for a particular force is not fixed. It rather depends on the motor task, in agreement with earlier observations by Tax et al. [93, 94, 95]. The present data generalize the observations of Tax et al. for various directions of force and movement.

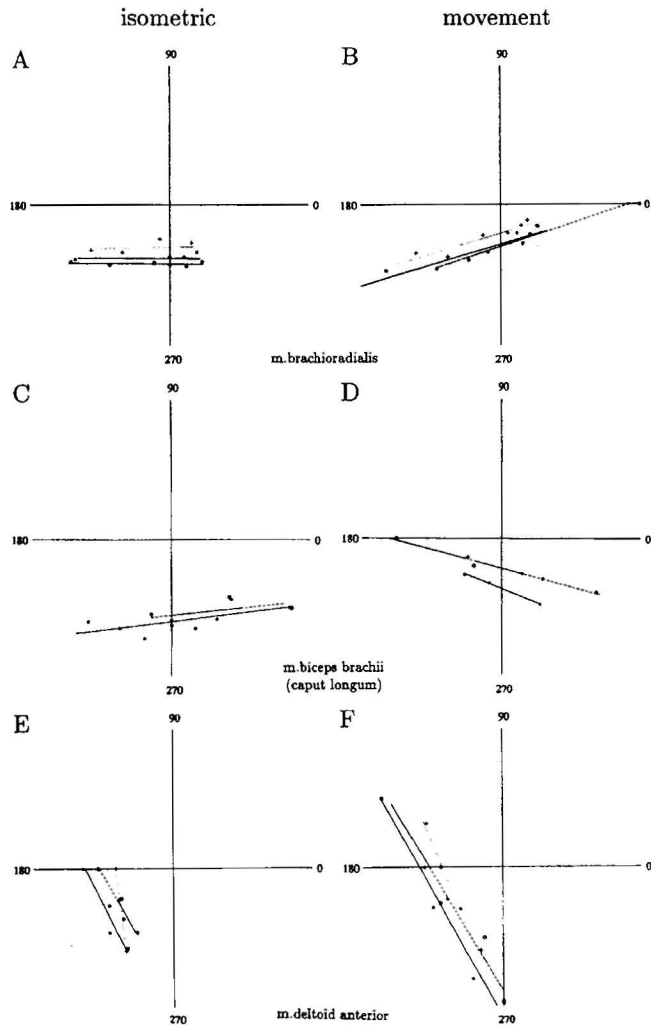


Figure 6.2: Recruitment data recorded from m. brachioradialis (top), m. biceps brachii caput longum (middle) and m. deltoideus anterior (bottom) in the isometric condition (left column) and movement condition (right column). Different symbols in each panel refer to recruitment thresholds of different motor-units. Straight lines are the result of a least squares linear fit to the recruitment data.

6.4.2 Amount of muscle activation

The other difference between EMG activity during isometric contractions and movements was the amplitude of the maximal EMG activity. For most subjects a larger

amplitude of EMG activity was observed for most muscles even though force at the wrist was the same in both conditions. This was in agreement with Miller et al. [70]. The mean increase of EMG activity was by a factor of 1.15 (SD = 0.33), 1.44 (SD = 0.32), and 1.20 (SD = 0.15) for m. brachioradialis, m. biceps brachii caput longum and m. deltoid anterior, respectively (see table 6.1). These ratios differed significantly from-unity for m. biceps caput longum and m. deltoid anterior. However, it should be noted that for some subjects, m. brachioradialis activity was occasionally smaller for movements than for isometric contractions (see e.g. figure 6.1A).

Figure 6.2 shows that the distance of the recruitment line to the origin was in most cases smaller for the recruitment data collected during the movement condition than during isometric contractions. A smaller recruitment threshold implies that more motor-units were recruited. This is at least qualitatively in agreement with the mean increase of surface EMG activity typical of the movement condition. The mean ratio of minimal recruitment thresholds in the isometric and movement conditions was 1.08 (SD = 0.34), 1.39 (SD = 0.46) and 1.20 (SD = 0.21) for m. brachioradialis, m. biceps brachii caput longum and m. deltoid anterior, respectively (see table 6.1). These results appear to be in close correspondence with the related ratios of surface EMG activity under movement and isometric conditions. In order to test the relation quantitatively, we calculated the correlation between the ratio of EMG values in the isometric and movement conditions and the ratio of recruitment thresholds for the same two conditions (see columns 2 and 3 in table 6.1). This included 14 EMG / recruitment threshold pairs for the three muscles (using the mean ratio for the recruitment thresholds when more than one motor-unit was recorded simultaneously). The r value was 0.6, which was significant with respect to a 5 % significance level. The slope of this relation for each muscle independently was 0.94 (SD=0.20) and 1.02 (SD=0.51) for data obtained from m. brachioradialis and m. biceps brachii, which is close to the value 1 for these muscles. Because only two pairs of EMG / recruitment data were available for m. deltoid anterior, no slope was fitted for this muscle. An analysis of the scatter of the data points relative to the line with a slope equal to one indicated that any differences between the changes in EMG amplitude and recruitment threshold of motor-units in the isometric and movement condition could not be attributed to any systematic deviations (see also data in table 6.1.) Rather, they had to be attributed to random fluctuations.

The fact that changes in EMG amplitude in the two experimental conditions were closely matched by changes in the recruitment threshold of motor units is further supported by several cases in m. brachioradialis in which a decrease, rather than an increase in amplitude was observed for the EMG activity during the movement task. In these cases, a corresponding increase in recruitment thresholds was found (see figure 6.1 and table 6.1), which leads to a smaller number of recruited motor-units,

and hence to a decrease in EMG amplitude.

Although the movement velocity in these experiments was typically rather small (2 cm/s, corresponding to about 2% of the muscle's rest length per-unit of time), we wished to test directly for the presence of possible force / velocity effects.

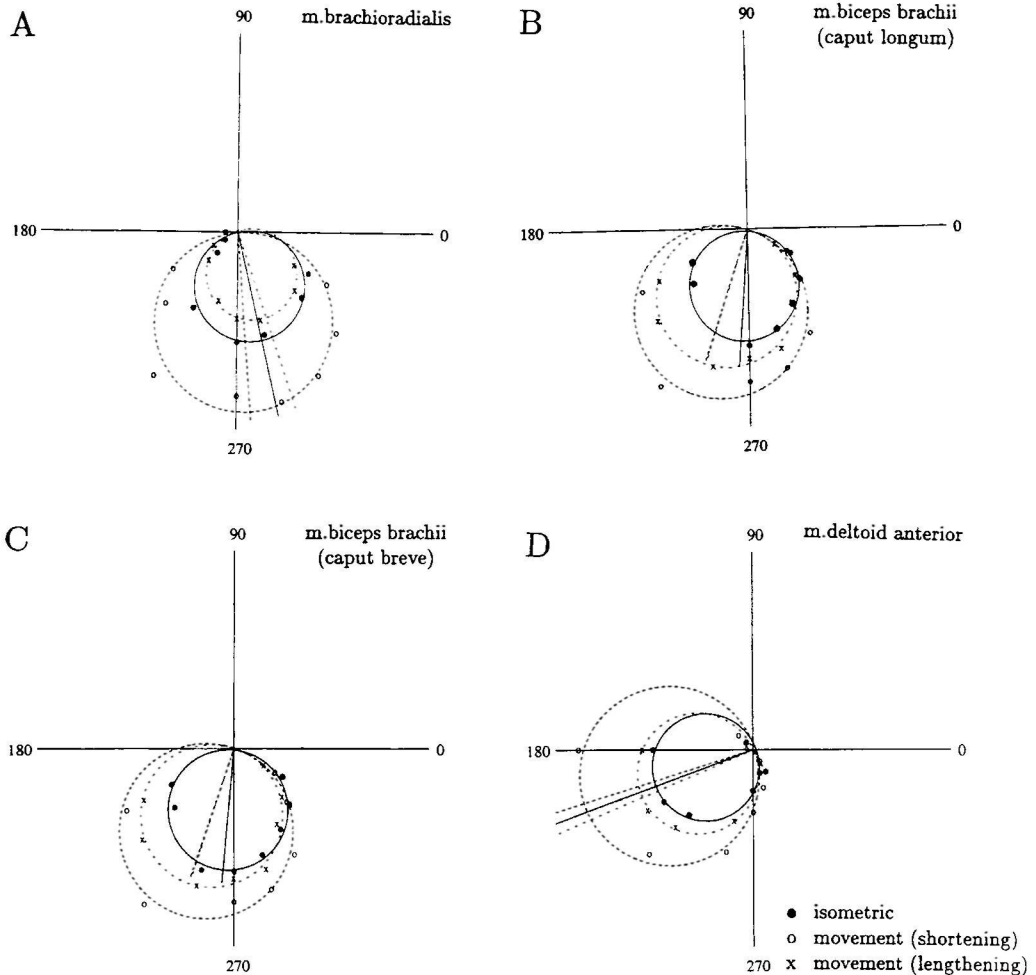


Figure 6.3: Surface EMG data for m. brachioradialis (top left), m. biceps brachii caput longum, (top right), m. biceps brachii caput breve (lower left) and m. deltoid anterior (lower right) for isometric contractions (filled circles; circle with solid line), shortening movements (open circles; circle with dashed line), and lengthening movements (crosses; circle with dashed/dotted line).

Therefore, we did four control experiments in which we tested both shortening and lengthening contractions. In these experiments, the subject was instructed to move the hand either in the direction opposite to the force (shortening contraction) or in the direction of the force (lengthening contraction) at a velocity of approximately 2 cm/s. The external force was fixed at a constant level of 50 N throughout the experiment.

If the force-velocity relation were to play a significant role, we would expect to find a greater EMG amplitude during shortening and a smaller amplitude during lengthening contractions compared to isometric contractions at the same force. Figure 6.3 shows the results of such an experiment. For both biceps brachii (caput breve) as well as m. deltoid anterior, the mean amplitude of activity for shortening and lengthening contractions exceeded that measured for isometric contractions. Only for m. brachioradialis (A) did we find a smaller mean amplitude of EMG for lengthening contractions relative to that for isometric contractions. This suggests a different relative activation for isometric contractions and contractions during movement. It also indicates that there may be a different relative activation during lengthening and shortening contractions. Because the differences for lengthening and shortening contractions relative to isometric contractions were not always in opposite directions, the force-velocity relationship cannot be the only explanation for the different EMG amplitude in the two conditions.

During these experiments we also measured the EMG activity in the long and lateral heads of m. triceps to check for any evidence of co-contraction. The EMG activity in these muscles was virtually absent (see figure 6.3D). If any activity was measured at all in these muscles, this EMG activity was oriented in the same way as that of m. biceps brachii, suggesting cross-talk from m. biceps brachii.

6.4.3 Firing rate at recruitment

The firing rate of motor units might also make a significant contribution to the observed changes in EMG activity in the movement condition. Figure 6.4 shows the initial firing rate at recruitment for all motor-units for m. brachioradialis, m. biceps caput longum and m. deltoid anterior as a function of the direction in which force was exerted, for both isometric and movement conditions (panels A, C and E and panels B, D and F, respectively). Because the initial firing rate varied between 7 Hz and 16 Hz, we normalized all initial firing rates by dividing them by the mean initial firing rate of that motor-unit in the isometric condition. This allowed all data to be plotted on the same scale. We fitted lines through the normalized initial firing rates as a function of the direction. These lines had a slope near zero (mean value 0.001 spike/second/deg) for both isometric and movement conditions. The slopes were

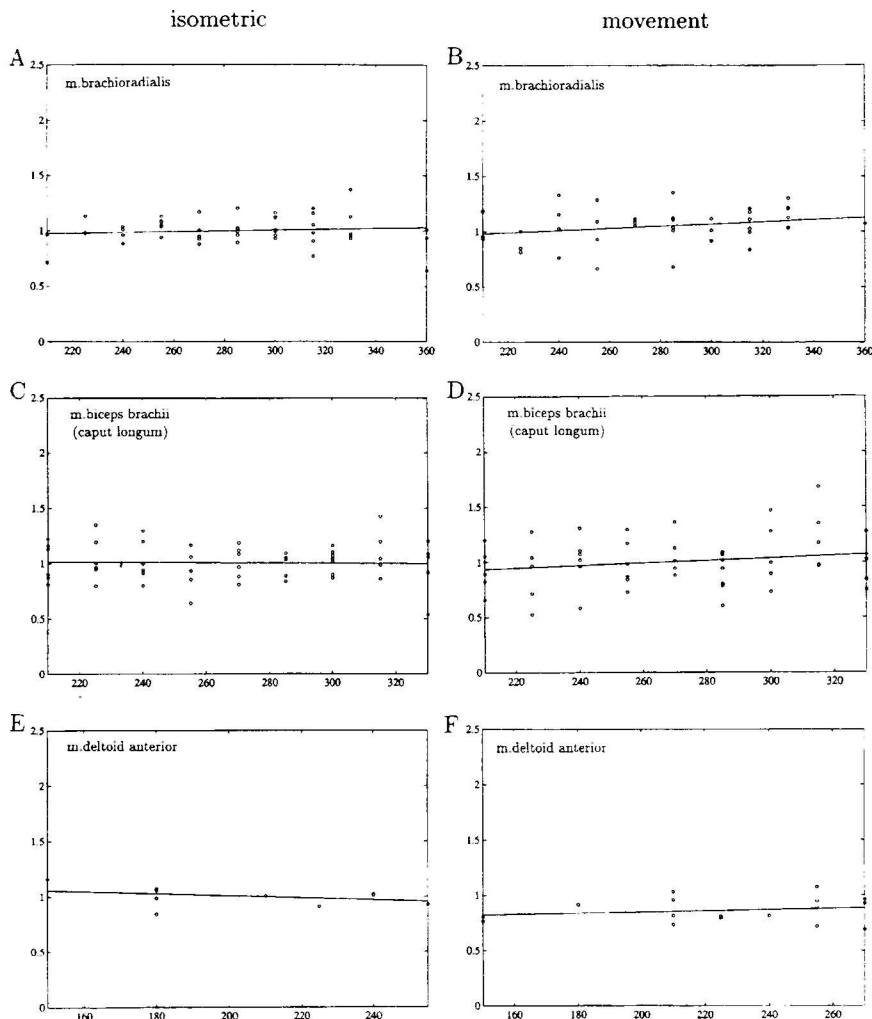


Figure 6.4: Normalized initial firing rates as a function of the direction of exerted force for all data from *m. brachioradialis* (top), *m. biceps brachii*, caput longum, (middle) and *m. deltoid anterior* (bottom) for isometric (left) and isotonic (right) conditions. The firing rates have been divided by the mean initial firing rate under isometric conditions for each motor-unit. A line has been fitted through these data. Vertical scale represents the (normalized) firing rate at recruitment in movement and isometric conditions. Horizontal axis represents direction of force or movement in degrees.

never significantly different from 0, which indicates that the initial firing rate did not depend on the direction of force or movement

Since the initial firing rate had no direction dependence, the initial firing rates from all directions could be averaged in order to investigate its contribution to the increase of surface EMG activity during movement. The ratio of initial firing rate under movement and isometric conditions was always close to 1. Averaged over all motor-units from a given muscle, we found ratios of 0.96 (0.17), 1.00 (0.16) and 1.02 (0.13) for *m. brachioradialis*, *m. biceps brachii caput longum* and *m. deltoideus anterior*, respectively (see table 6.1). This indicates that initial firing rate made no significant contribution to the changes in surface EMG activity during the movement condition.

6.5 Discussion

The main results of this study are the following: 1) The direction dependent EMG activity of muscles is different in isometric and in movement tasks. 2) The orientation of the lines which describe the recruitment thresholds of motor-units in the two experimental conditions differs in a fashion closely related to that of the EMG activity. 3) Changes in the amount of EMG activity in the two conditions can be attributed to changes in the recruitment threshold of motor-units. 4) There was no evidence for changes in firing rate at recruitment, as had been demonstrated in some previous studies [93, 95].

These results have several consequences for our understanding of the contribution of muscles to joint torque during isometric contractions and movements. These implications will be discussed in more detail below.

6.5.1 Direction dependent activation of muscles.

In a previous paper [97] we have shown that the direction dependent surface EMG activity for isometric contractions could be well fitted by a circle. The same result was found in this study. In addition, a circle also provided an adequate fit of the EMG data obtained during movements against an elastic load. According to Theeuwes et al [97] the good circle fit for the EMG data in the movement condition is compatible with the fact that recruitment thresholds fall along a straight line. The different orientation of the circles in the two experimental conditions indicates a different relative activation of muscles acting across the elbow joint in the two motor tasks.

This result corroborates and extends previous findings [46, 74, 75, 93, 94, 95, 70] of different relative activation of muscles depending on the motor task. Recently, Keshner et al [59] reported that in cat neck muscles a unique pattern of activity is

selected for both the vestibulocollic reflex and for voluntary tracking movements of the head in any animal. However, the patterns for the two behaviors differ, indicating that the central nervous system can generate movements in the same direction using different muscle patterns. The muscle activation differences reported in this study presumably result from the movement task differences and it raises the question of how many different task-dependent patterns of muscle activity might exist.

It is tempting to speculate about the neuronal origin of the task-dependent activation. In this context it is interesting that recent studies using magnetic stimulation of motor cortex [76, 20] have shown, that the effect of magnetic stimulation of motor cortex on muscle EMG is task-dependent. Since magnetic stimulation activates a large part of motor cortex, these results cannot tell us whether the output of motor cortex is different in different motor tasks or whether motocortical signals to spinal motoneurons and interneurons is modulated by task-dependent signals coming from other parts in the central nervous system.

Tax et al. found that the recruitment threshold of motor-units in *m. biceps brachii* was smaller for movements than for isometric contractions. The opposite result was found for *m. brachioradialis*. In contrast, we found that for both muscles, the recruitment threshold of motor-units was in general smaller for movements than for isometric contractions. The explanation for this apparent contradiction can be found in figure 6.2. If one considers isometric contractions and movements only in the direction 210 deg (as did Tax and colleagues), the recruitment threshold for motor-units in *m. brachioradialis* will indeed be higher during movement than isometric contractions (see figures 6.2A and 6.2B) and the opposite result will be found for *m. biceps* (see figures 6.2C and 6.2D). However, in the preferred activation direction for each condition, the mean recruitment threshold decreased for both muscles. This can be seen as a decreased distance from the origin to the recruitment lines during movement.

Tax et al. [93, 95] also found that firing rate at recruitment was different for isometric contractions and movements. The change in initial firing frequency was about 1 spike/s for the three major flexor muscles. We were unable to reproduce this finding. Any changes in initial firing rate at recruitment were much smaller than 1 spike/sec, and not considered to be significant. Tax et al [95] calculated that a change in firing rate at recruitment could account at most, for a few percent of the total flexion torque. Therefore, whether or not there were small changes in initial firing rate, any potential contribution to muscle torque would be very small, in good agreement with earlier studies [13, 14, 83].

In both isometric and movement trials, we used a slowly increasing force in order to determine the motor-unit recruitment threshold precisely. These recruitment thresholds depended on both the direction in which force was exerted [55] and on

the precise instructions to the subject [94, 95] Measuring the recruitment thresholds with adequate precision under real isotonic conditions would have required an unacceptably large number of trials per direction However, it has been reported in the literature (Tax et al 1990a, 1990b) that no differences were found in recruitment thresholds for real isotonic conditions and for movements against an elastic load Therefore, the results we have obtained during our movement trials may be expected to be valid for real isotonic conditions as well

The dependence of motor-unit recruitment behavior and EMG amplitude on the nature of the motor task raises questions of functional significance It has been suggested in the past (see e.g. van Ingen Schenau 1989, Gielen and van Ingen Schenau, 1992) that mono- and bi-articular muscles might have different functional roles which become particularly important because of energy constraints during movement tasks The changes in orientation of the recruitment lines and EMG data were frequently different for biceps and brachioradialis, and qualitatively in agreement with these theoretical predictions (see Gielen and van Ingen Schenau, 1992) Similar data have been obtained for the leg during cycling movements (see van Ingen Schenau et al , 1992) However, a biomechanical analysis and computer simulations have shown that these ideas do not provide a quantitatively fully correct explanation for the observed differences Another argument against this explanation is the fact, that the changes in orientation of both EMG activity and recruitment lines were not always on a consistent direction for different subjects (see table 6.1) Any special role for mono- and bi-articular muscles should give a consistent pattern of changes in direction selectivity

Moreover, let us assume that the task-dependent activation could be understood by the energy constraints of the movement task The question remains, why would this optimal activation during movement not also be appropriate for the isometric condition? To our knowledge, most models which attempt to explain how the musculoskeletal system deals with redundancy, for example, the minimization of total muscle torque (Yeo, 1976) or fatigue (Dul, 1984), predict the same activation for isometric and movement tasks Only ideas such as those of Loeb et al (1990), describing the control of the hindlimb of the cat during various phases in the walking cycle, leave room for a task-dependent activation

6.5.2 Task dependent changes in the amount of EMG activity.

The data in table 6.1 clearly indicate that the radius of the circle which describes the EMG data was larger for the movement condition than for the isometric condition It is not clear how the same flexion force at the wrist may be obtained when all major elbow muscles reveal increased EMG activity EMG recordings in m. triceps (long and lateral head) revealed an absence of activity during isometric force or movement in

flexion directions

It is possible that the activation of *m. pronator teres* and *m. extensor carpi radialis longus*, both of which have a mechanical advantage in flexion direction, was decreased. However, it is very unlikely that such an effect could counterbalance the increased activity of the primary elbow flexors, considering the small size and the mechanical advantage of the muscles. Furthermore, it is unlikely that the force-velocity relation can explain these results, since the shortening velocities were quite low (less than 2% of the rest length per second). Moreover, in a control experiment, *m. anterior deltoid* and both heads of *m. biceps* demonstrated that the EMG data was generally larger for the movement conditions than for isometric contractions.

At present we cannot provide a full explanation of these results, which would require a detailed modeling of the biomechanics and muscle properties. The present results (figure 6.4) suggest, however, that the relative activation during shortening and lengthening differs from that for isometric contractions and also that the relative activation of lengthening and shortening contractions may differ. The latter result would be in agreement with data from Nardone and Schieppati (1988, 1989). However, more data are necessary to quantify this statement.

At the very least, the fact that the directional activation of these muscles was different during isometric and movement conditions, and the fact that the amount of EMG activity differed during isometric shortening and lengthening contractions against the same force, clearly demonstrates that the isometric EMG force relation may not be used during other types of motor tasks.

Chapter 7

Estimating the contribution of muscles to joint torque from EMG activity.

Adapted from: Theeuwes M, Gielen CCAM, van Bolhuis B (1994) Estimating the contribution of muscles to joint torque from EMG activity. *Submitted to J Biomechanics*

7.1 Abstract

Because most joints in the human arm are crossed by a number of muscles which exceeds the number of degrees of freedom for those joints, the motor system can use a variety of muscle activation patterns for the same torque in each joint. We have developed a model to estimate the contribution of individual muscles to the total torque in a joint based on surface and/or intramuscular EMG recordings. If the mean EMG activity of the individual muscles is uniquely (not necessarily linearly !) related to the torque they produce, only a scaling factor has to be estimated to transform EMG activity into muscle torques. A set of linear equations can then be constructed which relates the contribution of each muscle to the total joint torque. If these equations are linearly independent, which is the case if the EMG activity of the individual muscles is modulated differently for forces in several directions, these scaling constants and hence the relative contributions of the individual muscles to the total joint torque can be estimated. This method is generalized for non-linear EMG-force relationships and can be used for various motor tasks for which the EMG-force relation is different from that for isometric forces.

With small modifications this method can also be used calculating the contribution of each muscle to joint torque from the recruitment behavior in subpopulations of motor-units in a muscle

7.2 Introduction

The force exerted at the end effector of a limb is the result of the torques in each of its joints. Since in general more than one single muscle is acting across a joint, it is hard to determine the individual contribution of each of the muscles to joint torque. However, there are several reasons why it is important to know the contribution of each single muscle to total joint torque. For example, there are various theories on the role of mono- and bi-articular muscles [52, 54] and about the role of muscles with parallel oriented muscle fibers and of muscles with a pennate structure [102, 79]. Knowledge of the contribution of individual muscles to joint torque in natural movements will make it possible to test these hypotheses and will contribute to a better understanding of muscle coordination in biologically redundant limbs.

In addition to these reasons a quantitative method for this purpose would also be highly desirable since recent studies have shown that the relative activation of muscles for a particular joint torque is not constant, but dependent on the motor task [93, 94, 95]. As a consequence, the relative contribution of muscles to joint torque is not constant but depends on the motor task. Quantitative information about the task-dependent contribution of muscles to joint torque may reveal more information on the particular role of mono- and bi-articular muscles [52, 28]. Moreover, such a method may be helpful in rehabilitation in order to evaluate the result of rehabilitation and physical therapy after motor traumata.

Usually, surface EMG recordings have been used to estimate the activation of various muscles and to determine their role in various movements. However, the absolute value of EMG activity depends on a variety of factors such as on the position of the surface electrodes relative to the active muscle fibers, on the thickness of subcutaneous fat layers, on blood vessels etc. Therefore, EMG activity by itself cannot provide a quantitative measure of the contribution of a muscle to joint torque. Moreover, the EMG-force relationship is not fixed but task-dependent such that EMG is not a unique measure for muscle force [70, 98].

In the past several studies have tried to estimate the relative contribution of muscles to joint torque. Usually, these studies had to make several additional assumptions. For example, Jørgensen and Bankov [57] based their predictions on the physiological cross-sectional area of muscles. Since each muscle may have several subpopulations of motor-units, each with a different activation, only a limited set of motor-units is

active at the same time for force in a particular direction [33, 106]. Therefore, the physiological cross-sectional area of a muscle is not representative for the area of muscle which is involved in the production of force in a particular direction. More in general, it is very hard to estimate the reliability of results from approaches which are based on assumptions on muscle physiology and on biomechanical properties [8].

Following another approach, van Zuyl en et al. [106] estimated the relative contribution of human flexor muscles to elbow flexion torque by assuming, that the numbers of intramuscularly recorded motor-units in motor-unit subpopulations in *m. biceps brachii*, *m. brachialis*, and *m. brachioradialis* are unbiased estimates of the relative number of motor-units in each of the subpopulations of motor-units. Since motor-unit subpopulations are not distributed randomly in a muscle [33] who demonstrated that in *m. biceps brachii* there are different motor-unit subpopulations in the middle, at the very lateral and at the very medial side of *m. biceps brachii*, *caput longum*) this assumption is at best a very rough approximation.

Following another approach, Hof and van den Berg [42, 43, 44, 45] and Olney and Winter [77] estimated muscle force using muscle models where the degree of muscle activation was estimated from EMG signals. However, the fact that the EMG-force relation is not the same under all conditions (e.g. for isometric and isotonic contractions) introduces an uncertainty in the estimates for muscle force. Other approaches [82, 34, 81, 104] have used optimization techniques which minimized or maximized some objective function. However, for many movements it is not easy to identify an objective criterion for minimization or maximization and, if one is found, it is still an open question whether the central nervous system uses the optimization of that particular criterion for the coordination of muscles.

In this study we tried to develop a method which makes fewer assumptions, which is generally applicable, and which can make use of both surface EMG data and intramuscularly recorded motor-unit data.

The aim of this paper is to present a general method to determine the contribution of a muscle to joint torque, when several muscles act across that joint. Our approach is basically similar to that described by Cnockaert et al. [9] since we also make the assumption that the EMG activity of a muscle in a particular motor task (e.g. for isometric or for isotonic contractions) is uniquely related to muscle force generated by a specific subpopulation of motor-units in that muscle. If one is able to measure the EMG activity of these muscles in force conditions in which the relative EMG activity in the muscles is different, one obtains an independent set of equations, which allow the determination of the contribution of each muscle. However, surface EMG frequently has the disadvantage that cross-talk from other muscles is hard to avoid, which makes a quantitative estimation of the contributions rather inaccurate. Therefore, we have extended the method to an estimation of the contribution of

each muscle based on the recruitment behavior of single motor-units in that muscle. Recently, we have described how the recruitment behavior of single motor-units can be used to describe the contribution of these motor-units to surface EMG (see chapter 5). In the present study we have used these results to relate the activity of single motor-units in a subpopulation to the EMG activity from that subpopulation. This procedure allows an accurate estimation of the contribution of the various groups of motor-unit subpopulations to joint torque.

7.3 Theory

The basic idea of the method is that the relative activation of all muscles acting across a joint remains constant when force exerted by the limb in a particular direction increases, as long as the instruction to the subject remains the same. This implies that the contribution to joint torque by all muscles increases proportionally when joint torque increases, irrespective of the slope of the EMG-force relationship for each of the muscles. This assumption is supported by numerous results in motor-unit studies [32, 33, 15, 106, 84, 56], which have demonstrated a common drive to synergistic muscles. Based on the available data this seems to be valid for arm muscles in the force range up to 50N at the wrist. In addition, we assume that the relationship between EMG and the actual muscle force which the muscle delivers, the EMG-muscle force ($EMG - F_m$) relationship, remains constant for all directions for a particular motor task. We also assume that the derivative of the EMG-force relation is positive-definite such that a unique force level for that muscle belongs to each EMG-value.

Usually, EMG activity is related to the force exerted by a limb. This force is the result of the contribution from many muscles. To distinguish this relation from the $EMG - F_m$ relationship, we will refer to the relation of EMG to total force exerted by the limb by " $EMG - F_t$ " relationship. With the assumption that the relative activation of muscles is the same for all force levels exerted by the limb, the two relationships $EMG - F_t$ and $EMG - F_m$ are the same apart from a scaling factor:

$$EMG(\alpha_m F_t) = EMG(F_m), \quad (7.1)$$

where α_m stands for the fraction of the total force produced by muscle m . In this study we will analyse data obtained for force in various directions ϕ at the wrist. If for a given direction ϕ for the force F_t the $EMG - F_t(\phi)$ relationship is known, then for each value of the EMG the force F_m produced by that muscle can be given as:

$$F_m(EMG) = \alpha_m F_t(\phi, EMG). \quad (7.2)$$

This equation says, that the force exerted by muscle m at a particular EMG activity for that muscle is the same for all forces \vec{F}_t at the limb for which that muscle produces the same amount of EMG activity, irrespective of the direction of force \vec{F}_t .

With these assumptions the precise contribution of a muscle to joint torque can be determined in the following way. For a multi-jointed limb the vector \vec{T} representing the torque in a joint can be derived from the lever arm \vec{r} and the force \vec{F}_t at the end-effector by the relation $\vec{T} = \vec{r} \times \vec{F}_t$. When the direction of the external force changes, the relative activation of muscles (and therefore also their relative contribution to joint torque) will change [2, 70, 97]. Since the contribution of each muscle to total joint torque is uniquely related to the EMG activity of that muscle, a set of linear equations relating the contribution to joint torque by each muscle to total joint torque can be constructed for various directions of force for a specific motor task. If these equations are linearly independent, which is the case if the relative amount of EMG activity for several muscles differs for various directions of force \vec{F}_t , this set can be solved and the proportionality constants between muscle torque and external torque for one direction can be obtained for each single muscle. In general, this set of equations will be overdetermined when the number of force directions exceeds the number of muscles acting across the joint. This overdetermination can be used to minimize the effect of stochastic noise on the EMG signals.

For reasons of clarity we will start by assuming a linear EMG-force relationship. The case for a nonlinear EMG-force relation can also be handled in a straightforward way and will be explained at the end of this section.

In case of a linear EMG-force relationship for each muscle, the EMG will also have a linear relationship with the torque $T_{m,j}$ which is contributed by muscle m to the total torque in joint j :

$$\vec{T}_{m,j} = \vec{C}_{m,j} \cdot (EMG_m - EMG_{m,rest}). \quad (7.3)$$

In this equation the EMG activity is corrected for the mean rectified EMG signals (usually due to noise) which are measured in a completely relaxed state. For the remainder of this section we will refer to $EMG_m - EMG_{m,rest}$ as simply EMG_m . If only forces and lever arms in one plane are considered, for example the horizontal $\hat{x} - \hat{y}$ plane as used in the Results section, torques will have only one component different from zero in the \hat{z} direction. Then the vectors $\vec{T}_{m,j}$ and $\vec{C}_{m,j}$ become scalars $T_{m,j}$ and $C_{m,j}$.

The total torque T_j in a joint j equals the vector product of the leverarm \vec{r}_j from the joint to the point where the external force is exerted, and the external force \vec{F}_t . However, it is also equal to the sum of the torque contributions $T_{m,j}$ from all

individual muscles m to total torque in joint j :

$$\sum_{m=1}^M T_{m,j} = \left(\vec{r}_j \times \vec{F}_t \right)_z = T_j. \quad (7.4)$$

By varying the direction ϕ of the external force \vec{F}_t in the horizontal plane, the EMG activity from the active muscles m across a joint j are modulated independently [2, 70, 97]. (If the ratio of activation of two muscles is constant for all directions of force in one movement task, only the combined torque of both muscles can be determined.) When N different directions ϕ_i are tested, this allows the construction of a set of N linear equations from which the coefficients $C_{m,j}$ can be solved:

$$\sum_{m=1}^M EMG_m(\phi_i) C_{m,j} = T_j(\phi_i), \quad i \in \{1, 2, \dots, N\}. \quad (7.5)$$

If N exceeds M , this system will be overdetermined and will be without a solution unless some of the equations are not linearly independent. Due to noise in the measurements of the EMG signals, this is unlikely. The overdetermination can be used in this case to minimize the effects of the noise. To do this, one has to find the residual vector \vec{R} with minimum length:

$$\|\vec{R}\|^2 = \sum_{i=1}^N \left(T_j(\phi_i) - \sum_{m=1}^M EMG_m(\phi_i) C_{m,j} \right)^2. \quad (7.6)$$

Taking the partial derivatives of $\|\vec{R}\|^2$ with respect to the coefficients $C_{m,j}$ and setting them equal to zero to find the minimum of $\|\vec{R}\|$, yields the "normal equations":

$$\sum_{m=1}^M \left(\sum_{i=1}^N EMG_m(\phi_i) EMG_l(\phi_i) \right) C_{m,j} = \sum_{i=1}^N EMG_l(\phi_i) T_j(\phi_i) \quad (7.7)$$

$l \in \{1, 2, \dots, M\}.$

These normal equations form a square matrix equation, which can be solved by a variety of methods [87]. Once the coefficients $C_{m,j}$ are solved, the individual muscle torques can be found by linear transformations of the EMG activities in each muscle as shown in Eq. (3). A non-negative least squares method for solving the matrix equation guarantees that flexor muscles produce only flexion torques and extensor muscles only extension torques because then the scaling constants $C_{m,j}$ are always positive.

The data of Miller et al. [70] and Tax et al. [93, 94, 95] have indicated that the $EMG - F_t$ relation may be different for isometric contractions and for movements.

Therefore, we do not assume that the $EMG - F_m$ relation for a muscle is the same for all motor tasks and we will solve the sets of linear equations (Eq. 5) for data obtained for each specific motor condition separately.

For non-linear EMG-force relationships, EMG in Eq. (3) has to be replaced by $\alpha_m \times F_t(\phi, EMG)$. Then the coefficients $C_{m,j}$ will give the relative contribution of the muscle to torque in joint j . This method can also be generalized to motor unit recruitment data, which will be described in the next subsection.

7.3.1 Motor-unit recruitment data

Motor-unit recruitment data can also be used to determine the relative contribution of muscles. These data can also provide insight in the contribution of subpopulations of motor-units within the same muscle as has been reported in the literature [32, 106]. To fit motor unit recruitment data into the equations above to calculate the individual contribution of a subpopulation of motor-units to the total torque in a joint, some assumptions have to be made. First we assume that motor-units of one subpopulation are recruited in an orderly manner according to the size principle described by Henneman [39]. This means that all motor-units in that subpopulation have a recruitment behavior which is modulated in the same way for forces in various directions. If for forces in a particular direction the recruitment threshold of one motor-unit is raised by a certain factor, this will be representative for the behavior of all other motor-units in the same subpopulation. This is confirmed by the finding that recruitment thresholds for forces in several directions lie on straight parallel lines as reported by ter Haar Romeny et al. [32] and van Zuylen et al. [106].

Secondly we assume that a line of recruitment thresholds represents a line of forces where the activation of the subpopulation of motor-units is constant. Hence, the contribution to joint torque by this subpopulation will also be constant along this line. With these two assumptions, the contribution to joint torque by this subpopulation of motor-units can be estimated up till a scaling factor. Since the recruitment thresholds of a motor-unit fall on a straight line, the external force at recruitment F_r can be described as:

$$F_r(\phi) = \frac{F_0}{\cos(\phi - \phi_0)}. \quad (7.8)$$

In this equation F_0 stands for the smallest recruitment threshold which can be found for this motor-unit in the preferred direction ϕ_0 . The forces, which are delivered by a single muscle m , are related to the external force $F_r(\phi)$ at recruitment by a scaling parameter $F_{m,0}$ which is independent of the direction ϕ . Then for a total force F

the contribution $F_m(\phi)$ of this muscle (or subpopulation of motor-units) will be:

$$F_m(\phi) = \frac{F}{F_r(\phi)} F_{m,0} = \frac{F}{F_0} \cos(\phi - \phi_0) F_{m,0}. \quad (7.9)$$

For torques instead of forces at the wrist in various directions, as reported by van Zuylen et al. [106], a similar expression results:

$$T_m(\phi) = \frac{T}{T_r(\phi)} T_{m,0} = \frac{T}{T_0} \cos(\phi - \phi_0) T_{m,0}. \quad (7.10)$$

where $T_r(\phi)$ is the torque at recruitment of a particular motor-unit for torques in a direction ϕ . Since EMG_m can be uniquely related to torque T_m generated by the muscle, the solution method to find the coefficients $C_{m,j}$ in Eq. (3) can also be used to find the contributions $T_{m,0}$ in Eq. (10).

7.4 Methods

We performed some experiments to validate the theory outlined above. The EMG activity of several muscles acting across the elbow (m. brachioradialis, m.biceps caput longum, m.biceps caput breve and m.triceps caput longum) was measured by means of surface electrodes in experiments in which subjects were instructed to exert isometric force at the wrist in various directions within the horizontal plane, or to make slow movements of the hand in various directions against a fixed external load. Data were collected in eight experiments with six subjects. None of them had any known history of neurological or musculoskeletal disorder.

7.4.1 Experimental paradigm

A detailed description of the experimental set up can be found in chapter 5. In the first paradigm (isometric condition) the subjects were asked to exert a constant isometric force (approximately 25 N) for 5 seconds in various directions in the horizontal plane. Each direction was tested three times in succession. At regular time intervals, the EMG activity was measured with the arm in a completely relaxed condition in order to correct the EMG signals for background activity, usually due to noise. Various directions of isometric force were tested in random order.

In the second and third paradigms (movements of the hand against or assisting an external force, also called shortening and lengthening contractions, respectively) the subject was asked to move the wrist in a direction along the pulling direction of

the cable. This force was equal to the force in the isometric condition (25 N). The subject was instructed to move the wrist slowly but at a constant velocity (about 2 cm/s) against a load provided by the torque motor. The direction of the movement was either opposite to the force exerted by the cable (shortening contraction) or in the same direction as that force (lengthening contraction). For these low hand velocities the relative shortening or lengthening of flexor muscles is rather small (about 2% restlength per second) such that any effects of the well known force-velocity relationship on exerted force at the wrist are very small. This procedure was repeated three times for each movement direction and for various movement directions in the horizontal plane.

In order to be able to compare the results found under the movement conditions with those found in the isometric conditions, in particular to avoid any possible effects of the force-length relationship, data were only included if the position of the wrist was within a distance of 3 cm of the position tested in the isometric condition. The maximal angular differences in elbow and shoulder joint angle corresponding to this range were 6 degrees and 4 degrees, respectively.

In the first series of 4 experiments only the first two paradigms were used. In following experiments all subjects were tested in all three experimental paradigms.

7.4.2 Surface EMG

Surface EMG data were collected using Ag/AgCl surface electrodes. The signals were differentially amplified and filtered with a 50 Hz notch filter and a fourth order Bessel filter with a passband of 10-150 Hz. The signals were sampled with a 12 bit A/D converter at 400 Hz. Force signals were simultaneously sampled at 400 Hz and could be measured with an accuracy of 0.1 N.

The mean EMG signal, determined when the muscle was relaxed, was subtracted from the mean EMG amplitude obtained from the three repeated isometric or isotonic trials. By these procedures, a single, average EMG value was calculated for each muscle and each direction. Polar plots were constructed for the EMG amplitude as a function of the direction of the applied force. For reasons explained in an earlier paper [97], a circle passing through the origin was fitted to these data.

7.4.3 Motor-unit data

The motor-unit data were taken from van Zuylen et al. [106]. In this study averaged data are presented for recruitment thresholds of motor units in various subpopulations in m. biceps brachii, m. brachioradialis, m. brachialis, m. triceps (lateral head, medial head and long head), m. supinator, and pronator teres for isometric contrac-

tions. For *m. pronator quadratus*, the pure antagonist of *m. supinator*, no data were available. For this muscle, we simulated data based on the data of its antagonist *m. supinator*. In the discussion it will be argued, that based on biomechanical considerations any other type of behavior for the motor-units in *m. pronator quadratus* is not possible. The effect of small variations in the precise, quantitative behavior of these motor-units appears to be small (see Results and Discussion).

7.5 Results

7.5.1 Analysis of EMG data

To test the theory outlined above, EMG activity was measured during isometric contractions and during movements opposite to or assisting a constant load. Figure 7.1 shows surface EMG data recorded from the elbow flexors *m. brachioradialis* (A), *m. biceps caput breve* (B), and *m. biceps caput longum* (C). The amount of EMG activity for isometric contractions of 25 N and for movements against and assisting a load of 25 N in various directions is plotted in polar coordinates. Different symbols refer to EMG activity in different conditions. Crosses refer to data collected in the isotonic shortening conditions, open circles to isotonic lengthening conditions and filled circles refer to data collected in the isometric condition. As reported in previous papers [70, 97] the EMG data for a particular condition (isometric or movement) are well described by a circle. Solid, dotted, and broken circles stand for the fit to the data in the isometric, isotonic shortening and isotonic lengthening condition, respectively. The circle fits help to illustrate that the EMG data for isometric and isotonic contractions are different. The EMG activity in isometric and isotonic conditions differs in the orientation of the data (direction sensitivity of muscle activation) and in the amount of EMG activity in both conditions: the amplitude of EMG activity is in general larger for movements than for isometric contractions against the same load (this is always the case for shortening movements and frequently also for lengthening movements) and it has its maximal activity in a different direction. These data, together with the previously published data [70, 97, 98] indicate that the relative contribution of flexor muscles to torque in the elbow joint is different for different motor tasks.

Surface EMG of the elbow extensor *m. triceps caput longum* (D) was recorded too in order to see whether any co-contraction of elbow flexor and extensor muscles was present. Panel D demonstrates that the amount of EMG activity in *m. triceps, caput longum*, is very small and that most EMG activity is found in a direction in which *m. biceps* shows the largest EMG activity. Evidently, this is due to cross talk and this result shows that if there is any activity of *m. triceps*, it cannot be measured

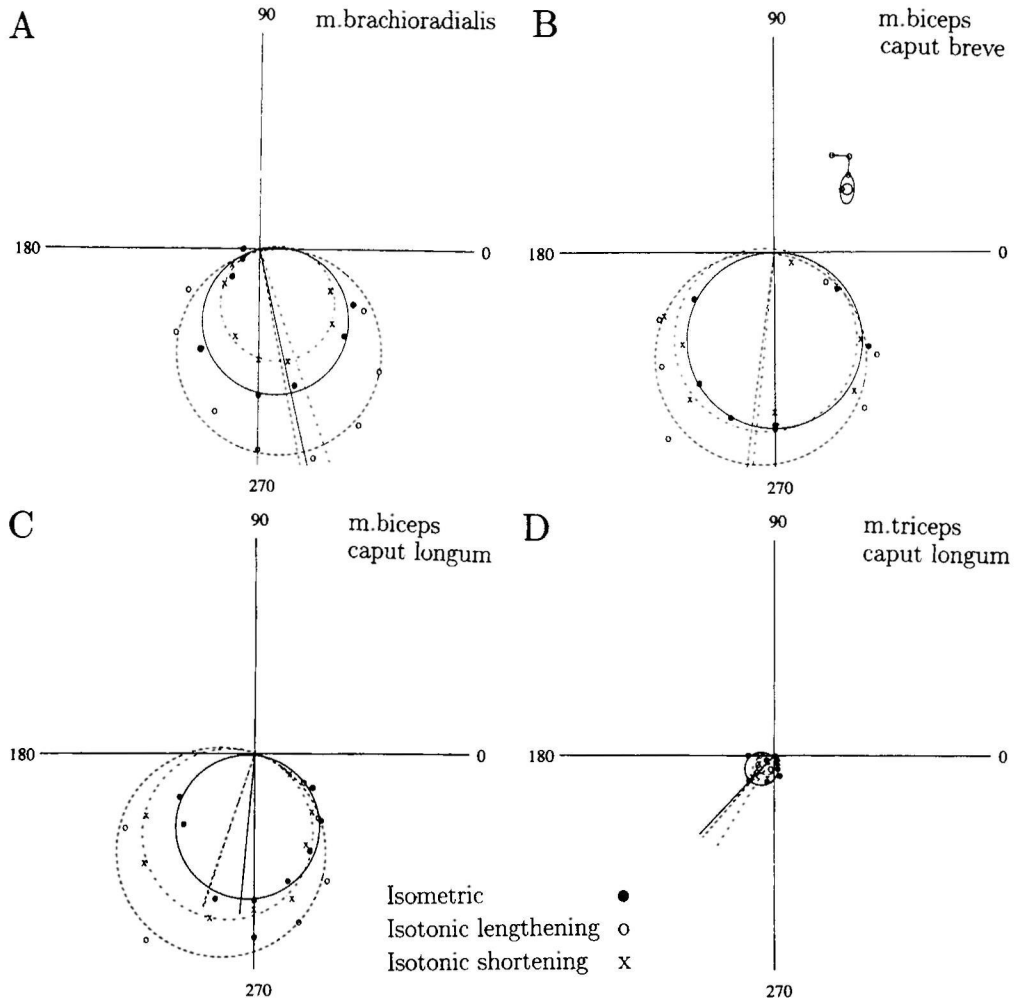


Figure 7.1: Surface EMG data obtained from m. brachioradialis (A), m. biceps brachii caput breve (B), m. biceps brachii caput longum (C) and m. triceps caput longum (D). The EMG data are plotted in polar plots. Each symbol represents the amount of EMG (distance to the origin) for a force of 25N in the indicated direction. The data shown in panels A, B and C have been plotted full scale. The data from m. triceps caput longum (D) have been plotted three times magnified because otherwise they would not be discernable. Crosses (x) refer to data collected in the isotonic shortening condition, open circles to the isotonic lengthening condition and filled circles refer to data collected in the isometric condition. Circle fits are shown by solid, dotted, and broken solid lines for the isometric, isotonic shortening and isotonic lengthening condition, respectively.

quantitatively because it is too small. This result was found in all experiments.

Because of cross talk from *m. biceps caput longum*, EMG signals could not be recorded reliably from *m. brachialis*. Since previous studies [106, 56] have reported the same activation pattern for *m. brachialis* and *m. brachioradialis*, we assumed, that both muscles received the same activation as a function of the direction of force and of movement. Therefore, we assumed that the behavior of both *m. brachioradialis* and *m. brachialis* were very similar. As a consequence, the contribution to elbow joint torque, estimated from the EMG activity of *m. brachioradialis*, represents the summed contribution of *m. brachialis* and *m. brachioradialis*.

For each of the three conditions (isometric contractions, shortening and lengthening contractions) the methods outlined in the theory section were applied to determine the scaling factors (see equation 7) to calculate the torque delivered by each of the individual muscles. The panels in figure 7.2 show the individual torques for each of the conditions and the total elbow torque for forces in various directions. The results for the isometric, the isotonic shortening and the isotonic lengthening conditions are shown at the upper left, upper right and the lower left, respectively.

The symbols in each of the panels in figure 7.2 represent the torque contributed by each muscle to the total torque in the elbow. The contribution from *m. brachioradialis* is represented by open circles and that from *m. biceps* by filled circles. Since the circle, which fits to the EMG data, has almost the same orientation for the short and long head of *m. biceps* (see figures 7.1B and 7.1C) for all subjects (no significant differences were observed for any subject), the mean EMG activity of the two heads of *m. biceps* was used. The sum of the torque contributions from *m. brachioradialis*, *m. brachialis* and *m. biceps* for all force directions is represented by a solid line. The dotted line indicates the total torque in the elbow calculated as the cross product of lever arm and external force at the wrist for all force directions in the horizontal plane. The deviations of the dotted circle relative to the solid line are small indicating that a good fit of the actual torque can be made from surface EMG for each of the conditions.

M. brachioradialis and *m. biceps* have a different relative contribution to total elbow torque in each of the three experimental conditions (see also Theeuwes et al [97, 98]). Examining the direction 270 deg, which is the direction for which the elbow flexion torque is largest, we found that the mean contribution from *m. brachioradialis* and *m. brachialis* together to the total torque in the elbow for the isometric, the isotonic shortening and isotonic lengthening conditions is 40%, 58% and 39%, respectively (see table 7.1). Ignoring the contribution from other muscles, which have a small contribution to elbow joint torque (such as *m. pronator teres* and *m. extensor carpi radialis*) the remainder of the total elbow torque (60%, 42%, and 61%) is provided by the two heads of *m. biceps*. These differences appeared to be significant.

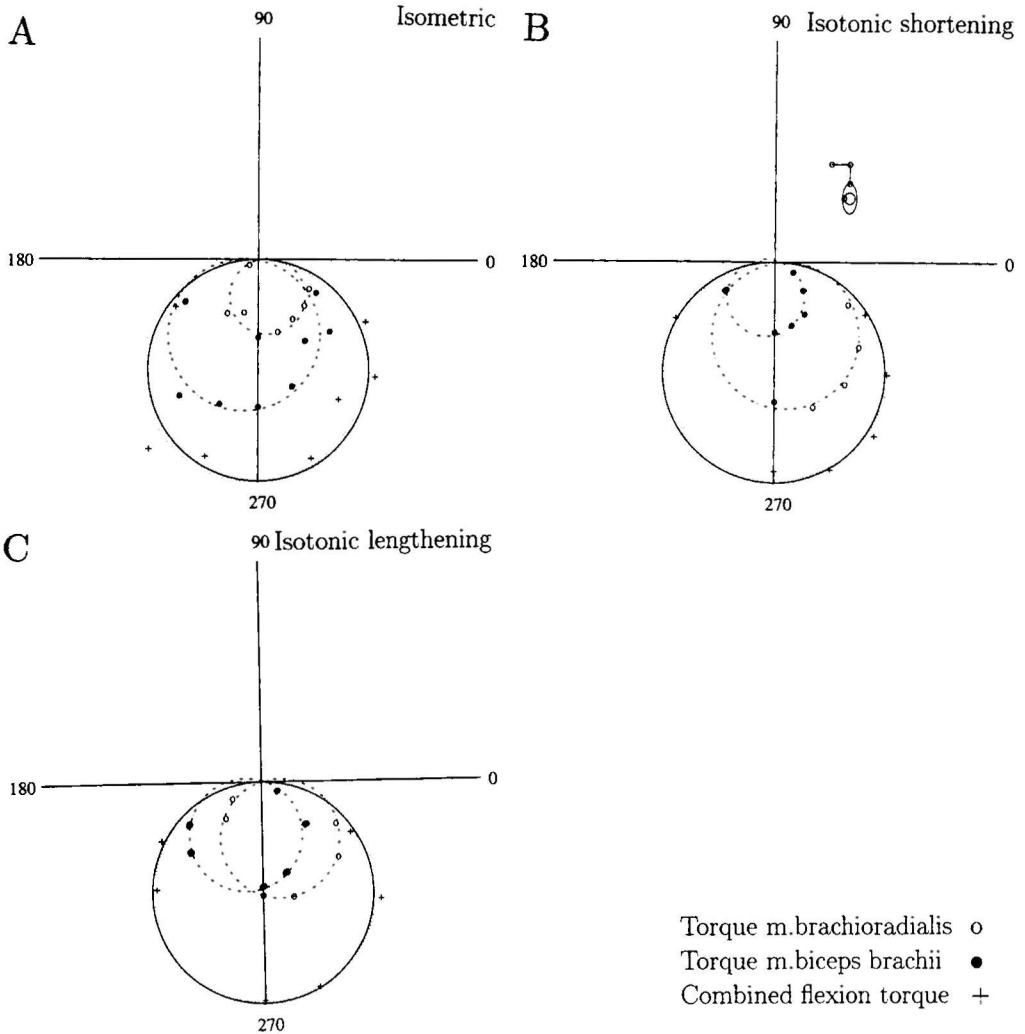


Figure 7.2: Contributions of m.brachioradialis/m.brachialis (open circles) and the two heads of m.biceps (solid circles) to the total torque in the elbow joint. The crosses represent the sum of torque of these muscles. The solid circle is fitted through these data. The torque in the elbow joint as calculated by the cross product of lever arm (wrist-elbow) and external force is indicated by the dotted circle. The broken circles have been fitted to the individual muscle torques.

for each condition in an ANOVA.

These results show that the contribution of m. brachioradialis and m. brachialis

Subject	Isometric	Shortening	Lengthening
EO	34	65	—
MT1	68	84	—
MT2	67	84	—
TT	—	46	—
SG1	22	60	45
SG2	33	45	39
BM	18	30	39
TD	—	50	33
Mean	40 (21)	58 (19)	39 (5)

Table 7.1: The estimated contributions from m.brachioradialis and m.brachialis to the total elbow torque when the subjects exert forces in direction 270 deg for isometric and isotonic (shortening and lengthening) contractions. These estimates are based on the measured surface EMG data using equation (7). If no data are given for a particular condition, either no data were available for that condition (this was the case for the lengthening condition in the initial experiments) or the standard deviation of the circle fit was relatively large, indicating a large variability in the EMG data.

to torque in the elbow joint is larger for isotonic shortening than for isometric contractions. The intersubject variability in the estimated predictions, however, is relatively large. Whether this scatter results from natural variability in the control of the arm muscles, or from noise in the measurements has to be investigated. This will determine how robust and practically useful this method will be. Two subjects were tested twice. The results showed some scatter, which is either due to variability in the control of the arm muscles for the same subject or to the fact that our method is sensitive to noise in the measurements.

Since the orientation of the circles, which are fitted to the EMG data, shows some variability between subjects, we have investigated the effect of small variations in the orientation of the EMG data on the estimate for the relative contribution of the flexor muscles to elbow torque. For this purpose we repeated the analysis with the EMG data presented in a previous paper [98]. We used the averaged data for subject AM in the Theeuwes et al. [98] paper, since multiple data sets were collected for this subject. We then calculated to what extent the relative contribution changed when the orientation of the EMG data was changed by 2 degrees in either clockwise or counterclockwise direction. The results for these (artificially simulated) data are shown in figure 7.3. For these data we used a preferred direction of 278 and 290 for m. brachioradialis under isometric and isotonic shortening conditions, respectively,

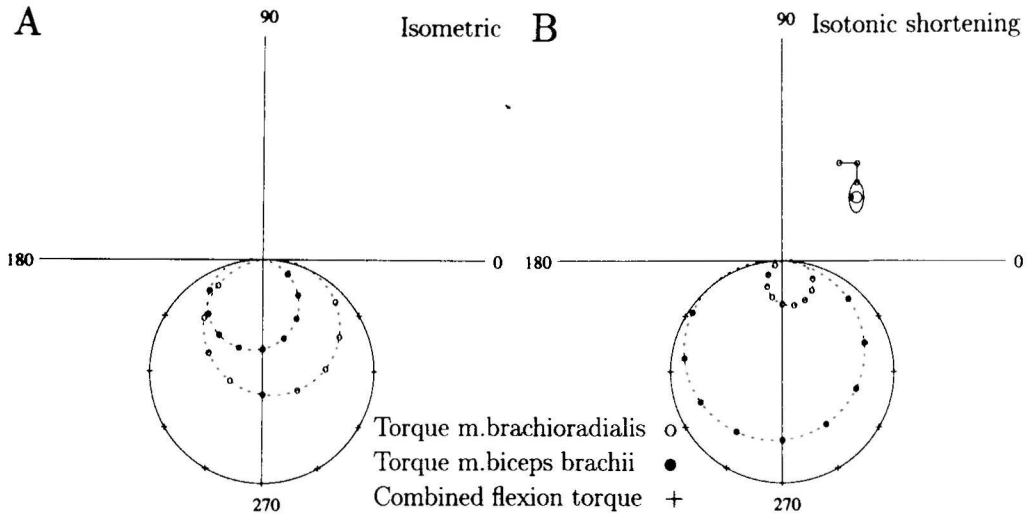


Figure 7.3: Mean EMG data for isometric (A) and isotonic shortening (B) condition obtained from averaged data of subject AM (see chapter 6). The large circle represents the flexion torque in the elbow joint for a force of 25N in various directions in the horizontal plane. The radius of the broken circles is the result of the procedure to estimate the torque contributions of m. brachialis/m. brachioradialis and m. biceps to torque in the elbow joint.

and of 258 and 260 for m. biceps.

The simulated EMG data for the isometric condition for two sets of muscles were represented by a circle through the origin with a maximal amplitude in the preferred direction ϕ_i (278 and 258 deg for m. brachioradialis and m. biceps brachii, respectively) [97, 98]. The torque produced by these muscles, which is proportional to the amplitude of the EMG activity, can then be given as $T_i = \tau_i \times \cos(\phi - \phi_i)$, where τ_i denotes the amplitude of the torque exerted by muscle i and the cosine modulates the torque for different directions of force. The sum $T_1 + T_2$ must be equal to the externally required torque $T_e = |\vec{r} \times \vec{F}_e| = \cos(\phi - 270^\circ)$, where we have taken unity for the amplitude of the external force and the lever arm from wrist to elbow. This torque has its maximal amplitude in the direction 270 deg when lever arm and external force are orthogonal. It is easy to calculate the radii of the torque circles and thus also their relative torque contributions: $\tau_1 = \frac{\cos \phi_2}{\sin(\phi_2 - \phi_1)}$ and $\tau_2 = \frac{\cos \phi_1}{\sin(\phi_1 - \phi_2)}$. Substitution of the preferred directions ϕ_1 and ϕ_2 in these expressions shows that when the combination of preferred directions for m. brachioradialis and m. biceps shifts from (278, 258) to (280, 260), the relative contribution of m. brachioradialis to

the total torque decreases by almost 10 % and the relative contribution for *m. biceps* increases by the same amount. Shifts in the opposite direction, however, resulted in a 10 % increase of the relative contribution from *m. brachioradialis* and the same decrease for *m. biceps*. Because standard deviations of 2 degrees in the orientation of the EMG data are common for our data, the variability in the estimated relative contribution of muscles by our procedure is about 10%. Because of the trigonometric relationship for the estimated contribution of the muscles, the influence of noise will be dependent on the precise preferred directions.

In another effort to investigate the confidence levels of our results we added Gaussian white noise to the same data such that the signal/noise ratio was equal to 10. The preferred direction of the muscles corresponded to the mean values found by Theeuwes et al. [98]. Adding noise to the EMG data resulted in variations of 3% and 9% for the torque contribution for isometric and isotonic shortening data, respectively, relative to the estimates made without noise. These results indicate that our method is not very sensitive for noise on the EMG data. However, small variations in the orientation of the circle which fit the EMG data give relatively large (10%) variations in the estimated torque contribution of muscles.

7.5.2 Estimation of contributions to joint torque based on motor-unit recruitment data.

Estimation of the relative contribution of individual muscles to the total torque in a joint can also be made based on motor-unit recruitment data. An extensive report on the recruitment behavior of motor-units in human elbow muscles for various combinations of isometric torque in flexion/extension and pronation/supination directions is given by van Zuylen et al. [106]. These authors reported on subpopulations of motor-units within the same muscle with a distinctively different recruitment behavior despite the fact that all motor-units have the same mechanical effect because they share the same tendons [33]. These subpopulations have to be handled as separate muscle-units. Based on the paper by van Zuylen et al. [106] we took all 13 subpopulations of motor-units into account which were reported in that study. The recruitment threshold of motor-units in these subpopulations as a function of the combination of flexion/extension (F/E) torque and supination/pronation (S/P) torque is summarized in figure 7.4 and can also be found in van Zuylen et al. [106].

Because no data were available for *m. pronator quadratus*, we assumed a recruitment behavior for its motor-units opposite to that of its antagonist *m. supinator*. The consequences of this choice will be discussed later.

For all subpopulations of motor-units shown in figure 7.4 we calculated the muscle activation for combinations of torques in flexion/extension and supination/pronation

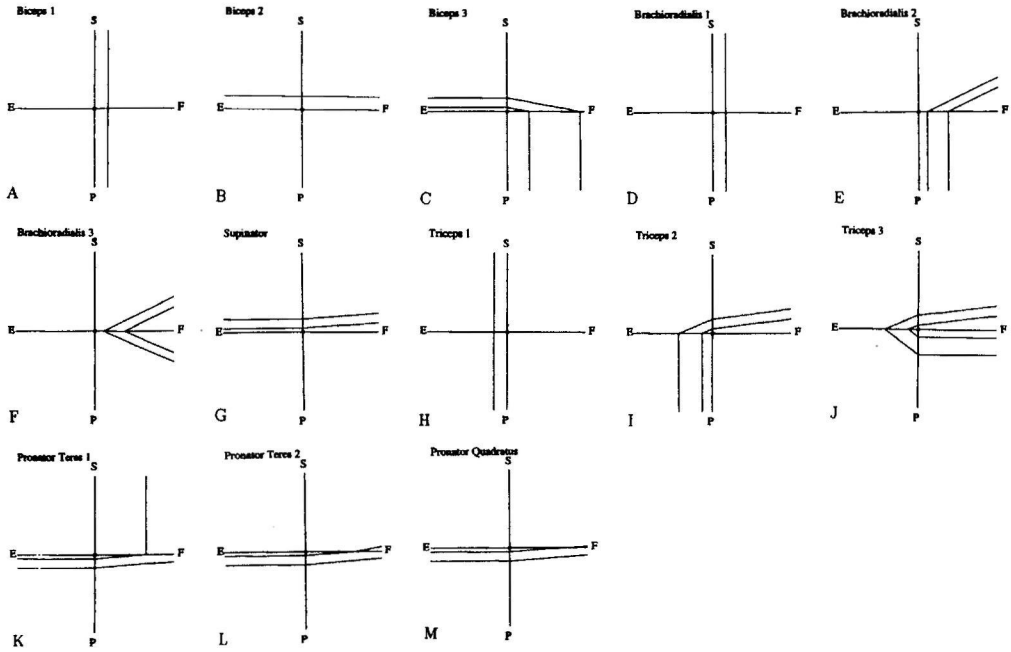


Figure 7.4: The behavior of the recruitment thresholds as a function of the combination of flexion (F), supination (S), extension (E) and pronation (P) for several elbow muscles and subpopulations of motor-units within a muscle. In the panels are shown m.biceps subpopulation 1 (A), m.biceps subpopulation 2 (B), m.biceps subpopulation 3 (C), m.brachioradialis subpopulation 1 (D), m.brachioradialis subpopulation 2 (E), m.brachioradialis subpopulation 3 (F), m.supinator (G), m.triceps subpopulation 1 (H), m.triceps subpopulation 1 (H), m.triceps subpopulation 2 (I), m.triceps subpopulation 3 (J), m.pronator teres subpopulation 1 (K), m.pronator teres subpopulation 2 (L) and m.pronator quadratus (M). These data are taken from van Zuylen et al. [106].

direction. Since the parameters ϕ_0 and $\frac{T}{T_0} \cos(\phi - \phi_0)$ can be derived from the recruitment behavior shown in figure 7.4 the contribution $T_{m,0}$ from muscle m can be calculated for the total torque T in direction ϕ using the set of equations obtained with equation (10). Figure 7.5 shows the shape of the torque contribution of the subpopulations of motor-units with a recruitment behavior illustrated in figure 7.4 for various combinations of Flexion/Extension-torques and Supination/Pronation-torques. If the recruitment thresholds fall along a straight line (such as in figure 7.4A) the torque contribution is given by a circle. If the recruitment behavior of a motor-unit is described by different line segments, as for m. biceps subpopulation 3 (figure 7.4C), a

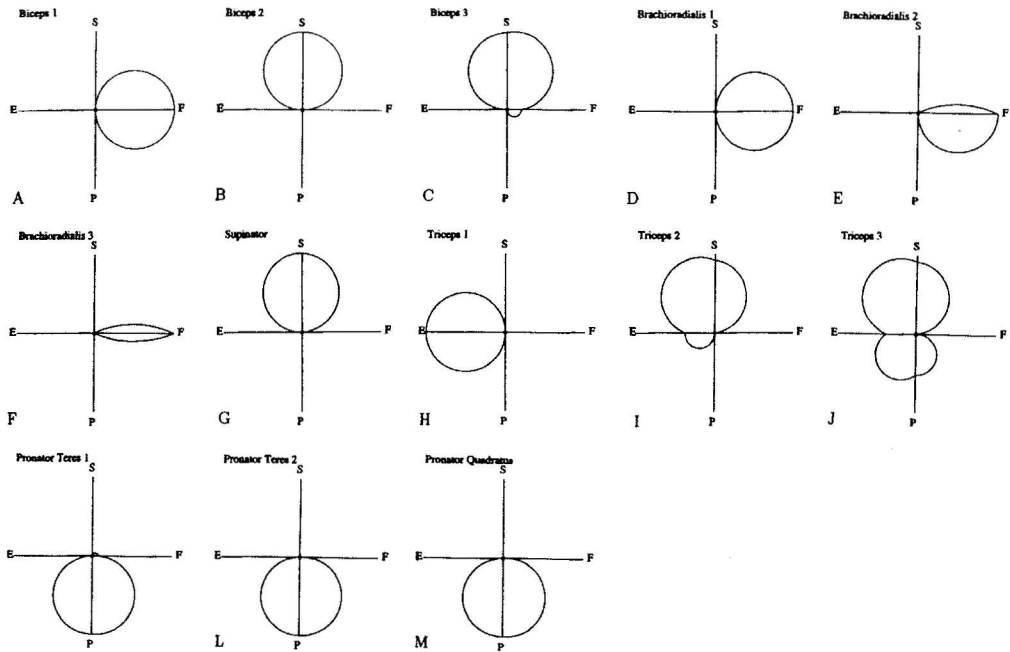


Figure 7.5: The results of the estimation procedure to estimate the torque contribution of various subpopulations of motor-units as a function of the combination of flexion (F), supination (S), extension (E) and pronation (P). The recruitment thresholds of these motor-units are shown in figure 7.4. In the panels are shown m.biceps subpopulation 1 (A), m.biceps subpopulation 2 (B), m.biceps subpopulation 3 (C), m.brachioradialis subpopulation 1 (D), m.brachioradialis subpopulation 2 (E), m.brachioradialis subpopulation 3 (F), m.supinator (G), m.triceps subpopulation 1 (H), m.triceps subpopulation 1 (H), m.triceps subpopulation 2 (I), m.triceps subpopulation 3 (J), m.pronator teres subpopulation 1 (K), m.pronator teres subpopulation 2 (L) and m.pronator quadratus (M).

transformation can be found for each of the line segments. With the requirement of continuity the concatenation of circle segments in figure 7.5 can be derived.

Only a scaling constant representing the relative contribution of these subpopulations to the total torque T has to be determined. As described in the theory section, a matrix equation similar to equation 7 can be constructed for these data. One should replace EMG_m by $\frac{T}{T_o} \cos(\phi - \phi_0)$ and $C_{m,j}$ by $T_{m,0}$. Some muscles generate torques which have components both for flexion/extension and for supination/pronation. The ratio of the flexion/extension and supination/pronation torque components is defined by the anatomical lever arms of the muscles [19, 68, 89]. The

modulation of these torque components, however, must be the same because all subpopulations share the same origin and insertion of tendons. For each direction both the required flexion/extension torque and the supination/pronation torque have to be satisfied. This results in two equations per direction with just one unknown scaling parameter per muscle or subpopulation of motor-units.

A singular value decomposition has been used to find the eigenvalues and eigenvectors of the matrix with coefficients $T_m(\phi)$ obtained with the equations (7) and (10) in order to find the scaling constants necessary to relate the recruitment behavior of individual muscles or of subpopulations of motor-units to the total joint torque. Three eigenvalues were equal to zero, which means that there exists a three dimensional solution space instead of just one single unique solution. One dimension of this solution space comes from the three subpopulations in m.biceps. The activation pattern of subpopulation 3 of this muscle (see figure 7.4C) can be constructed by a linear combination of activation patterns of subpopulations 1 and 2 (see figures 7.4A and 7.4B). The recruitment behavior of subpopulation 3 is the same as that for subpopulation 1 in the (F/P)-quadrant, the same as that for subpopulation 2 in the (S/E)-quadrant and the same as the combination of these subpopulations in the (F/S)-quadrant.

The second dimension of this solution space comes from the use of m. biceps subpopulation 2 and 3 for supination torques in addition to m.supinator. Two subpopulations from m. biceps are active when a torque with a component in supination direction is present. Because m.biceps has a mechanical contribution to flexion torque, this contribution to flexion torque, which is generated during supination, has to be canceled. This can be done by activating the subpopulations 2 and 3 in m. triceps (see figures 7.4I and 7.4J). The activity of subpopulation 1 of m.triceps, which is activated for extension torques only (figure 7.4H), is then also determined because it has to contribute the extension torque which is not provided by subpopulations 2 and 3.

The third dimension of this solution space comes from motor-units labeled "m.pronator teres 2" for pronation torques. This muscle contributes mechanically to torque in flexion and pronation direction. The undesired flexion torques, when a pure pronation torque has to be generated, can be compensated by activation of m.triceps subpopulation 3, which is the only subpopulation of m. triceps which can be activated in the Flexion/Pronation-quadrant. The activation of m.pronator teres relative to the activation of m. pronator quadratus determines the relative contribution of the subpopulations 2 and 3 of m.triceps.

Given these three degrees of freedom in the solution space, the activation of the other pools of motor-units is uniquely determined. The use of m.pronator teres subpopulation 2 determines the ratio between m.triceps subpopulation 2 and 3. Only

subpopulation 3 can compensate the flexion torque of *m. pronator teres*. *M. pronator quadratus* generates the remainder of the pronation torque.

For torques with a supination component the maximal activation of the subpopulations 1 and 3 in *m. biceps* is determined by the slope of the recruitment lines for *m. supinator* in the Flexion/Supination-quadrant. For joint torques with mainly a flexion component, activation of subpopulations 1 and 3 leads automatically to a contribution from these muscles to supination as well. Because the total joint torque already has a small supination component, which is now mainly generated by *m. biceps*, the contribution from *m. supinator* has to be small. The slope of the recruitment line for *m. supinator* determines to what extent the relative contribution from *m. supinator* to the total supination torque in the elbow decreases for joint torques with a smaller torque component for supination. For these joint torques, the relative contribution from *m. biceps* subpopulations 1 and 2 to the supination torque and hence to the flexion torque in the elbow can increase.

Similarly, the maximal activity of motor-units in subpopulations 1 and 3 of *m. biceps* is also determined by the slope of recruitment lines of motor-units in *m. pronator quadratus* in the (F/P)-quadrant. Here *m. biceps* generates a mechanical contribution to supination torque when it is activated for flexion torques. This undesired supination torque has to be compensated for by *m. pronator quadratus*, which gives a lower recruitment threshold for pronation when flexion torques are involved. The flexion torque can be provided by *m. biceps*, *m. pronator teres* and *m. brachioradialis*. Given the contribution from *m. biceps* and *m. pronator teres*, the flexion torque which is not generated by these muscles must be generated by *m. brachioradialis*.

Without additional constraints, except the requirement that all muscles must have an activation which is not negative, the three degrees of freedom in the solution space can not be removed and within the solution space each solution has equal likelihood. Therefore only ranges of relative contributions can be given. The ranges of relative contributions of the individual muscles to torques in pure flexion, supination, extension and pronation torques are given in table 7.2. The main contribution (57% to 80%) to the flexion torque comes from motor-units from subpopulation 1 in *m. brachioradialis* and *m. brachialis*. Subpopulation 2 in these muscles provides less than 4% of the total torque. Subpopulation 3 is not used at all. The subpopulations 1 and 3 in *m. biceps brachii* contribute 20%-43% to flexion torque (Subpopulation 2 is not activated for a torque without a supination component). Subpopulation 2 in *m. pronator teres* is predicted to provide at most 2% of the flexion torque. The subpopulation 1 in *m. pronator teres* is not used at all. Supination torque is mainly provided by *m. supinator* (87%-100%) and for a small part by *m. biceps* subpopulations 2 and 3. *M. pronator quadratus* generates 88%-100% of the pronation torque. *M. pronator teres 2* generates no more than 12% of the pronation torque. Because

	F	S	E	P
M.biceps 1+3	20-43 %	-		
M.biceps 2+3	-	0-13 %		
M.brachioradialis 1+2	57-80 %			
M.brachioradialis 3	-			
M.supinator		87-100 %		
M.triceps 1			66-100 %	
M.triceps 2+3			0-34 %	
M.pronator teres 1	-			-
M.pronator teres 2	0-2 %			0-12 %
M.pronator quadratus				88-100 %

Table 7.2: Lists of ranges for the relative contributions of individual muscles and subpopulations of motor-units within a muscle to the total elbow torque for pure flexion (F), supination (S), extension (E) and pronation (P). These estimates are based on recruitment data reported in van Zuylen et al., [106].

the maximal activation of m. triceps subpopulations 2 and 3 is determined by the activation of pronator teres 2 (subpopulation 3) and by the activation of m. biceps (subpopulations 2 and 3), the contributions from these subpopulations to flexion torque is at most 34%. Subpopulation 1 in m. triceps generates the remaining 66%-100% of the extension torque.

7.6 Discussion

In order to understand the coordination of muscle activation patterns several studies have proposed constraints, which give rise to a reduction of degrees of freedom [18, 103, 28]. In this study we have chosen another approach in which we started from the experimental data. Based on these data, we have tried to estimate the relative contribution of muscles to joint torque.

A closer look at tables 7.1 and 7.2 reveals that the predictions based on the data obtained by Theeuwes et al ([98]; see table 7.1) and that based on the data obtained by van Zuylen et al. ([106]; table 7.2) for the relative contribution to torque in the elbow joint by m.brachialis and m. brachioradialis are not quite in agreement, although the same procedure was used to estimate the torque contribution in both cases. The data in table 7.1 are well in agreement with earlier estimates [57, 106]. On the other hand, the data in table 7.2 are estimated such that a good fit was obtained not only for flexion/extension of the elbow but also for supination/pronation.

Therefore, more information was available to estimate the data in table 7.2. The most likely explanation is that the data in both tables are reliable and that the differences have to be explained by the fact, that the data of van Zuylen et al. [106], which led to the data in table 7.2, were obtained for an elbow joint angle of 110 deg, instead of 90 deg as in our study. Since the relative activation of elbow flexor muscles changes with elbow joint angle [26] and since the mechanical advantage of *m. biceps brachii*, *m. brachialis*, and *m. brachioradialis* changes in a different way with elbow joint angle [107], the different position of the arm may quite well explain the differences in tables 7.1 and 7.2.

Several attempts to estimate the relative contribution of muscles to the total torque in a joint have been reported [57, 9, 106]. Jørgenson and Bankov [57] estimated the relative contribution based on the physiological cross sectional area of the muscles. Because of the existence of multiple subpopulations of motor-units within one muscle with different activation patterns [106], the physiological cross sectional area is not a good criterion for the estimation of the relative contribution from individual muscles to total joint torque.

Cnockaert et al. [9] made their estimates based on the integrated EMG activity from *m. biceps* and *m. brachioradialis*. They made the assumption that the EMG activity from a muscle was linearly related to the torque from a muscle. The EMG activity of these muscles was measured under three conditions: flexion, flexion with supination and flexion with pronation. From these three conditions they constructed a matrix equation similarly to ours. Our method for estimating of the relative contribution from individual muscles to the total joint torque has several advantages over the method they proposed. 1) Our method can also be used for non-linear EMG-force relationships. 2) It is difficult to measure EMG very accurately. Therefore, it is advisable to construct an overdetermined matrix equation, as we do, to reduce the effect of noise. The estimation by Cnockaert et al. [9] for the relative contributions to the total flexion torque in the same condition could differ by more than 40%. These differences are substantially larger than the 10% standard deviation which we typically find. 3) Our method is more general and can be extended for more muscles and torques in other joints which can be helpful to estimate the activation of bi-articular muscles. Both the method proposed by Cnockaert et al. [9] and by us for estimating the relative contribution from individual muscles to the total torque in a joint, is limited in use if multiple subpopulations of motor-units are active. Because then the same amount of EMG, even without noise, can correspond to different torques, the reliability of these methods decreases tremendously. To incorporate the activity from these subpopulations correctly, intramuscular EMG activity has to be measured because the contributions from the individual subpopulations can not be separated from surface EMG directly.

Estimates of the relative contributions from individual muscles or subpopulations of muscles based on intramuscular EMG activity have been reported by van Zuylen et al., [106]. They assumed that the number of recordings of motor-units belonging to one of the subpopulations in m. biceps and triceps brachii from which they obtained recordings, was a reliable estimate for the distribution of muscle fibers over the individual subpopulations. Furthermore they assumed that the contribution of subpopulations is proportional to the number of muscle fibers in each of the subpopulations. The first assumption may be heavily biased because recordings from motor-units near the boundaries of the muscle are very difficult to obtain. However, the estimate of 38% for the contribution of m.biceps to flexion torque falls in the range for the estimated contribution of m.biceps which is predicted by our method (see table 7.2).

The recruitment behavior of m.pronator quadratus has not been measured directly. From this deep muscle no surface EMG recordings can be obtained. Intramuscular recordings are very difficult because this muscle is very thin. Because scratching of the bone underneath this muscle with a needle, while inserting the intramuscular electrodes, would cause severe pain to the subject, no attempts have been made to record from this muscle. Therefore we made an initial guess of the recruitment behavior for m. pronator quadratus based on the behavior of its antagonist m. supinator. For several variations on this initial guess, we constructed a matrix equation as described in the Theory and Results section to make estimations of the relative contributions of individual muscles and subpopulations of motor-units to the joint torque. For the recruitment behavior shown in figure 7.4M the discrepancy between the externally required elbow torque and the sum of the individual contributions from muscles and subpopulations of motor units was virtually absent. Any deviations from this behavior resulted in an increased discrepancy. This suggests that our assumption about the recruitment behavior of motor-units in m. pronator quadratus was quite plausible.

The methods outlined above which make estimations based on the EMG activity of muscles or subpopulations of muscles, can not separate the contributions from muscles with the same recruitment behavior and with the same activation pattern unless they have a distinctly different mechanical effect. For m. brachioradialis and m. brachialis the relative contributions from the individual muscles can not be distinguished, because they show similar activation patterns [56]. Only the combined contribution from these muscles could be estimated.

Hoofdstuk 8

Inleiding en samenvatting

8.1 Algemene inleiding

De coordinatie van de spieren en gewrichten in de arm om bepaalde taken uit te voeren lijkt eenvoudig voor gezonde mensen. De oorzaak voor dit schijnbaar gemak waarmee deze coordinatie tot stand wordt gebracht, is gelegen in de ontelbare malen dat we deze taken hebben uitgevoerd. We kennen deze taken als het ware van buiten en kunnen ze uitvoeren, zonder dat wij ons er van bewust zijn hoe we dat doen. Vragen als "welke spieren moeten gebruikt worden" en "in welke mate moeten ze samentrekken" en "welke hoeken moeten de gewrichten hebben", worden niet expliciet gesteld. Mensen hebben besturingstrategieën ontwikkeld voor spieren en gewrichten waarvan ze zich niet actief bewust zijn. Stelt U zich eens voor dat plotseling een mens de beschikking zou krijgen over vier armen, zoals de Hindoeïstische god Shiva op de omslag van dit proefschrift. Om dit tweetal extra armen te besturen, kan hij er niet op vertrouwen dat de vaardigheden die hij verworven heeft voor het oorspronkelijke paar armen, zonder meer bruikbaar zijn zonder veel bewust denkwerk. Waarschijnlijk zal de functie van deze nieuwe armen beperkt blijven tot eenvoudige statische taken, zoals het vasthouden van voorwerpen die dan bewerkt kunnen worden m.b.v. de oorspronkelijke twee armen. Alhoewel zo'n persoon een grotere flexibiliteit heeft, d.w.z. meer vrijheidsgraden, zal hij deze niet volledig hoeven te benutten voor alledaagse taken, daarvoor is hij al adequaat genoeg uitgerust met zijn oorspronkelijk paar armen. Voor deze taken is zijn nieuwe motorische systeem dus redundant.

Allereerst moge het duidelijk zijn dat het menselijk motorisch systeem niet echt redundant is: elke schade aan het effector systeem zal op de een of andere manier tot uiting komen door vermindering van functionaliteit. Voor eenvoudige taken worden echter niet alle vrijheidsgraden van het menselijk motorisch systeem eenduidig

vastgelegd. Zo leiden bijvoorbeeld verschillende combinaties van gewrichtshoeken in elleboog, schouder en pols tot dezelfde 3-D positie van het puntje van de wijsvinger. In zo'n geval ontstaat er een probleem omdat er meerdere oplossingen beschikbaar zijn voor het einddoel, maar dat slechts een daarvan gekozen moet worden. Welke oplossing de beste is, moet bepaald worden door extra randvoorwaarden. Dit kan vergeleken worden met een tochtje van plaats A naar plaats B. Er zijn diverse alternatieve wegen beschikbaar. Wanneer tijd een belangrijke randvoorwaarde is, ligt de keus voor de snelweg voor de hand. Anderzijds zal de keus voor een weg met meer natuurschoon tot een keus voor een meer rustieke weg leiden. Afhankelijk van de randvoorwaarden zal dus een andere oplossing voor het redundantie-probleem gekozen worden.

Vergelijkbare redundantie-problemen bestaan er voor de menselijke arm, zowel op gewrichtsniveau als op spierniveau. Er zijn diverse hypothesen voor randvoorwaarden en strategieën gepostuleerd om deze redundanties op te lossen op gewrichtsniveau [90, 22, 11] en op spierniveau [18, 103, 52]. Alhoewel diverse hypothesen over de manier, waarop het menselijk motorisch systeem deze schijnbare redundantie zou kunnen oplossen, beschikbaar zijn, zijn er onvoldoende experimentele data beschikbaar om onderscheid te kunnen maken tussen de diverse hypothesen en om na te gaan of enige hypothese afdoende verklaringen en voorspellingen biedt. Een van de voornaamste doelen van het in dit proefschrift beschreven onderzoek was het verschaffen van meer experimentele waarnemingen om daarmee diverse hypothesen te kunnen toetsen.

8.1.1 Redundantie op gewrichtsniveau

Elk van onze armen bezit op gewrichtsniveau vele vrijheidsgraden. Voor bepaalde taken, zoals het vermijden van hindernissen of het serveren van een erg vol kopje koffie, zijn vrijwel alle beschikbare vrijheidsgraden noodzakelijk. De meeste taken zijn echter op verschillende wijzen uit te voeren. Dit probleem bestaat ook in de robotiek voor robotarmen met meerdere gewrichten. De positie van de hand c.q. manipulator in drie dimensies kan bereikt worden door vele combinaties van gewrichtshoeken. De besturingsstrategie, om de hand langs een pad te bewegen, kan er op gericht zijn om de hoekveranderingen in de gewrichten te minimaliseren. Dit lijkt op het eerste gezicht heel wenselijk, maar er kan aangetoond worden dat de arm een andere set gewrichtshoeken heeft wanneer de hand na een beweging weer dezelfde beginpositie bereikt. De oriëntatie van een arm, die op dergelijke wijze bestuurd wordt, hangt af van zijn voorgeschiedenis [60]. Het meerdere malen afleggen van een bepaald pad leidt tot een arm met gewrichtshoeken die de fysiologische grenzen overschrijden, hetgeen onaanvaardbaar is. Ook de eigenlijke beweging van de hand, van de ene positie naar de andere, zal op een andere wijze gemaakt worden, afhankelijk van de

precieze orientatie van de arm en afhankelijk van voorgaande motorische handelingen, waardoor planning lastiger wordt.

Het redundantie-probleem voor de menselijke arm kan voor een uitgebreid scala aan taken bestudeerd worden. Het beginnen met een erg eenvoudige taak, zoals het wijzen met gestrekte arm, lijkt een natuurlijke keuze. De wijsrichting van een gestrekte arm legt slechts 2 van de 3 vrijheidsgraden van de schouder vast, namelijk de elevatie (omhoog/omlaag) en de azimuth (links/rechts). De mate van endo-/exorotatie van de bovenarm en pronatie/supinatie van de onderarm, de rotatie van deze ledematen om hun lengteas, ook wel torsie genoemd, wordt niet vastgelegd door de wijsrichting. Wanneer proefpersonen gevraagd wordt om deze taken diverse malen uit te voeren, doen ze dat altijd op dezelfde manier (afgezien van kleine afwijkingen van ongeveer een graad). Blijkbaar benutten zij steeds dezelfde besturingsstrategie. Verrassender is het dat meerdere proefpersonen een erg vergelijkbare strategie gebruiken. Een algemeen geldende randvoorwaarde voor dit soort strategieën lijkt voor de hand te liggen (zie hoofdstukken 2 en 3). Wanneer eenmaal voor deze eenvoudige taak volledig begrepen is hoe de redundantie wordt opgeheven, dan kan dit inzicht gebruikt worden om complexere taken te bestuderen.

Wijzen met gestrekte arm naar een (bewegend) doel werd ook uitgekozen als taak in onze experimenten vanwege een sterke analogie met het kijken naar een (bewegend) doel. Dit laatste is al gedurende lange tijd uitgebreid onderzocht. In beide gevallen worden slechts twee vrijheidsgraden vastgelegd door de wijs- c.q. kijkrichting. De mate van endo-/exorotatie en pronatie/supinatie van de arm en de mate van torsie van het oog is onbepaald voor deze specifieke taak. Sinds de observaties van Donders in 1848 [16] is het bekend dat de torsie van het oog op unieke wijze afhangt van de kijkrichting. Wanneer de orientatie van het oog voor een bepaalde kijkrichting als referentie genomen wordt, dan kunnen de orientaties van het oog voor alle andere kijkrichtingen verkregen worden door middel van rotaties vanuit de referentie-orientatie om vaste assen die in een plat vlak liggen, het zogenaamde Listingvlak [36]. Deze rotaties kunnen weergegeven worden m.b.v. rotatievectoren waarvan de richting parallel is aan die van de rotatie-as en waarvan de grootte afhangt van de rotatiehoek. Voor een speciale referentie, de zogenaamde primaire positie, staat het Listingvlak, dat alle rotatievectoren bevat die de rotatie vanuit de referentie-orientatie naar de actuele oog-orientatie beschrijven, loodrecht op de kijkrichting van die referentie. Deze bevindingen bleken niet alleen voor fixaties van het oog, maar ook voor bewegingen van het oog van toepassing te zijn [100].

Vergelijkbare resultaten werden voor de arm en het hoofd gevonden door Hepp et al. [41]. Zij vonden dat de orientaties voor de arm ook door rotatievectoren in een plat vlak beschreven konden worden. Dat vlak was wel aanzienlijk dikker dan het vlak voor oogbewegingen (standaard deviaties van ongeveer 6 graden in plaats van 1

graad, zoals gevonden voor oogbewegingen). De grotere dikte schreven zij toe aan het grotere bereik van de endo-/exorotatie voor de bovenarm en de pronatie/supinatie van de onderarm in vergelijking tot het bereik van de torsiebewegingen van het oog. Een alternatieve verklaring voor het verschil in dikte van de vlakken voor oog- en armbewegingen was dat proefpersonen vrijwillig de mate van endo-/exorotatie en pronatie/supinatie kunnen veranderen, dit in tegenstelling tot de torsiecomponent van de oog-orientatie die niet vrijwillig veranderd kan worden.

De grotere flexibiliteit en veelzijdigheid van de arm werd door Hepp et al. [41] als verklaring gegeven voor de vondst dat de orientatie van de vlakken van rotatievectoren afhankelijk is van de richtingen waarin gewezen wordt (nagenoeg loodrecht op de gemiddelde wijsrichting van de arm), terwijl het vast t.o.v. het hoofd is voor oogbewegingen. De vlakken met rotatievectoren voor de arm, de hand en het hoofd zijn vrijwel parallel. Een mogelijke verklaring hiervoor zou kunnen zijn dat dit een strategie weergeeft voor de coördinatie van oog- en handbewegingen. Voor een gegeven werkgebied zouden het oog, het hoofd en de arm een gemeenschappelijk 2-dimensionaal refrentieframe kunnen delen waardoor de 9-dimensionale ruimte van alle mogelijke orientaties voor oog, hoofd en arm gereduceerd kan worden tot een 2-dimensionale ruimte. Berekeningen en coördinatie van hun interactie zouden dus efficient georganiseerd kunnen worden. Onderzoek naar deze organisatie was de achterliggende motivatie voor het onderzoek dat beschreven wordt in hoofdstukken 2 en 3.

8.1.2 Redundantie op spierniveau

Niet alleen het aantal gewrichten is redundant voor bepaalde eenvoudige taken, dat geldt ook voor het aantal spieren dat een gewricht omspant. Het ellebooggewricht, bijvoorbeeld, wordt omspannen door een aantal spieren dat het aantal vrijheidsgraden van dat gewricht overtreft. Het ellebooggewricht heeft twee vrijheidsgraden: flexie/extensie (buigen/strekken van de onderarm) en pronatie/supinatie (rotatie van de hand naar binnen/buiten). Aangezien spieren niet kunnen duwen, maar alleen trekken, zouden 4 spieren genoeg kunnen zijn voor deze twee vrijheidsgraden. Meer dan 7 spieren, echter, dragen bij aan flexie/extensie en pronatie/supinatie. Dit impliceert dat dezelfde momenten gegenereerd kunnen worden door een oneindig aantal combinaties van spieractivatie-patronen.

Voor flexiemomenten zijn m.brachioradialis, m.brachialis en m.biceps de belangrijkste spieren. Deze drie spieren kunnen het gewenste flexiemoment in de elleboog elk afzonderlijk, of in combinatie, genereren. Alleen het totaal van hun bijdragen wordt voorgeschreven door het vereiste flexiemoment. Co-contractie van antagonisten zoals m.triceps maakt de situatie nog complexer.

Het aantal spieren is al redundant voor flexie /extensie- en pronatie-/supinatie-momenten. Dat spieren niet als enkelvoudige samenhangende structuren beschouwd kunnen worden, laat de redundantie nog verder toenemen. De oorzaak hiervan is deels anatomisch, maar ook voor een deel het gevolg van de verschillende aansturing van diverse subpopulaties van motor-units binnen dezelfde spier. M biceps, bijvoorbeeld, is met een enkele pees bevestigd aan de onderarm, en met twee pezen aan de schouder. Deze twee delen, de lange en de korte kop, hebben verschillende activaties. Binnen de lange kop van de biceps zijn weer drie subpopulaties van spiervezels aangetoond met elk een eigen activatiepatroon [33, 106]. M biceps draagt, ten gevolge van de aanhechting van zijn pees aan de onderarm, tegelijkertijd bij aan zowel flexie als supinatie in het ellebooggewricht. De activatie van de subpopulaties motor-units bleek af te hangen van specifieke combinaties van supinatie- en flexiemomenten, ondanks het feit dat het mechanisch effect van alle subpopulaties gelijk is.

Het aantal spieren en subpopulaties, van motor-units binnen een spier, dat het ellebooggewricht omspant is groot en derhalve kan een oneindig aantal combinaties van spieractivatie-patronen bijdragen aan hetzelfde moment in een gewricht. Ondanks deze redundantie wordt een vergelijkbaar spieractivatiepatroon gevonden bij alle proefpersonen voor een specifieke motorische taak [3, 21]. Hierdoor wordt gebruik van een algemeen geldende randvoorwaarde of coordinatiestrategie gesuggereerd.

Om deze randvoorwaarde of strategie te onderzoeken, moet het verkrijgen van kennis over hoe de spieractiviteit wordt gecoördineerd tijdens isometrische contracties en tijdens bewegingen in verschillende richtingen, de eerste stap zijn. De bijdrage van elke spier afzonderlijk aan het totale moment in een gewricht, kan niet direct gemeten worden. Een scala van variabelen geeft echter wel indirect informatie over de spiercoördinatie. Wanneer deze variabelen gemeten worden tijdens diverse motorische taken, kunnen de relatieve verschillen in de spiercoördinatie onderzocht worden. Externe variabelen, zoals de kracht uitgeoefend door de pols, zowel qua grootte als qua richting, en de positie en de tijdsafgeleide daarvan, de snelheid, kunnen direct gemeten worden met strain gauges en goniometers. Met behulp van deze variabelen en inverse dynamica, kunnen de totale momenten en gewrichtshoeken gemeten worden.

Met enige anatomische kennis kunnen deze data ook inzicht bieden in de spierlengte en de veranderingen daarvan. Deze grootheden zijn van invloed op de maximale kracht die een spier kan uitoefenen wegens de kracht-lengte en kracht-snelheidsrelaties [69]. De interne variabelen, zoals de bijdragen van individuele spieren aan het totale moment in een gewricht, kunnen niet direct gemeten worden. Voor deze metingen zou het noodzakelijk zijn om krachtstransducers te implanteren in de pezen van alle spieren.

Een benaderingswijze die vriendelijker is voor de proefpersoon, maar minder direct, is het meten van de elektrische activiteit van spiervezels, het zogenaamde Electro

Myo Gram (EMG) Een variabele die vaak gebruikt wordt om het EMG, dat aan de oppervlakte, dus op de huid, gemeten wordt, te quantificeren is het gelijkgerichte signaal gemiddeld over een bepaalde tijd [65] De signalen van spiervezels dicht bij de oppervlakte elektroden geven een grotere bijdrage dan die van spiervezels die ver weg liggen vanwege spatiele filtering hetgeen ook nog eens de vorm van de actiepotentialen verandert Dit betekent dat de amplitude van het signaal afhangt van de precieze plaats van de oppervlakte elektroden t o v de actieve spiervezels De amplitude wordt ook beïnvloed door de dikte van de onderhuidse vetlaag en de aanwezigheid van bloedvaten Daarom is de absolute waarde van het gemeten oppervlakte EMG niet direct nuttig om een indruk te verkrijgen van de activatie van een spier Men kan alleen twee EMG-waardes met elkaar vergelijken en uitspraken doen over de relatieve activiteit van de spieren op de tijdstippen dat de signalen van het oppervlakte EMG gemeten werden

Gedetailleerdere informatie over individuele spiervezels kan verkregen worden uit de signalen gemeten door intramusculaire elektroden Omdat een aantal individuele spiervezels samen wordt geactiveerd door een motoneuron, gezamenlijk motor-unit genoemd, genereren alle spiervezels, die door dit motoneuron worden geactiveerd, simultaan hun actiepotentialen De gecombineerde actiepotentialen van alle tot die ene motor-unit behorende spiervezels resulteren in karakteristieke signalen door hun relatieve geometrische positie t o v de electrode en door de eigenschappen van de volumegeleider [96] Actiepotentialen van verschillende motor-units kunnen onderscheiden worden op grond van hun specifieke golfvormen zoals die gemeten worden m b v intramusculaire elektroden

Krachtsproductie door een spier komt op een uitermate ordelijke manier tot stand De motor-units worden in een vaste volgorde gerecruteerd t g v het "size principle", geformuleerd door Henneman [39] Wanneer de input van de motor-unit een bepaalde waarde overschrijdt, dan wordt die motor-unit gerecruteerd en begint kracht te leveren Gedurende elke twitch-contractie van de motor-unit neemt de kracht toe, bereikt zijn maximum en neemt vervolgens weer langzaam af Na een bepaalde refractaire periode kan de motor-unit opnieuw geactiveerd worden De frequentie, waarmee dat gebeurt, wordt de vuurfrequentie genoemd Voor een groter input-sig-naal aan de motoneuronen neemt de vuurfrequentie van alle gerecruteerde motor-units langzaam toe Ook worden voor grotere inputsignalen steeds meer motor-units gerecruteerd Door middel van intramusculaire waarnemingen kan het activatiepatroon van individuele motor-units, mogelijk behorende tot verschillende subpopulaties, bestudeerd worden zowel qua recruitment-drempel als qua vuurfrequentie

Omdat intramusculaire afleidingen zo specifiek zijn, kunnen ze informatie verschaffen over het organisatieschema van individuele motor-units, hetgeen onmogelijk is met oppervlakte EMG afleidingen Anderzijds bieden deze afleidingen alleen in-

formatie over een beperkt deel van de spier. Oppervlakte EMG en intramusculaire afleidingen samen kunnen dus inzicht verschaffen in het activatiepatroon van spieren vanuit een ander perspectief en waardevolle informatie toevoegen aan de kennis die met de andere methode verkregen is. Dit wordt beschreven in de hoofdstukken 4 tot en met 7.

8.2 Overzicht en samenvatting

8.2.1 Hoofdstukken 2 en 3

Om te bestuderen hoe de redundantie in de menselijke arm op gewrichtsniveau wordt opgelost, hebben wij wijsbewegingen met een gestrekte arm onderzocht. Deze bewegingen hebben sterke analogieën met oogbewegingen die uitgebreid onderzocht zijn. Hepp et al., [41] postuleerden een gemeenschappelijk referentiefraam voor oog-, hoofd- en handbewegingen. Berekeningen en coordinatie van hun interactie zouden hierdoor efficiënt georganiseerd kunnen worden. De experimenten, die in de hoofdstukken 2 en 3 beschreven worden, bevestigden de resultaten van Hepp et al. [41] dat de oriëntatie van de arm, de hand en het hoofd tijdens wijsbewegingen beschreven kan worden door middel van rotatievectoren die in een 2-dimensionaal vlak liggen. Ook vonden we dat de oriëntatie van dit vlak ongeveer loodrecht staat op de gemiddelde wijsrichting.

Deze resultaten leken de hypothese van een gemeenschappelijk 2-dimensionaal referentievlak voor oog-, hoofd- en handbewegingen te bevestigen. De oriëntatie van dit vlak zou dan aangepast worden aan het werkgebied van wijsrichtingen. Analyse, echter, van wijsbewegingen in een klein gedeelte van het grote werkgebied, geselecteerd uit een set data van wijsbewegingen in dat grote werkgebied, liet zien dat het vlak waarin de rotatievectoren liggen ongeveer loodrecht stond op de gemiddelde wijsrichting in dat kleine werkgebied en niet loodrecht op de gemiddelde wijsrichting in het grote werkgebied. De onvermijdelijke conclusie moest zijn dat het vlak van rotatievectoren zelf niet plat is, maar gekromd. Het gefitte platte vlak dat voor kleine werkgebieden wordt gevonden, is slechts een lokale benadering van het gekromde vlak. De redundantie voor arm-oriëntaties tijdens wijsbewegingen wordt opgeheven door de randvoorwaarde dat de rotatievectoren in dit gekromde vlak moeten liggen.

Vergelijkbare resultaten werden niet alleen voor de hand gevonden, maar ook voor de bovenarm en het hoofd. De oriëntatie van al deze ledematen werd beschreven door rotatievectoren in op vergelijkbare wijze gekromde vlakken en niet in platte vlakken zoals gevonden voor oogbewegingen. Op het eerste gezicht zou er nog een gemeenschappelijk referentiefraam kunnen bestaan voor hoofd, bovenarm en onderarm. Vergelijking van de vlakken van rotatievectoren gaf echter aan dat dit

niet het geval was omdat zij significante verschillen vertoonden, ondanks de globale gelijkenis

8.2.2 Hoofdstuk 4

Om de besturing van de redundantie op spierniveau te onderzoeken, is allereerst de spieractivatie onderzocht. Dit onderzoek begon met behulp van oppervlakte EMG (hoofdstuk 4). Vervolgens werd meer gedetailleerde informatie verkregen met gecombineerde intramusculaire en oppervlakte EMG afleidingen (hoofdstukken 5 en 6). In hoofdstuk 7 worden de inzichten, hiermee verworven, gebruikt om kwantitatief de bijdrage van spieren te schatten. Hoe de oplossing van de redundantie tot stand komt, kan met deze methodes bepaald worden. Hopelijk zal nader modelmatig onderzoek uitwijzen waarom deze oplossing door het motorisch systeem gekozen wordt om het redundantie-probleem op te lossen.

In hoofdstuk 4 wordt de relatieve activatie van verschillende elleboog- en schouderpijpen gemeten met behulp van oppervlakte elektroden voor een constante kracht in diverse richtingen tijdens isometrische contracties en tijdens bewegingen tegen een externe kracht. Gedurende isometrische (statische) contracties, vertoonde elke spier een specifiek activatiepatroon. Voor elke spier was er een bepaalde richting, de voorkeursrichting, waarin die spier zijn grootste activiteit vertoonde. Dit betekent ook dat die spier zijn grootste bijdrage levert aan de totale extern vereiste kracht voor die richting. Voor andere richtingen nam de activiteit, en dus de bijdrage van de spier aan de extern vereiste kracht, langzaam af met de cosinus van de hoek tussen de voorkeursrichting en de richting van de extern uitgeoefende kracht. Wanneer deze cosinus-afhankelijkheid in een polaire plot gezet wordt, dan levert dat cirkels door de oorsprong op in de richting van de voorkeursrichting.

Voor bewegingen tegen een externe kracht kon de richtingsafhankelijkheid ook met een cosinus van de hoek tussen de voorkeursrichting en de richting van de extern uitgeoefende kracht beschreven worden. De voorkeursrichtingen van de spieren tijdens bewegingen bleken te verschillen van die voor isometrische contractie, terwijl de gemeten krachten en de richting waarin zij werden uitgeoefend hetzelfde waren. Dat de spieren hun grootste EMG activiteit en dus hun grootste bijdrage aan de externe kracht in een andere richting vertoonden, terwijl de totale externe krachten uitgeoefend aan de pols gelijk waren, betekent dat de spieren verschillende relatieve bijdragen leveren aan de externe kracht tijdens deze twee experimentele condities. Niet alleen de voorkeursrichting van de spieren was anders voor isometrische contracties en bewegingen. Ook de gemeten amplitude van het EMG was anders. Tijdens bewegingen werd een EMG amplitude gemeten, die was toegenomen t.o.v. die tijdens isometrische contracties. Opmerkelijk is dat veelal de EMG activiteit van alle spieren

bleek toe te nemen. Dit impliceert dat er andere EMG-kracht relaties moeten zijn voor de spieren onder deze omstandigheden.

8.2.3 Hoofdstukken 5 en 6

Om deze resultaten te kunnen verklaren, hebben wij de EMG activiteit tegelijkertijd gemeten met oppervlakte en intramusculaire elektroden. De cosinus-afhankelijkheid waarmee de EMG activiteit voor een constante kracht in verschillende richtingen beschreven kan worden, kan verklaard worden op grond van het recruitment-gedrag van motor-units. De recruitment-drempel blijkt alleen af te hangen van de component van de externe kracht in een bepaalde, d.w.z. de "voorkeurs-" richting. In een polaire figuur blijken de recruitment-drempels van de motor-units op een rechte lijn te vallen. Gebaseerd op het size principle en het resultaat dat de recruitment-drempels, van motor-units met verschillende recruitment-drempels, op parallelle lijnen liggen, nemen wij aan dat bij recruitment van een bepaalde motor-unit het EMG altijd gelijk is. Daarom moet het EMG ook afhangen van de component van de externe kracht in die bepaalde richting, die dus gelijk is aan de voorkeursrichting van de spieren zoals die voor oppervlakte EMG gevonden wordt. Voor een constante externe kracht varieert deze component met de cosinus van de hoek tussen de voorkeursrichting en de richting van de externe kracht. De veranderingen in richting, die werden gevonden voor het oppervlakte EMG tussen isometrische contracties en bewegingen, kunnen verklaard worden door overeenkomstige veranderingen in de orientatie van de lijn gefit door de recruitment-drempels als functie van de richting van de extern uitgeoefende kracht.

De amplitudeveranderingen van de oppervlakte EMG data konden ook kwantitatief verklaard worden door het recruitment-gedrag van de motor units. Wanneer de recruitment-drempel afneemt, dan neemt de amplitude van het oppervlakte EMG toe. Een afgenomen recruitment-drempel betekent dat bij gelijke kracht, meer motor-units actief zullen zijn en derhalve dat ook het oppervlakte EMG zal toenemen. De totale amplitudeveranderingen van het oppervlakte EMG konden toegeschreven worden aan veranderingen van de recruitment-drempel aangezien geen veranderingen in vuurfrequentie van motor-units werden waargenomen.

8.2.4 Hoofdstuk 7

De verklaring van de amplitudetoename van het oppervlakte EMG, in termen van afname van de recruitment-drempels, laat de vraag waarom een groter aantal motor-units actief is tijdens bewegingen terwijl dezelfde krachten worden uitgeoefend als tijdens isometrische contracties, onbeantwoord. De kracht/snelheids-relatie kan niet

de enige oorzaak zijn voor de veranderingen, aangezien dan tegenovergestelde resultaten (dus afnames van de amplitude van het oppervlakte EMG) gevonden zouden moeten worden wanneer proefpersonen dezelfde krachten uitoefenen, maar daarbij in tegengestelde richting bewegen, wat niet het geval was. Een tweede resultaat, beschreven in hoofdstukken 4 en 6, was dat de voorkeursrichting voor isometrische contracties en contracties tijdens bewegingen verschillend is. Omdat de totale uitgeoefende kracht hetzelfde is, moet geconstateerd worden dat de relatieve bijdrage aan het gewrichtsmoment van de individuele spieren anders is. Co-contractie van antagonistische spieren kon als verklaring voor beide resultaten verworpen worden omdat de EMG activiteit van antagonistische spieren nagenoeg afwezig was.

Kwantificatie van de bijdrage van individuele spieren aan het totale gewrichtsmoment, in plaats van alleen maar een vage kwalitatieve beschrijving, was noodzakelijk om deze resultaten te beschrijven. Hiervoor hebben wij een methode ontwikkeld, om de momenten van individuele spieren af te leiden op grond van hun EMG. De basale aanname hierbij is dat de EMG-kracht relatie voor verschillende richtingen een geschaalde versie is van de werkelijke relatie tussen de EMG activiteit en de kracht die door elke spier zelf geproduceerd wordt. Alleen de schalingsconstanten moeten nog bepaald worden om de relatieve bijdrage van een spier aan het totale gewrichtsmoment te schatten. Doordat het totale gewrichtsmoment berekend kan worden, het is namelijk het uitproduct van de externe kracht uitgeoefend op de pols en de momentsarm van elleboog tot pols, verkrijgt men een relatie tussen de schalingsconstanten en het totale gewrichtsmoment. Wanneer dat gedaan wordt voor diverse richtingen, waarvoor de relatieve bijdrage van de actieve spieren anders is, dan kan een set lineaire vergelijkingen opgesteld worden, waaruit deze schalingsconstanten bepaald kunnen worden.

Deze methode blijkt te werken, maar is erg gevoelig voor ruis, waardoor het praktisch nut onduidelijk is. Robuuster is waarschijnlijk de vergelijkbare methode gebaseerd op intramusculaire recruitment-data. Deze laatste methode biedt de mogelijkheid om de activatie en dus de momentsbijdrage van individuele subpopulaties van motor-units apart te meten. Hierdoor kan inzicht verkregen worden in de coördinatie van spieren rond een gewricht op een wijze die veel gedetailleerder is dan met alleen oppervlakte EMG.

Bibliography

- [1] Bernstein N (1967) The problem of co-ordination and localization. In: *The co-ordination and regulation of movements*. Pergamon, New York, pp 15-59.
- [2] Buchanan TS, Almdale DPJ, Lewis JL, Rymer WZ (1986) Characteristics of synergic relations during isometric contractions of human elbow muscles. *J Neurophysiol* 56, pp 1225-1241.
- [3] Buchanan TS, Rovai GP, Rymer WZ (1989) Strategies for muscle activation during isometric torque generation at the human elbow. *J Neurophysiol* 62, pp 1201-1212.
- [4] Calancie B, Bawa P (1990) Motor unit recruitment in humans. In Binder MD and Mendell LM (eds): *The orderly recruitment of motor units*. Oxford University Press, pp 75-95.
- [5] Caminiti R, Johnson PB, Urbano A (1990) Making arm movements within different parts of space: Dynamic aspects in the primate motor cortex. *J Neurosci* 10, pp 2039-2058
- [6] Capaday C, Stein RB (1986) Amplitude modulation of the soleus H-reflex in the human during walking and standing. *J Neurosci* 6, pp 1308-1313.
- [7] Carpenter RHS (1988) Movement of the eyes, PION, London.
- [8] Challis JH and Kerwin DG (1994) Determining individual muscle forces during maximal activity: model development, parameter determination, and validation. *Hum Movement Science* 13, pp 29-61.
- [9] Cnockaert JC, Lensel G, Pertuzon E (1975) Relative contribution of individual muscles to the isometric contraction of a muscle group. *J Biomech* 8, pp 191-197.

- [10] Crawford JD, Vilis T (1991) Axes of rotation and Listing's law during rotations of the head. *J Neurophysiol* 3, pp 407-423.
- [11] Cruse H, Brüwer M (1987) The human arm as a redundant manipulator: The control of path and joint angles. *Biol Cybern* 57, pp 137-144.
- [12] Cruse H, Brüwer M, Dean J (1993) Control of three- and four-joint arm movement: strategies for a manipulator with redundant degrees of freedom. *J Motor Behavior* 25, pp 131-139.
- [13] De Luca CJ (1979) Physiology and mathematics of myoelectric signals. *IEEE Trans Biomed Eng* 26, pp 359-370.
- [14] De Luca CJ, Lefever RS, McCue MP, Xenakis AP (1982) Behaviour of human motor units in different muscles during linearly varying contractions. *J Physiol* 359, pp 107-118.
- [15] De Luca CJ, Mambrito B (1987) Voluntary control of motor units in human antagonist muscles: coactivation and reciprocal activation. *J Neurophysiol* 58, pp 525-542.
- [16] Donders FC (1848) Beitrag zur Lehre von den Bewegungen des menschlichen Auges. *Holländ Beitr Anat Physiol Wiss* 1, pp 104-145.
- [17] Donders FC (1875) Ueber das Gesetz der Lage der Netzhaut in beziehung zu der Blickebene. *Albrecht v. Graefes Arch. f. Ophtal.* 21, pp 125-130.
- [18] Dul J, Johnson JE, Shiavi R, Townsend MA (1984) Muscular synergism II. A minimum fatigue criterion for load sharing between synergistic muscles. *J Biomech* 17, pp 675-684.
- [19] Fick R (1911) Handbuch der Anatomie und Mechanik der Gelenke. III Teil: Spezielle Gelenk- und Muskelmechanik. Jena Verlag von Gustaf Fischer, pp 274-332.
- [20] Flament D, Goldsmith P, Buckley CJ, Lemon RN (1993) Task dependence of responses in first dorsal interosseus muscle to magnetic brain stimulation in man. *J Physiol* 464, 361-378.
- [21] Flanders M, Soechting JF (1990) Arm muscle activation for static forces in three-dimensional space. *J Neurophysiol* 64, pp 1818-1837.
- [22] Flash T (1987) The control of hand equilibrium trajectories in multi-joint arm movements. *Biol Cybern* 57, pp 257-274.

- [23] Georgopoulos AP, Kalaska JF, Caminiti R, Massey JT (1982) On the relations between the direction of two-dimensional arm movements and cell discharge in primate motor cortex *J Neurosci* 2, pp 1527-1537
- [24] Georgopoulos AP, Kalaska JF, Crutcher MD, Caminiti R, Massey JT (1984) The representation of movement direction in the motor cortex: single cell and population studies. In: Edelman GM, Gall WE, Cowan WEM (eds) *Dynamic aspects of neocortical function*, Wiley, New York, pp 501-524
- [25] Georgopoulos AP, Kettner RE, Schwartz AB (1988) Primate motor cortex and free arm movements to visual targets in three-dimensional space II. Coding of the direction of movement by a neuronal population *J Neurosci* 8, pp 2928-2937
- [26] Gielen C C A M and van Zuyl en EJ (1986) Coordination of forearm muscles during flexion and supination: application of the tensor analysis approach *J Neurosci* 17, pp 527-539
- [27] Gielen S, van Ingen Schenau GJ, Tax T, Theeuw en M (1990) The activation of mono- and bi-articular muscles in multi-joint movements. In: Winters JM, Woo SLY (eds) *Multiple muscle systems: biomechanics and movement organization*. Springer, New York, pp 302-311
- [28] Gielen CCAM, van Ingen Schenau GJ (1992) The constrained control of force and position in multi-link manipulators *IEEE Trans Systems, Man and Cybernetics*, 22, pp 1214-1219
- [29] Glenn B, Vilis T (1992) Violations of Listing's Law after large eye and head gaze shifts *J Neurophysiol* 68, pp 309-318
- [30] Gottlieb GL, Agerwal GC (1971) Dynamic relationship between isometric muscle tension and the electromyogram in man *J Appl Physiol* 30, pp 345-351
- [31] Gustafsson B, Pinter MJ (1985) On factors determining orderly recruitment of motor units: a role for intrinsic membrane properties *TINS* 8, pp 431-433
- [32] ter Haar Romeny BM, Denier van der Gon JJ, Gielen CCAM (1982) Changes in recruitment order of motor units in the human biceps muscle *Exp Neurology* 78, pp 360-368
- [33] ter Haar Romeny BM, Denier van der Gon JJ, Gielen CCAM (1984) Relation of the location of a motor unit in human biceps muscle and its critical firing levels for different tasks *Exp Neurology* 85, pp 631-650

- [34] Hatze H (1976) The complete optimization of human motion *Math Biosci* 28, pp 99-135
- [35] Hauste W (1989) Considerations on Listing's law and the primary position by means of a matrix description of eye position control *Biol Cybern* 60, pp 411-420
- [36] Helmholtz H von (1866) *Handbuch der physiologischen Optik* Voss, Hamburg
Engl transl (1962) Helmholtz' treatise on physiological optics Dover, New York
- [37] Henneman E, Somjen G, Carpenter DO (1965) Functional significance of cell size in spinal motoneurons, *J Neurophysiol* 28, pp 581-598
- [38] Henneman E, Somjen G, Carpenter DO (1965), Excitability and inhibibility of motoneurons of different sizes, *J Neurophysiol* 28, pp 599-620
- [39] Henneman E (1981) Recruitment of motoneurons the size principle In *motor unit types, recruitment, and plasticity in Health and Disease Progress in Clinical Neurophysiology* 9 Karger, Basel, pp 26-60
- [40] Hepp K, Hepp-Reymond M-C, (1989) Donders' and Listing's law for reaching and grasping arm synergies *Soc Neurosci Abstr* 15, p 604
- [41] Hepp K, Haslwanter T, Straumann D, Hepp-Reymond M-C, Henn V (1992) The control of arm, gaze and head by Listing's law In Caminiti R, Johnson PB, Burnod Y (eds) *Control of Arm Movement in Space Neurophysiological and Computational Approaches* Springer, Heidelberg, pp 307-320
- [42] Hof AL and van den Berg JW (1981a) EMG to force processing I An electrical analogue of the Hill muscle model *J Biomech* 14, pp 747-758
- [43] Hof AL and van den Berg JW (1981b) EMG to force processing II Estimation of the parameters of the Hill muscle model for the human triceps surae by means of a calf ergometer *J Biomech* 14, pp 759-770
- [44] Hof AL and van den Berg JW (1981c) EMG to force processing III Estimation of model parameters for the human triceps surae and assessment of accuracy by means a torque plate *J Biomech* 14, pp 787-792
- [45] Hof AL and van den Berg JW (1981d) EMG to force processing IV Eccentric-concentric contractions on a spring-flywheel set-up *J Biomech* 14, pp 787-792

- [46] Hoffer JA, Loeb GE, Sugano N, Marks WB, O'Donovan MJ, Pratt CA (1987) Cat hindlimb motoneurons during locomotion III. Functional segregation in sartorius. *J Neurophysiol* 57, pp 554-562.
- [47] Hogan N (1985) The mechanics of multi-joint posture and movement control. *Biol Cybern* 52, pp 315-331.
- [48] Hore J, McCloskey DI, Taylor JL (1990) Task-dependent changes in gain of the reflex response to imperceptible perturbations of joint position in man. *J Physiol* 429, pp 309-321.
- [49] Hore J, Goodale M, Vilis T (1990) The axis of rotation of the arm during pointing. *Soc Soc Neurosci Abstr* 16, p 1086.
- [50] Hore J, Watts S, Vilis T (1992) Constraints on arm position when pointing in three dimensions: Donders' law and the Fick gimbal system. *J Neurophysiol* 68, pp 374-383.
- [51] van Ingen Schenau GJ, Bobbert MF, Rozendal RH (1987) The unique action of bi-articular muscles in complex movements. *J Anat* 155, pp 1-5.
- [52] van Ingen Schenau GJ (1989) From rotation to translation: constraints on multi-joint movements and the unique action of bi-articular muscles. *Hum Mov Sciences* 8, pp 865-882.
- [53] van Ingen Schenau GJ, Boots PJM, de Groot G, Snackers RJ, van Woensel (1992) The constrained control of force and position in multi-joint movements. *J Neurosci* 46, pp 197-207.
- [54] Jacobs R, van Ingen Schenau GJ (1992) Control of an external force in leg extensions in humans. *J Physiol* 457, pp 611-626.
- [55] Jongen H (1989) Theories and experiments on muscle coordination during isometric contractions. *Thesis*, University of Utrecht, The Netherlands.
- [56] Jongen HAH, Denier van der Gon JJ, Gielen CCAM (1989) Activation of human arm muscles during flexion/extension and supination/pronation tasks: a theory on muscle coordination. *Biol Cybern* 61, pp 1-9.
- [57] Jørgenson K, Bankov S (1971) Maximum strength of elbow flexors with pronated and supinated forearm. In: *Medicine and Sport 6: Biomechanics II*, Karger, Basel, pp 174-180.

- [58] Kalaska JF, Caminiti R, Georgopoulos AP (1983) Cortical mechanisms related to the direction of two-dimensional arm movements: Relations in parietal area 5 and comparison with motor cortex. *Exp Brain Res* 51, pp 247-260.
- [59] Keshner EA, Baker JF, Banovetz J, Peterson BW (1992) Patterns of neck muscle activity in cats during reflex and voluntary head movements. *Exp Brain Res* 88, 361-374.
- [60] Klein CA, Huang CH (1983) Review of pseudoinverse control for use with kinematically redundant manipulators. *IEEE Trans Syst, Man, Cybern, SMC-13*, pp 245-250.
- [61] Krauth J (1988) Distribution-free statistics: an application oriented approach. Elsevier, Amsterdam
- [62] Kukulka CG, Clamann HP (1981) Comparison of the recruitment and discharge properties of motor units in human brachial biceps and adductor pollicis during isometric contractions *Exp Brain Res* 219, pp 45-55.
- [63] LeFever RS, De Luca CJ (1976) The contribution of individual motor units to the EMG power spectrum. *Proc 29th Ann. Conf. Engineering in Medicine and Biology*, p 56.
- [64] Leigh RJ, Maas EF, Grossman GE, Robinson DA (1989) Visual cancellation of the torsional vestibulo-ocular reflex in humans. *Exp Brain Res* 75, pp 221-226.
- [65] Lippold OJC (1952) The relation between integrated action potentials in human muscle and its isometric tension. *J Physiol* 117, pp 492-499.
- [66] Loeb GE (1985) Motoneurone task groups: coping with kinematic heterogeneity. *J Exp Biol* 115, pp 137-146.
- [67] Loeb GE, Levine WS, He J (1990) Understanding sensorimotor feedback through optimal control. *Cold Spring Harbor Symposia on Quantitative Biology* 55, pp 791-803.
- [68] Lohman AHM (1976) Vorm en beweging: leerboek van de mens. *Deel II: platen*. Bohn, Scheltema en Hoeksema, Utrecht.
- [69] McMahon TA (1984) Muscles, Reflexes and Locomotion. Princeton University Press.

- [70] Miller LE, Gielen CCAM, Theeuwens M, Doorenbosch D (1992) The activation of mono- and biarticular muscles in multijoint movements. In: Caminiti R, Johnson PB, Burnod Y (eds) *Control of Arm Movement in Space. Neurophysiological and Computational Approaches*. Springer, Heidelberg, pp 1-15.
- [71] Miller LE, Theeuwens M, Gielen CCAM (1992) The control of arm pointing movements in three dimensions. *Exp Brain Res* 90, pp 415-426.
- [72] Nakayama K (1975) Coordination of extraocular muscles. In: Lennerstrand G, Bach-y-Rita P (eds.) *Basic mechanisms in ocular motility and their clinical implications*. Pergamon Press, New York, pp 193-207.
- [73] Nakayama K (1983) Kinematics of normal and strabismic eyes. In: Shor CM, Ciuffreda (eds.) *Vergence eye movements: Basic and clinical aspects*. Butterworths, Boston, pp 543-564.
- [74] Nardone A, Scieppati M (1988) Shift of activity from slow to fast muscle during voluntary lengthening contractions of the triceps surae muscles in humans. *J Physiol* 395, pp 363-381.
- [75] Nardone A, Romano C, Schieppati M (1989) Selective recruitment of high-threshold human motor units during voluntary isotonic lengthening of active muscles. *J Physiol* 409, pp 451-471.
- [76] Nielsen J, Petersen N, Deuschl G, Ballegaard M (1993) Task-related changes in the effect of magnetic brain stimulation on spinal neurones in man. *J Physiol* 471, pp 223-243.
- [77] Olney SJ, and Winter DA (1985) Prediction of knee and ankle moments of force in walking from EMG and kinematic data. *J Biomech* 19, pp 9-20.
- [78] van Opstal J, Hepp K, Hess B, Straumann D, Henn V (1991) Two- rather than three-dimensional representation of saccades in monkey superior colliculus. *Science* 252, pp 1313-1315.
- [79] Otten B (1988) Concepts and models of functional architecture in skeletal muscle. *Exercise Sport Sci Rev* 16, pp 89-137.
- [80] Patla AE, Hudgins BS, Scott R.N. (1982) Myoelectric signal as a quantitative measure of muscle mechanical output. *Med Biol Eng Comput* 20, pp 319-328.
- [81] Pedotti A, Krishnan VV and Stark L (1978) Optimization of muscle force sequencing in human locomotion. *Math Biosci* 38, pp 57-76.

- [82] Penrod D.D., Davy D.T., Singh D.P. (1974) An optimization approach to tendon force analysis. *J Biomech* 7, pp 123-129.
- [83] Person RS, Kudina LP (1972) Discharge frequency and discharge pattern of human motor units during voluntary contraction of muscle. *Electroenceph Clin Neurophysiol* 32, pp 471-483.
- [84] Powers RK, van den Noen S, Rymer WZ (1989) Evidence of shared, direct input to motoneurons supplying synergist muscles in humans. *Neurosci Lett*, 102, pp 76-81.
- [85] Riek S, Bawa P (1992) Recruitment of motor units in human forearm extensors. *J Neurophysiol* 68, pp 100-108.
- [86] Robinson DA (1975) Oculomotor control signals. In Lennerstrand G, Bach-y-Rita P (eds) *Basic Mechanisms of Ocular Mobility*, Pergamon Press, Oxford, pp 337-378.
- [87] Scheid F (1968) Numerical analysis. *Schaum's outline series*. McGraw-Hill.
- [88] Segal RL (1992) Neuromuscular compartments in the human biceps brachii muscle. *Neurosci Lett* 140, pp 98-102.
- [89] Sobotta J, Becher H (1972) Atlas der Anatomie des Menschen. Band I: Regionen, Knochen, Bänder, Gelenke und Muskeln des menschlichen Körpers. Urban & Schwarzenberg, München.
- [90] Soechting JF, Terzuolo CA (1986) An algorithm for the generation of curvilinear wrist motion in an arbitrary plane in three-dimensional space. *J Neurosci* 19, pp 1393-1405.
- [91] Straumann D, Hepp K, Hepp-Reymond M-C, Haslwanter T (1990) Human eye, head and arm rotations during reaching and grasping. *Soc Neurosci Abstr* 16, p 1087.
- [92] Straumann D, Haslwanter T, Hepp-Reymond M-C, Hepp K (1991) Listing's law for eye, head and arm movements and their synergistic control. *Exp Brain Res* 86, pp 209-215.
- [93] Tax A, Denier van der Gon JJ, Gielen CCAM, van den Tempel CMM (1989) Differences in the activation of m.biceps brachii in the control of slow isotonic movements and isometric contractions *Exp Brain Res* 76, pp 55-63.

- [94] Tax AAM, Denier van der Gon JJ, Gielen CCAM, Kleyne M (1990) Differences in central control of m.biceps brachii in movement tasks and force tasks. *Exp Brain Res* 79, pp 138-142.
- [95] Tax AAM, Denier van der Gon JJ, Erkelens CJ (1990) Differences in coordination of elbow flexor muscles in force tasks and in movement tasks. *Exp Brain Res* 81, pp 567-572.
- [96] Theeuwes MMHJ (1989) The influential needle. *Master thesis*, University of Nijmegen.
- [97] Theeuwes M., Gielen CCAM, Miller LE, Doorenbosch C (1994) The relation between surface EMG and recruitment thresholds of motor units in human arm muscles during isometric contractions. *Exp Brain Res*, in press.
- [98] Theeuwes M., Gielen CCAM, Miller LE (1994) The relative activation of muscles during isometric contractions and low-velocity movements against a load. Submitted to *Exp Brain Res*.
- [99] Tweed D, Vilis T (1987) Implications of rotational kinematics for the oculomotor system in three dimensions. *J Neurophysiol* 58, pp 832-849.
- [100] Tweed D, Vilis T (1990) Geometric relations of eye position and velocity vectors during saccades. *Vision Res* 30, pp 111-127.
- [101] Vereijken B, van Emmerik REA, Whiting HTA, Newell KM (1992) Free(z)ing degrees of freedom in skill acquisition. *J Motor Behavior* 24, pp 133-142.
- [102] Woittiez RD, Huijing PA, Boom HBK, Rozendal RH (1984) A three-dimensional muscle model: a quantified relation between form and function of skeletal muscles. *J Morphol* 182, pp 95-113.
- [103] Yeo BP (1976) Investigations concerning the principle of minimal total muscular force. *J Biomech* 9, pp 413-416.
- [104] Zajac FE, Wicke RW, and Levine WS (1984) Dependence of jumping performance on muscle properties when humans use only calf muscles for propulsion. *J Biomech* 17, pp 513-523.
- [105] Zajac FE (1990) Coupling of recruitment order to the force produced by motor units: the "size principle hypothesis" revisited. In: Binder MD and Mendell LM (eds) *The orderly recruitment of motor units*. Oxford University Press, pp 96-111.

- [106] van Zuylen EJ, Gielen CCAM, Denier van der Gon JJ (1988) Coordination and inhomogeneous activation of human arm muscles during isometric torques. *J Neurophysiol* 60, pp 1523-1548.
- [107] van Zuylen EJ, van Velsen A, and Denier van der Gon JJ (1988b) A biomechanical model model for flexion torque of human arm muscles as a function of elbow angle. *J Biomech* 15, pp 183-190.

Publications

- Gielen S, van Ingen Schenau GJ, Tax T, Theeuwen M (1990) The activation of mono- and bi-articular muscles in multi-joint movements. In: Winters JM, Woo SLY (eds). *Multiple muscle systems: biomechanics and movement organization*. Springer, New York. pp 302-311.
- Miller LE, Gielen CCAM, Theeuwen M, Doorenbosch D (1992) The activation of mono- and biarticular muscles in multijoint movements. In: Caminiti R, Johnson PB, Burnod Y (eds) *Control of Arm Movement in Space. Neurophysiological and Computational Approaches*. Springer, Heidelberg, pp 1-15.
- Miller LE, Theeuwen M, Gielen CCAM (1992) The control of arm pointing movements in three dimensions. *Exp Brain Res* 90, pp 415-426.
- Theeuwen MMHJ, Gootzen THJM, Stegeman DF (1993) Muscle Electric Activity I: A Model Study on the Effect of Needle Electrodes on Single Fiber Action Potentials. *Ann Biomed Eng* 21, pp 377-389.
- Stegeman DF, Gootzen THJM, Theeuwen MMHJ, Vingerhoets HJM (1994) Intramuscular potential changes caused by the presence of the recording EMG needle electrode. *Electromyogr Clin Neurophysiol*, in press.
- Theeuwen M., Gielen CCAM, Miller LE, Doorenbosch C (1994) The relation between surface EMG and recruitment thresholds of motor units in human arm muscles during isometric contractions. *Exp Brain Res*, in press.
- Theeuwen M., Gielen CCAM, Miller LE (1994) The relative activation of muscles during isometric contractions and low-velocity movements against a load. Submitted to *Exp Brain Res*.
- Theeuwen M, Gielen CCAM, van Bolhuis B (1994) Estimating the contribution of muscles to joint torque from EMG activity. Submitted to *J Biomech*

Nawoord

Het beeld dat sommige mensen hebben van een wetenschapper, die alleen in zijn ivoren toren de meest ingenieuze theorie bedenkt, is pertinent onjuist. In mijn geval is zelfs de meeste tijd onder het maaiveld doorgebracht. Bovendien zou ik nooit in staat zijn geweest deze promotie in mijn eentje tot stand te brengen. Ik heb dan ook gebruik mogen maken van de hulp van velen en hierbij wil ik hen dan ook van harte danken. Mocht ik iemand vergeten hebben te danken, dan bied ik daarvoor mijn excuses aan.

Zonder de belangeloze inzet van vele proefpersonen hadden de experimenten nooit uitgevoerd kunnen worden. Sommigen zullen zichzelf kunnen herkennen in de initialen in een van de tabellen van dit proefschrift. Anderen zullen misschien vergeefs zoeken naar tastbare tekenen van hun inspanningen. Allen hebben bijgedragen aan de continue verbetering van de opstelling, wijze van experimenteren en nader inzicht in de diverse vraagstellingen van dit proefschrift. Aangezien fysici geen invasieve handelingen mogen verrichten, was de hulp van een tweetal artsen bij het inbrengen van de intramusculaire elektroden van cruciaal belang. Zowel Jaak Duysens als Leo Geeraedts hebben op doeltreffende wijze menig proefpersoon met naald en draad behandeld. Ton van Dreumel en Hans Kleijnen hebben hun onschatbare talenten ingezet om van de grond af een efficiënte experimentele opstelling te bouwen. Hun bliksemacties hebben verscheidene experimenten gered, vooral in het begin, toen kinderziektes in de opstelling nog wel eens de kop opstaken.

Vier mensen hebben de afgelopen vier jaar speciaal bijgedragen aan het tot stand komen van dit proefschrift. Zij hebben mij bijgestaan tijdens het opzetten, uitvoeren en analyseren van experimenten in de breedst mogelijke zin en het schrijven van de diverse artikelen. Bovendien hielden zij het gedurende lange tijd dagelijks met mij uit. Allereerst was dat natuurlijk Caroline Doorenbosch met haar mateloos doorzettingsvermogen. Net zoals zij deed ook Ron Hogeweg zijn afstudeerstage van de faculteit bewegingswetenschappen aan de VU bij ons in Nijmegen met groot enthousiasme. Because Lee Miller was too lazy to learn Dutch during the two years which he spent in our department, these sentences are written in English. His many

merits, however, outnumber this small shortcoming. He managed to build the experimental set-up in a minimum amount of time and even after his return to Chicago, he continued to contribute to most articles. En natuurlijk lest best Stan Gielen. Hij heeft aan de wieg van mijn project gestaan en meegeholpen het tot een goed einde te brengen als o.m. "de ideale proefpersoon" en dagelijks begeleider. Vooral zijn enthousiasme, inspiratie en overzicht van de relevante stand van zaken waren onmisbaar en zeer stimulerend

Behalve deze mensen die een directe bijdrage hebben geleverd aan het onderzoek, heeft menigeen meegeholpen om randvoorwaarden te scheppen waardoor dit proefschrift voltooid kon worden. Allereerst natuurlijk alle "MBFys-ers" voor de prettige werksfeer op de afdeling. Speciaal wil ik hier noemen Toine Tax, directe voorganger en verschaffer van wijze raad waar ik waarschijnlijk veel te weinig gebruik van heb gemaakt, en Siebren Schaafsma, o.a. sparring partner op de tennisbaan. De werkzaamheden en uiteraard de goedkeuringen van de manuscriptcommissie, te weten Jaak Duysens, Caspar Erkelens en Gerrit-Jan van Ingen-Schenau, hebben de laatste obstakels voor de promotie uit de weg geruimd. De laatste versie werd nog eens kritisch onder de loupe genomen door Marianne van Gool. Tenslotte wil ik mijn ouders bedanken voor hun vertrouwen en stimulatie. Vol ongeduld hebben zij gewacht op het ei dat nu eindelijk gelegd is.

Curriculum Vitae

Redundantie heeft twee betekenissen, namelijk overtolligheid en overvloedigheid. De eerste betekenis is negatief van aard. De tweede betekenis is juist erg positief en als zodanig dient dan ook het begrip redundantie in dit proefschrift opgevat te worden, namelijk de overvloedigheid aan vrijheidsgraden die tot gevolg heeft dat er meerdere oplossingen bestaan voor een enkele bepaalde taak.

Dit is niet alleen op de coördinatie van gewrichten en spieren van toepassing, maar ook op de ontwikkeling van ieder mens van baby tot volwassene. In principe heeft iedereen een groot aantal capaciteiten (vrijheidsgraden). Slechts een klein gedeelte hiervan kan uiteindelijk tot ontwikkeling worden gebracht. Toen ik als baby ter wereld kwam, kreeg ik al het nodige in aanleg mee. Binnen die mogelijkheden, die als harde randvoorwaarden aanwezig waren, kon ik mij nog op een schier oneindig aantal verschillende wijzen ontwikkelen, zowel qua persoonlijkheid als qua opleiding. Deze redundantie, waarmee iedereen geconfronteerd wordt, werd langzamerhand steeds meer gereduceerd door interacties met mijn omgeving en keuzes, die ik heb gemaakt.

Op de diverse lagere scholen en op de brugklas van het "Serviam" bestond mijn keus eigenlijk uit het niet kiezen en zo veel mogelijk keuzes open laten. Eenmaal op dit pad, lagen de keuzes om naar het gymnasium te gaan, te kiezen voor de β -richting en merendeels exacte vakken voor de hand. Dat daarbij vele vakken moesten afvallen was onvermijdelijk. Ophalen en zo nodig bijspijkeren van deze kennis is een van mijn vrijheidsgraden waarvan ik tot nu toe weinig gebruik heb gemaakt. Aan het eind van de middelbare school moest er toch een keus gemaakt worden. De studie Fysica aan de Katholieke Universiteit Nijmegen bood een sluipteg om te kiezen voor een geslaagd compromis tussen leuke alternatieven zoals wiskunde en informatica en natuurlijk natuurkunde zelf. Door mijn afstudeerwerk in de richting Medische Fysica, onder plezierige begeleiding van Theis Gootzen en Dick Stegeman, kwam ik, net als thuis, ook zijdelings in aanraking met een ander alternatief, namelijk medicijnen. Gedurende een jaar hield ik mij toen bezig met het modelleren van de elektrische volumegeleiding bij actiepotentialen van spieren (zie mijn afstudeer-scriptie). De keuze om mij te verdiepen in de interpretatie van deze signalen en van de bewegingen

en krachten die zij tot gevolg hebben (zie dit proefschrift), lijkt misschien wel een keuze om niets anders te kiezen, maar werd toch bewust gemaakt.

Ondanks de gigantische reductie in mijn vrijheidsgraden die ik tot nu toe tot stand heb gebracht, zijn er nog steeds oneindig veel over. Welke ik beroepsmatig zal gaan gebruiken, zal voor een deel bepaald worden door mijn keuze voor een bepaald segment in de arbeidsmarkt, maar ook voor een groot deel door de randvoorwaarden die de markt stelt.

